Addis Ababa University

College of Technology and Built Environment (CTBE)
SCHOOL OF CIVIL AND ENVIRONMENTAL ENGINEERING

SCHOOL OF GRADUATE STUDIES

MASTERS OF SCIENCE IN CIVIL ENGINEERING

THESIS

ON

Evaluation of Gravelly Clay Blanket Foundation Treatment and Remedial Measures for Piping Control in Embankment Dam: A Case Study of Kalid Dijo Dam

A Thesis Submitted to the School of Graduate Studies of Civil and Environmental Engineering of College of Technology and Built Environment (CTBE) SCHOOL OF CIVIL AND ENVIRONMENTAL ENGINEERING in Partial Fulfillment Of the Requirements for the Degree of Master of Science in Civil Engineering (Dam Engineering)

By: Hafsoa Getu

Advisor: Tezera Friew (PhD)

October 2025

Addis Ababa, Ethiopia

APPROVAL SHEET

ADDIS ABABA UNIVERSITY
SCHOOL OF GRADUATE STUDIES
COLLEGE OF TECHNOLOGY AND BUILT ENVIRONMENT (CTBE)
SCHOOL OF CIVIL AND ENVIRONMENTAL ENGINEERING
(Major in Dam Engineering)

This is certify that the thesis prepared by Hafsoa Getu, entitled: " **Evaluation of Gravelly Clay Blanket Foundation Treatment and Remedial Measures for Piping Control in Embankment Dam: A Case Study of Kalid Dijo Dam** " and submitted in fulfillment of the requirements for the Degree of Master of Science complies with the regulations of the Addis Ababa University and meets the accepted standards with respect to the originality and quality.

By :
Hafsoa Getu

Approved by Board of Examiners:

Dr. Tezera Firew		19/12/25
Advisor	Signature	Date
Aletsanat Nigatu (PhD)		15/12/25
Internal Examiner	Signature	Date
Dr. Ing. Tensay Gebremedhin		16/12/25
External Examiner	Signature	Date
PG Program Coordinator School of Civil & Environmental Engineering		
Chairman	Signature	Date

DECLARATION

I, Hafsoa Getu, hereby certify that the information contained in this paper was acquired and provided in compliance with laws and ethical standards. I have conducted my research with honesty, integrity, and transparency, striving to adhere to the highest standards of academic and professional ethics.

I further declare that, under these rules of conduct, I have accurately referenced and cited any data, ideas, and results that are not original to this work. I have meticulously acknowledged the contributions of other researchers and authors by providing appropriate citations throughout this thesis. I have taken care to avoid any form of plagiarism, ensuring that all sources are properly attributed.

By my signature below, I confirm that the work included in this thesis is entirely original to me. I have diligently conducted my research, crafted my arguments, and presented my findings based on my own efforts and intellect. Any assistance received from colleagues, advisors, or other individuals has been acknowledged and duly credited.

I further confirm that all information sources used in the preparation of this thesis have been correctly cited, referring to the original works and authors consistently and accurately. I have utilized a recognized citation style and followed its guidelines to ensure the proper documentation of my sources.

I understand the importance of academic integrity and take full responsibility for the accuracy and integrity of this research work. In the event that any discrepancies or issues are discovered, I am committed to addressing them promptly and transparently.

By signing below, I affirm that this certification is true and accurate to the best of my knowledge.

Signature: ______________________________

Date: __________________________________

ACKNOWLEDGEMENT

My deepest gratitude is to Allah, who consistently assists me in overcoming life's difficulties with success and joy.

I also sincerely thank my dear family for their love and encouragement. I am deeply grateful to my research advisor, Dr. Tezera Firew, for his genuine understanding and compassionate guidance. Additionally, I would like to extend my heartfelt gratitude to Mesfin Kere, a senior engineer.

I also extend my gratitude to Ethiopian Engineering Corporation for supplying most of the information essential for my research.

Finally, I wish to sincerely thank my friends from the Dam Engineering class of 2014 E.C., namely Mesfin K. Alemayehu M., Esubalew M., Amdemariam S. and Tegegn F., for their camaraderie and excellent academic support throughout the challenging past two years.

ACRONYMS AND ABBREVIATIONS

°	: Degrees (angle units)
BH	: Borehole
BSB	: British Standard
C	: Creep ratio or flow coefficient
E	: Porosity
ECDSWCo	: Ethiopian Construction Design and Supervision Works Corporation
EEC	: Ethiopian Engineering Corporation
FS	: Safety Factor
FSL	: Full Supply Level
g	: Acceleration due to gravity
GC	: Gravely Clay
GeoStudio	: Software suite for geotechnical analysis
GIS	: Geographical Information System
GNSS	: Global Navigation Satellite System
GPa	: Gigapascal
Gs	: Specific Gravity of soil particles
H	: Head loss or hydraulic head difference
H	: Hydraulic head difference
Ha	: hectare
ICOLD	: International Commission on Large Dams
K	: Coefficient of permeability
Km	: Kilometer
L	: Length of seepage path
Lugeon	: Unit of measurement for rock permeability
m.a.s.l.	: Meters above sea level
m^3/sec/m^2	: Cubic meters per second per square meter
MCM	: Million Cubic Meters
MLIT	: Ministry of Land, Infrastructure, Transport and Tourism
n	: Porosity
n.d.	: no date (as applied to referenced sources that do not have a date of publication)
P	: Potential (implied in seepage and pressure)

PGA	: Peak Ground Acceleration
U/S	: Upstream
D/S	: Downstream
Q	: Discharge or flow rate
Quake/W	: Seismic response analysis module within GeoStudio
RMR	: Rock Mass Rating system
SEEP/W	: Seepage analysis module within Geo-Studio
SPT	: Standard Penetration Test
UCS	: Uniaxial Compressive Strength
USCS	: Unified Soil Classification System
USSD	: U.S. Society on Dams
UTM	: Universal Transverse Mercator
VES	: Vertical Electrical Sounding
x, y, z	: Easting, Northing and Elevation — coordinate axes in modeling
α	: Angle of internal friction
β	: slope angle
Δ	: Change or difference (e.g., in head or pressure)

TABLE OF CONTENTS

LIST OF FIGURES

LIST OF TABLES

No table of figures entries found.

ABSTRACT

This thesis aimed to evaluate gravelly clay blanket and Remedial Measures for Piping Control in the dam foundation at Kalid Dijo Dam, employing a comprehensive methodology that integrated extensive geotechnical investigations, geological surveys, laboratory testing, and advanced numerical modeling with GeoStudio 2022. The primary objective was to assess the effectiveness of Gravelly Clay Blanket and foundation modifications in controlling seepage and enhancing dam stability. The analysis focused on static seepage and slope stability assessments across multiple critical sections of the dam, specifically at chainages 0+520, 0+770, 1+123, 1+228, and 1+670, using detailed geotechnical data and flow path evaluations.

The results demonstrated that the proposed foundation treatments such as increasing the thickness of impermeable gravelly clay layers and installing cutoff slurry walls substantially reduced water flux by approximately 85–90%, effectively lowering hydraulic gradients and minimizing the risk of piping. Validation work through flow path and flux comparison confirmed the reliability of the numerical models, indicating that the optimized foundation configurations can prevent internal erosion phenomena under static conditions. The safety factors derived from static slope stability analyses consistently exceeded critical thresholds, further affirming the structural integrity of the dam with the implemented modifications. Overall, the outputs substantiate that site-specific foundation interventions, supported by rigorous modeling and validation, are vital in mitigating piping risks, ensuring long-term dam safety, and conserving water resources.

Keywords: *gravelly clay blanket, internal erosion, piping, GeoStudio, water flux, slope stability*.

1. INTRODUCTION

1.1 General Background

Dams are vital for national growth as they provide flood protection, drinking water, agriculture, electricity, transportation, and tourism benefits. Dams have many valuable purposes, but they also pose threats to both property and life since they could end up failing and result in disastrous flooding. Owners and controllers of dams conduct routine examinations and inspections to identify potential causes of failure and implement preventative measures to lower the associated risks. Since no strategy for averting failure can ever be assured and loadings exceeding specified limits can never be totally avoided, projecting potential failures and developing preparations for them is another essential part of risk reduction. Programs for public education, the creation of alert systems and protocols, and the creation of efficient evacuation protocols are a few examples of these strategies. Dam owners can also utilize analysis of the effects of flooding and dam collapse to rank the risks posed by the various dams in their inventory. This prioritization approach makes it easier to employ human and financial resources efficiently in order to improve public safety and lessen the risk of dam failure.

In the event of failure of a dam by overtopping/or piping, a breach is formed on the dam hull, which gradually expands in terms of hours or even minutes. The water stored behind the reservoir is then set free uncontrollably in great amounts and causes damage along its route in great proportions. A flood caused by a dam breach may be much larger in magnitude and behave much differently than a natural flood (Asburry and Goodell, 2009). In the absence of preemptive measures geared towards such a risk, such as an emergency action plan, settlements and the properties located downstream of the dam and on the route of such a dam failure flood are put to great risk. Dam break analyses provide information on the consequences of a possible dam failure for risk estimation and rescue planning purposes. The development of effective emergency action plans and the design of early warning systems heavily rely on prediction results (Zagonjolli, 2007).

Among the primary and main purposes of constructing a dam is to store water and use it for irrigation. The World Commission of Dam estimates that around 30-40% of irrigated land relies on dams. It is estimated that 60% of the food production that comes to the market is dependent on dam water for its irrigation. In developing countries like Ethiopia, dam and irrigation projects are not only about development, but also survival. Therefore, the proper and timely utilization of water resources by constructing dam and their conveyances is vital for economic development.

1.2 Project Description

1.2.1 Project Overview

The Khalid Dijo Dam and Irrigation Project is being built in the Silt Zone of the Southern Nations, Nationalities and Peoples Regional State (SNNPRS) of Ethiopia, across the Dijo seasonal river, around Dalucha town, about 200 km from Addis Ababa. The project covers an area of 71895 ha and has a population of 90,032 (2007). The Woreda region, which includes 17 rural Kebeles, has a total area of 7047'N and 38015'E, with an elevation of 1950 m.a.s.l. and a terrain slope ranging from steep to almost plain. The dam is intended to irrigate 1000 hectares of land. The Woreda region has 17 rural Kebeles and is located at 7047'N and 38015'E. The Kalid Dijo dam is designed as a zoned earthen-rock fill dam with a central clay core. It has a maximum height of 26m measured from the river bed and a crest width of 8m which is the dam is under construction.

One of the basic requirements for the design of earth-rock fill dams is to ensure safety against internal erosion, piping, and the development of excessive pore pressures in the dam. The materials for the Kalid Dejo dam foundation is unwelded tuff with ash fall deposits. This material usually provides good bearing capacity, but can be highly vulnerable to (affected by) internal erosion. In consideration of such potential problems associated with the behavior of such foundation materials, it is recommended that the material not be excavated, removed, and replaced with a superior quality material, but the Engineer proposed that this soft material covered by a GC (gravel + clay) blanket all over the dam foundation.

1.2.2 Project Location Map

Kalid Dijo Dam site is located in the Rift Valley River Basin with geographic coordinates of 868194 UTM Northing and 413216 UTM Easting. The location map of the project area is shown in Figure 1.1.

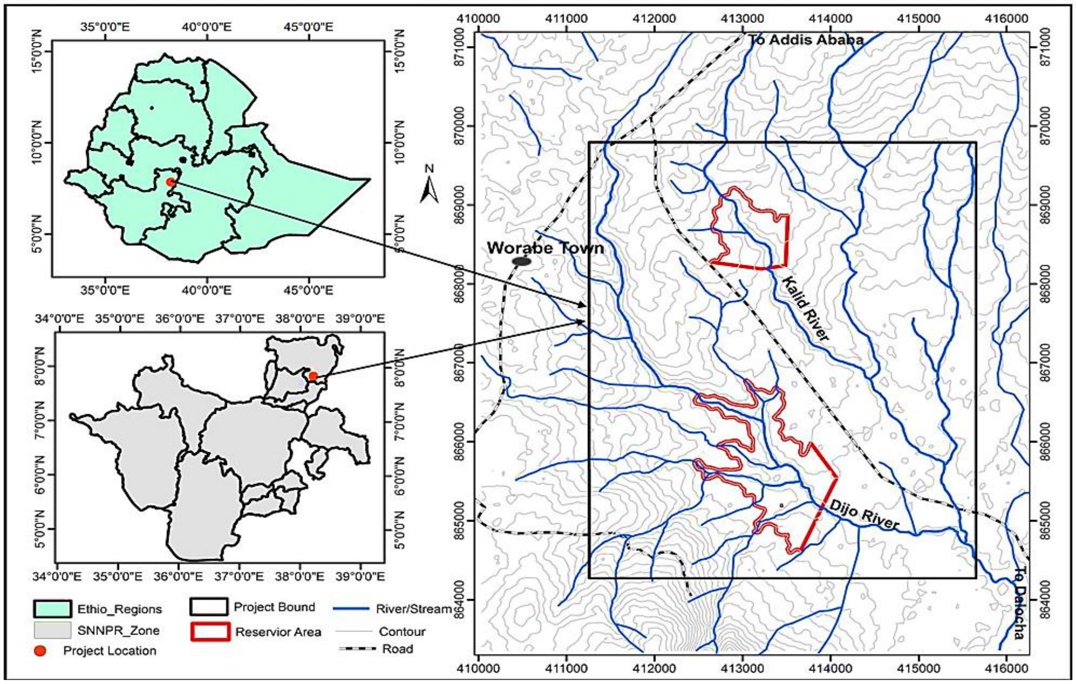

Figure 1. 1. Location map and salient features of Kalid Dijo Dam (EEC, 2019)

1.3 Statement of the problem

Piping in earth dams occurs when water seeps through the dam, carrying soil particles away from critical structures such as the embankment, filters, drains, foundation, or abutments. One of the primary causes of dam failure is piping through the dam foundation, which can lead to catastrophic breaches within a few hours once internal erosion becomes apparent. Given that internal erosion may arise during normal operations, it poses a greater risk to dam integrity than extreme loading scenarios like floods and earthquakes.

The Kalid Dijo dam foundation has been identified as having ash deposits based on geotechnical and geological investigations conducted by the Ethiopia Engineering Corporation (insert the firm that wrote the referenced report, and the year(2019). These ash deposits, which are in continuous contact with groundwater and the reservoir, present a significant risk for piping. To mitigate this risk, the design consultant has recommended the installation of a gravelly clay blanket throughout the dam-foundation interface as a countermeasure against potential piping and erosion failures.

This study has focused on evaluating the effectiveness of the recommended foundation treatment measures, specifically the use of gravelly clay blankets, employing geotechnical analysis software GeoStudio 2022 for the assessment.

1.4 Research questions

The research questions that will be answered at the end of this thesis are:

1) Does the recommended gravelly clay blanket and cutoff cement slurry treatment adequately control the piping or internal erosion problem?
2) Will it be structurally stable to construct the Kalid Dijo dam, including a gravelly clay blanket and remedial options to mitigate the potential piping problems in the foundation?
3) What are the cost implications of implementing these remedial measures, and are they economically viable for ensuring long-term dam safety?

1.5 Objective of the Study

1.5.1 General Objective

The main objective of this research is the Evaluation of Gravelly Clay Blanket foundation treatment and Remedial Measures for Piping Control in the foundations of the Kalid Dijo dam.

1.5.2 Specific Objective

The specific objectives of the study include:

1) To assess the effectiveness of the gravelly clay blanket layer in preventing internal erosion within the dam foundation, ensuring it meets its intended performance criteria.
2) To analyze the Steady State slope stability of the Kalid Dijo dam by incorporating the proposed gravelly clay blanket layer and other remedial options into the foundation design using seepage analysis results as essential input parameters.
3) To provide targeted recommendations for foundation improvement measures that may apply to similar geological and foundational challenges, specifically addressing issues arising from ash deposits at potential dam sites for future projects.

1.6 Scope of Work

The scope of this study is to evaluate the performance of the gravelly clay blanket layer in controlling piping and internal erosion within the dam foundation.

By using an integrated geotechnical analysis software known as Geostudio 2022, the study will apply laboratory test results, geotechnical data, and various parameters to calculate the occurrence of piping based on different blanket thicknesses.

1.7 Limitations of the Study

The results of this study will have the following limitations:

1) This study focuses solely on the foundation of the dam.
2) The research addresses piping issues only within the dam foundation.

2 LITERATURE REVIEW

This section deals with the literature reviews focused on the basic background concepts, theories, assumptions, considerations, methods of analysis, and sound engineering practices that are applicable to controlling and monitoring internal erosion and piping on embankment dams.

2.1 History of Piping of Dams in the World

Piping in dams refers to the process where internal erosion occurs due to water seeping through the dam or its foundation, leading to the transportation of soil particles and potentially compromising the structural integrity of the dam. Understanding the history of piping in dams is crucial for developing effective engineering practices and preventive measures. This paper provides an overview of the significant historical developments and notable incidents related to piping in dams worldwide.

2.1.1 Early Recognition and Incidents

The awareness of piping as a critical issue in dam safety can be traced back to the early 20th century. One of the earliest documented cases of piping occurred in 1912 with the failure of the Austin Dam in Pennsylvania, USA. The dam collapsed due to internal erosion caused by water seeping through its foundation, leading to a catastrophic flood that claimed the lives of 78 people (Caldwell, 1989).

In Europe, the St. Francis Dam in California, which failed in 1928, is another notable case. Although the primary cause of the failure was a geological fault, piping was a contributing factor. The disaster resulted in 431 deaths and highlighted the need for better understanding and prevention of internal erosion in dam structures (Rogers, 1992).

2.1.2 Advances in the Mid-20th Century

The mid-20th century saw significant advancements in the understanding and prevention of piping in dams. Research efforts were directed towards understanding the mechanics of soil erosion and the conditions under which piping occurs. The development of modern soil mechanics by Karl

Terzaghi and others provided a theoretical framework for analyzing seepage and internal erosion in earthen dams (Terzaghi, 1936).

The 1950s and 1960s witnessed a series of dam failures that emphasized the importance of addressing piping. The Malpasset Dam in France, which failed in 1959, was one such case. The dam's failure, which resulted in over 400 deaths, was primarily attributed to piping through the foundation rock, exacerbated by high pore pressures (Vaughan, 1969)

2.1.3 Modern Understanding and Mitigations

In recent decades, significant progress has been made in the detection, monitoring, and mitigation of piping in dams. Advanced technologies such as geophysical methods, piezometers, and seepage monitoring systems have been developed to detect early signs of internal erosion (Fell et al., 2005).

The use of filters and drainage systems within dam structures has become a standard practice to prevent the initiation and progression of piping. Filters are designed to allow water to pass through while retaining soil particles, thereby mitigating the risk of internal erosion. The design criteria for filters were refined through extensive research and field studies, significantly reducing the incidence of piping-related failures (Sherard et al., 1984).

2.2 Internal Erosion and Piping

Before 2009, the term *piping* was broadly used to describe various internal erosion mechanisms. As the dam engineering field advanced, *piping* now specifically refers to a subset of internal erosion where an open tunnel or ‘pipe’ forms within the dam or its foundation.

According to ICOLD Bulletin 164 (2015), piping is a potential progression of internal erosion that begins with backward erosion along cracks or high-permeability zones and results in a continuous tunnel connecting the upstream and downstream sides of the embankment or foundation. Essential prerequisites for piping include a water flow path or source, an unprotected exit, and erodible material within the flow channel. Erosion progresses as particles are removed, creating a void that temporarily halts further erosion when it collapses. Failure occurs when this process continues, breaking the core or steepening the downstream slope to instability.

Foundations with highly porous strata comprising gravel, sand, or cavities are particularly susceptible, as significant seepage can degrade soil and promote pipe formation. High seepage rates accelerate soil erosion, increasing water and soil flow, which can lead to dam settlement and eventual failure.

2.2.1 Seepage through the Dam and Foundation

Seepage is the movement of water through soil, occurring when water levels differ across a structure like a dam or sheet pile. All embankment dams experience some seepage, but it becomes problematic only if it transports dam materials, leading to internal erosion.

Controlling seepage is vital to prevent foundation erosion. Precise estimation of seepage volume is crucial for economic and technical reasons. Water flow within the dam induces seepage forces, pore pressures, and hydraulic gradients. Excessive forces can cause slope instability or piping, risking dam failure.

Seepage may manifest anywhere on the downstream face, beyond the toe, or on the abutments, often initially as dense vegetation or moist spots. Indicators of seepage include marsh vegetation such as reeds or mosses, rust-colored bacteria deposits, and cone-shaped soil boils around outlets—signs that soil erosion is occurring.

Unchecked seepage transporting silt can severely weaken the foundation, leading to failure. It is especially important to monitor areas around spillways and conduits, where piping is most likely to develop.

In stratigraphic terms, the ash storage field primarily features fluvial and alluvial deposits, with layers of clay, sand, and gravel, though gravelly soils predominate.

2.3 Mechanism of Piping

Piping refers to the formation of an open channel that extends from one point to another, as defined by Lane (1934). When seepage forces act horizontally or vertically, they can mobilize soil particles along their path, potentially leading to the development of soil channels known as piping. Proper management and mitigation of seepage through foundations are essential to prevent piping and the loss of material. In the case of dams built on alluvial foundations, excessive seepage gradients from downstream can cause phenomena such as blowouts, boiling, or liquefaction, which may compromise slope stability and result in pipe failure. High hydraulic gradients and pre-existing foundation conditions can lead to piping failure, where water transports soil particles and shapes the foundation into pipe-like structures. Piping is a specific type of seepage failure characterized by reservoir water exerting a tractive force on soil particles, causing their removal at unprotected seepage exit points. According to a synthesis by Foster et al. (2000a) referencing data from ICOLD and other studies, approximately 46% of dam failures are attributable to piping. Piping erosion in earth dams can be classified into four categories based on the type of erosion involved: Concentrated Leak Erosion, Backward Erosion, Suffusion (internal instability), and Soil Contact Erosion (Bonelli 2013; ICOLD 2015; USACE and USBR 2015).

2.3.1 Concentrated Leak Erosion

Fell and Fry (2007) describe Concentrated Leak Erosion as the process where soil is eroded within a fracture or a network of interconnected voids in an earth dam or its foundation (see Figure 2.4).

2.3.2 Internal Instability (Suffusion)

According to Bonelli (2013), suffusion is the mechanism by which finer particles in broadly graded or gap-graded soil are transported away, leaving behind only the larger grains that maintain the soil's structure. In internally unstable soils, only the larger grains form the soil skeleton, while the finer particles move freely within the voids (see Figure 2.4).

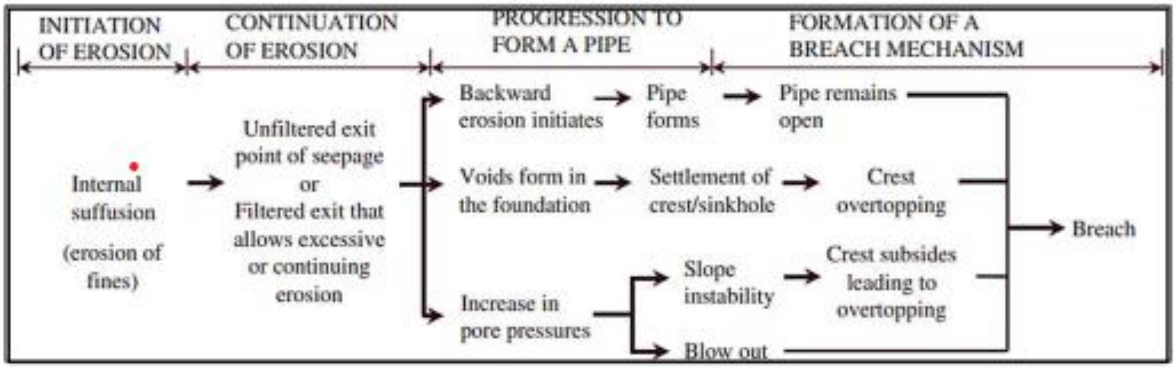

Figure 2. 1. Failure path diagram due to foundation-suffusion (Foster, 1999)

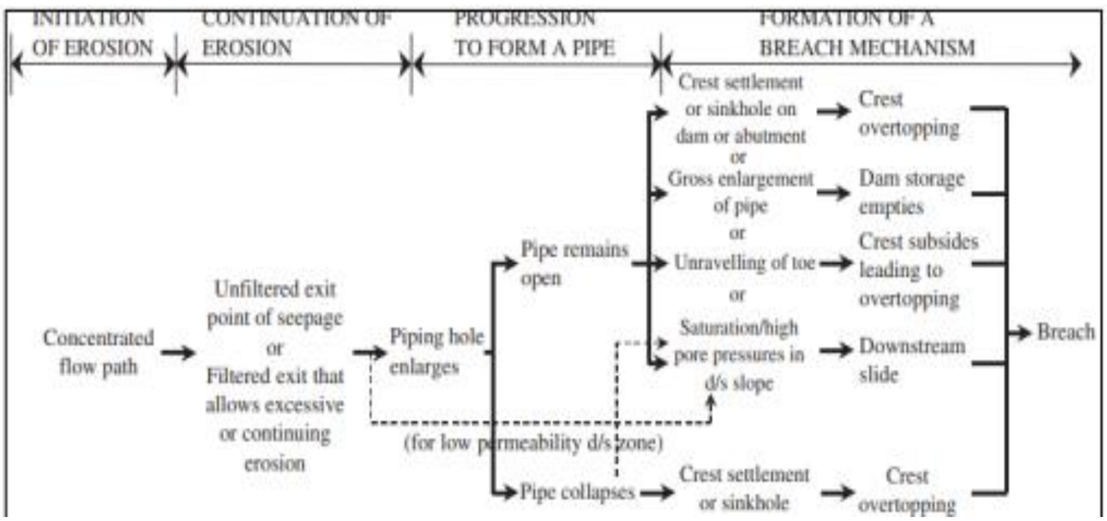

Figure 2. 2. Failure path diagram due to foundation-backward erosion (Foster, 1999)

2.3.3 Heave Piping Failure

Heave is a condition where a building's foundation enlarges upward, potentially destabilizing the structure. High gradient conditions can reduce the effective vertical stresses to zero, leading the soil to become fluid-like or form quicksand. The critical exit gradient, or heave equation, as proposed by Terzaghi (1943), is given by:

$$i_{cr} = \frac{\gamma_b}{\gamma_w} \qquad \text{Eq.2.1}$$

where γ_b = buoyant unit weight of the soil

γ_w = unit weight of water

The Terzaghi rule (1929) is a useful criterion for heaving control, with a safety factor of 3-4.

2.3.4 Backward-Erosion Piping (BEP)

Terzaghi described piping as the gradual removal of particles caused by backward erosion at concentrated leakage exit points (Terzaghi 1922, 1939, 1943). The onset of bio-piping (BEP) occurs when a "heave" or zero effective stress condition develops in sands, as noted by Terzaghi et al. in 1996. Hydraulic systems enable water to seep through the soil and exit vertically at the downstream end. This process results in the formation of a pipe-like channel beneath the dam, which moves upstream in the opposite direction, a phenomenon known as backward erosion piping. The process is triggered when the hydraulic gradient becomes sufficiently strong, reducing the flow path and accelerating particle removal. Backward erosion pipe failure happens when the hydraulic gradient exceeds the critical hydraulic gradient.

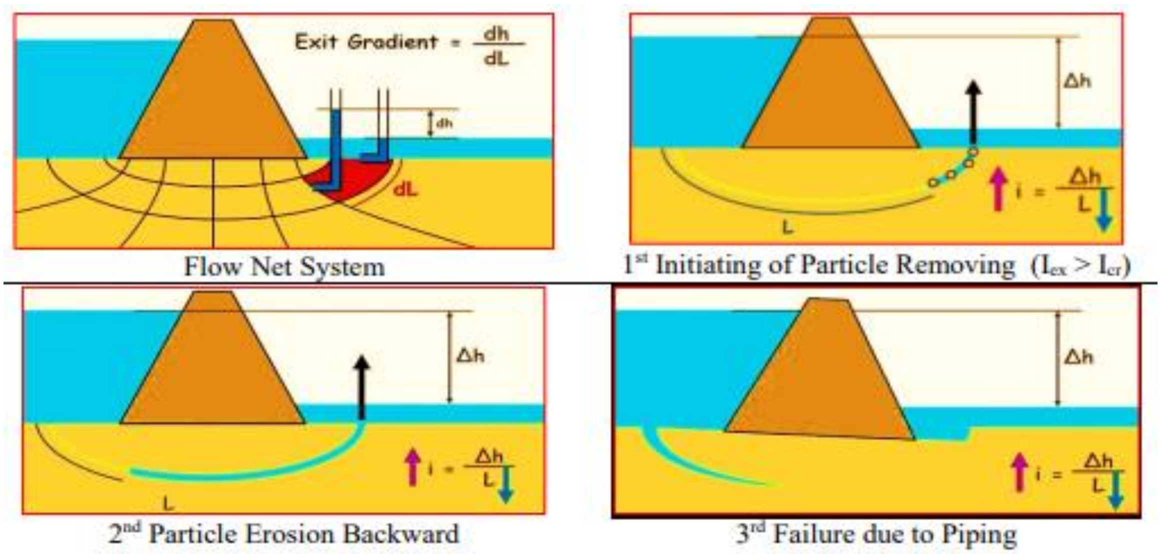

Figure 2. 3. Process of failure due to piping backward erosion

In the situation of a critical hydraulic gradient, the force of water and the particle's force are balanced, and the soil grain particles become buoyant. The line-of-creep approaches of Bligh (1910), Lane (1935), and Khosla's Theory are all techniques for determining the crucial gradient for a pipe's advancement.

2.4 Consequences of piping of the dam

Piping is a critical failure mechanism in dams that occurs when internal erosion creates continuous pathways for water flow through the dam structure. This process can lead to significant consequences, compromising the dam's integrity and potentially resulting in catastrophic failure. Understanding the theoretical aspects and consequences of piping is essential for dam safety and risk management. Piping in dams represents a significant threat to dam safety, necessitating a comprehensive understanding of its mechanisms and consequences. By applying rigorous monitoring, risk assessment, and management practices, engineers and dam safety professionals can mitigate the risks associated with piping, ensuring the continued safety and resilience of dam structures and the communities they serve. The consequences of piping in dams can be severe, impacting various aspects of dam safety and downstream communities:

2.4.1 Dam Failure

Piping is a precursor to dam failure in many instances. Once significant internal erosion occurs, the dam's ability to withstand hydraulic forces diminishes, increasing the risk of sudden collapse.

Dam failures can occur due to various factors, including design flaws, construction defects, inadequate maintenance, natural disasters, or unforeseen environmental conditions. Below are Below are the general overviews of the theories behind dam failures, and some notable embankment dam failures attributed to internal erosion, supported by references where applicable.

2.4.2 Notable Modern Incidents

Despite advancements in technology and engineering practices, piping remains a concern in dam safety. The Teton Dam failure in Idaho, USA, in 1976 is a stark reminder of the potential consequences of piping. The dam failed due to a combination of seepage and internal erosion, resulting in 11 deaths and significant economic losses (MacDonald & Langridge-Monopolis, 1984).

More recently, the Oroville Dam incident in California in 2017 highlighted the ongoing challenges in dam safety management. Although the primary issue was the failure of the spillway, concerns about internal erosion and piping were raised during the crisis, underscoring the need for continuous vigilance and maintenance (USSD, 2018).

Table 2.1 Typical notable embankment dam failures attributed to internal erosion,

No.	Dam Name / Year	Description
1	Malpasset Dam, France (1959)	Failed due to internal erosion of the sandy soil core, causing catastrophic downstream flooding and casualties.
2	Vajont Dam, Italy (1963)	Internal erosion triggered a landslide into the reservoir, producing a wave that overtopped the dam.
3	Teton Dam, USA (1976)	Foundation and embankment erosion led to sudden failure, with significant downstream damage.
4	Kelly Barnes Dam, USA (1977)	Erosion of the earth embankment core caused a sudden breach, resulting in fatalities.
5	Shakira Dam, Uzbekistan (1980)	Core erosion caused a breach, flooding downstream and damaging infrastructure.
6	Val di Stava Dam, Italy (1985)	Foundation erosion led to toxic tailings release, with fatalities and environmental impact.
7	Hengchun Dam, Taiwan (2009)	Core erosion caused a breach, inundating downstream areas with casualties.
8	Luis Eduardo Magalhães Dam, Brazil (2007)	Core erosion led to a breach, causing fatalities and regional destruction.
9	Miyagase Dam, Japan (2010)	Embankment breach due to erosion, damaging infrastructure and agriculture.
10	Xiaolangdi Dam, China (2020)	Embankment weakening during heavy rainfall caused a breach and localized flooding.
11	Melamchi Water Supply Project, Nepal (2020)	Spillway erosion caused a breach, disrupting the water supply and causing casualties.
12	Sardoba Reservoir Dam, Uzbekistan (2020)	Internal erosion and structural weaknesses resulted in a breach and downstream flooding.

2.5 Causes of Internal Erosion and Piping

Embankment dams, primarily constructed of soil and rock materials, are vulnerable to internal erosion, a process where water seeps through the dam's material, gradually eroding it and potentially leading to catastrophic failure if left unchecked. Piping, a specific form of internal erosion, involves the formation of concentrated seepage channels within the dam structure, which can compromise its integrity over time. Understanding the causes of piping and internal erosion is crucial for designing and maintaining safe embankment dams. Piping and internal erosion represent significant risks to the stability and safety of embankment dams. According to ICOLD (2019), "Internal Erosion of Dams and their Foundations. Bulletin 161. Paris and USSD (2018)", with a good understanding of the underlying causes, such as hydraulic gradients, soil properties, construction deficiencies, environmental factors, and the effectiveness of seepage control measures, engineers can design and maintain dams more effectively. Implementing rigorous monitoring and maintenance protocols based on these principles is essential for ensuring the long-term safety and functionality of embankment dams.

2.5.1 Hydraulic Gradient

The hydraulic gradient plays a fundamental role in initiating piping. When there is a significant difference in water pressure across the dam body, particularly if the upstream water pressure exceeds the downstream pressure, it creates favorable conditions for seepage. This pressure differential can force water through potential pathways such as voids or discontinuities in the dam material, initiating erosion and eventually forming pipes.

2.5.2 Soil Properties and Erodibility

The composition and characteristics of the dam materials greatly influence their susceptibility to piping. Fine-grained soils like silts and clays are more cohesive and less prone to erosion compared to coarser materials such as sands and gravels. However, even cohesive soils can erode if subjected to sustained seepage velocities or if disturbed during construction or maintenance activities.

2.5.3 Construction and Design Deficiencies

Poor construction practices, inadequate compaction of materials, or improper placement of filters and drainage features can create pathways for seepage within the dam. If filters designed to prevent soil erosion are not properly installed or fail over time, they can allow fine particles to be washed away, leading to internal erosion.

2.5.4 Seepage Control Measures

Effective seepage control measures are essential for mitigating internal erosion. Filters made of well-graded, stable materials placed at critical locations within the dam (such as upstream and downstream shells, core zones, and foundation interfaces) help to reduce seepage velocities and filter out fine particles that could initiate piping.

2.5.5 Environmental and Operational Factors

Environmental factors such as heavy rainfall, rapid drawdowns, or seismic events can increase water pressures and seepage velocities, accelerating the potential for piping. Similarly, changes in reservoir levels or operational procedures that alter the hydraulic conditions within the dam can influence the likelihood of internal erosion.

2.6 The Three Theories for Piping

2.6.1 Bligh's Creep Theory for Seepage Flow

According to this theory, water gradually moves along the bottom of the structure in a contour pattern. The length of the creep refers to the distance water travels along this contour. It is assumed that the head loss is proportional to the length of the creep. However, Bligh's limitation was that he did not differentiate between the lengths of creep that were oriented horizontally versus vertically. Bligh stated that ensuring safety against piping could be achieved by providing a sufficient creep length, represented by

$$L = C.H, \qquad \text{Eq.2.2}$$

Where C is the soil's Bligh's coefficient.

2.6.2 Lane's Weighted Creep Theory

The empirical "Weighted-Creep" hypothesis was formulated by Professor E. W. Lane after analyzing dam designs from around the world, encompassing 200 dams. According to this hypothesis, the flow path along a dam's base and its vertical contact forms a line of flow, with vertical contact being more influential than horizontal contact. For horizontal creep, the theory suggested assigning a weight factor of 1/3, whereas vertical creep was given a weight factor of 1.0. Although the flow pathways are considered differently, Lane's empirical relationship is comparable to Bligh's.

The empirical calculation procedure developed by Lane's equation, known as the weighted creep method, is shown below:

$$\mathbf{Ln = cH} \text{ and } c = Ln/H \qquad \text{Eq.2.3}$$

Where Ln = minimum safe flow length

c = safe weighted creep ratio

H = hydrostatic head across the structure

It is noted that the hydraulic gradient, H/L, becomes equal to 1/C as a result.

2.6.3 Khosla's Theory and Concept of Flow Nets

The main principle of this theory is that seepage water moves along a series of streamlines, rather than following the bottom contour as Bligh initially suggested. In the case of homogeneous soil, this theory employs the Laplacian equation to describe steady seepage conditions. The theory represents two families of curves, streamlines and equipotential lines that intersect at right angles, as described by the following equation. The resulting diagram, which illustrates both sets of curves, is known as a Flow Net.

This theory's central tenet is that seepage water flows through a series of streamlines rather than following the bottom contour as Bligh had originally proposed. For homogeneous soil, the Laplacian equation has been used for this theory under the condition of steady seepage. The streamline and the equipotential line, two sets of curves that meet one another orthogonally, are represented by the following equation. A Flow Net is the name for the resulting flow diagram that displays both curves as shown in Figure 2.7.

$$\frac{d^2\phi}{dx^2} + \frac{d^2\phi}{dz^2} \qquad \text{Eq.2.5}$$

where ϕ = flow potential = Kh,

K = coefficient of permeability of soil as defined by Darcy's law

h = the residual head at any point with the soil

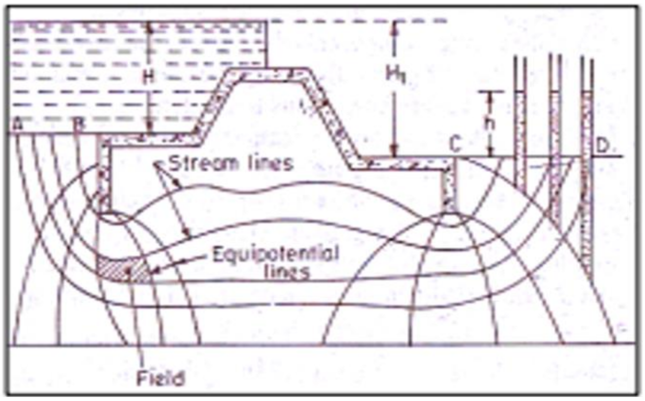

Figure 2. 4. Khosla's flow net

Khosla's exit gradient, G_E, is computed by the following formula:

$$G_E = \frac{H}{d} * \frac{1}{\pi\sqrt{\lambda}} \qquad \text{Eq.2.5}$$

where b = floor length

d = vertical cut-off of depth

H = maximum seepage head

$$\lambda = \frac{1+\sqrt{1+a^2}}{2}$$

a = b/d

2.6.4 Exit and Critical Gradient

A tangential force f is generated by water seeping through the subsoil and is always tangential to the streamline. The weight of the soil particle submerged in the fluid causes the streamlines to bend upward, producing a tangential force f that has a downward force w and a vertical component f1 as well. The submerged weight needs to be heavier than the upward vertical component of f1 to prevent soil particle dislodgement, guarantee soil stability, and avoid erosion and piping. The water pressure gradient dp/dl determines the force of the vertical component that points upward. The force f1 equals the weight of the soil particle immersed, suggesting a critical gradient if the exit gradient is critical.

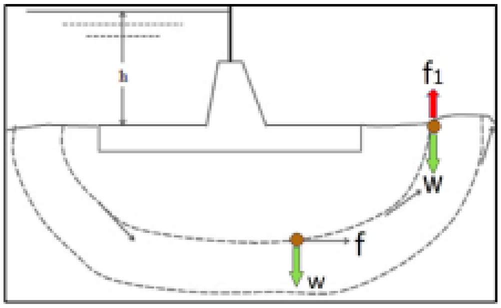

Where;
f_1 is the upward disturbing force on the grain,
w = Submerged Weight,
f = Pressure gradient at a point,
Gs = Specific Gravity,
n = Porosity,
γ_w = unit weight of water
$dp/dl = \gamma_w * dh/dl$, $dh/dl = (G_s - 1)(1-n)$

Figure 2. 5 Exit and critical gradient

In the equations below, according to EM 1110-2-190, icr will be approximately 1 if normal sand Gs, e, and n values are utilized. According to their research, the ranges for the escape gradient's factor of safety range from 1.5 to 15, depending on the soil's properties and any potential seepage situations.

$$\boxed{i_{cr} = (G_s - 1)(1 - n)} \quad \text{......Equation 1}$$

$$\boxed{n = \frac{e}{1+e}} \quad \text{......Equation 2}$$

$$\boxed{i_{cr} = \frac{G_s - 1}{1+e}} \quad \text{......Equation 3}$$

$$\boxed{I_e = (h_1 - h_2)/L} \quad \text{......Equation 4}$$

$$\boxed{FS = \frac{i_{cr}}{i_e}} \quad \text{Equation 5}$$

Where;

Gs = Specific Gravity
e = Void Ratio
n = Porosity
FS = Factor of Safety
I_e = Exit Gradient
h_1 = U/S hydraulic head
h_2 = D/S hydraulic head
L = Length flow path

Eq.2.6

2.7 Techniques for Foundation Piping Control

According to Arora K.R. (2004), the hydraulic gradient (i) is impacted by the percolation route (L). The exit gradient will decrease to a safe level as the path's length is increased. The following tactics might prolong the percolation process. The Exit Gradient decreases as the flow length increases.

2.7.1 Increasing The Dam's Base Width

The percolation length is extended by lengthening the base of the dam (Figure 2.1) to the extent required by the design in order to protect pipelines. The option of extending the flow channel exists, but the increased volume of embankment dam fill material makes the project unfeasible.

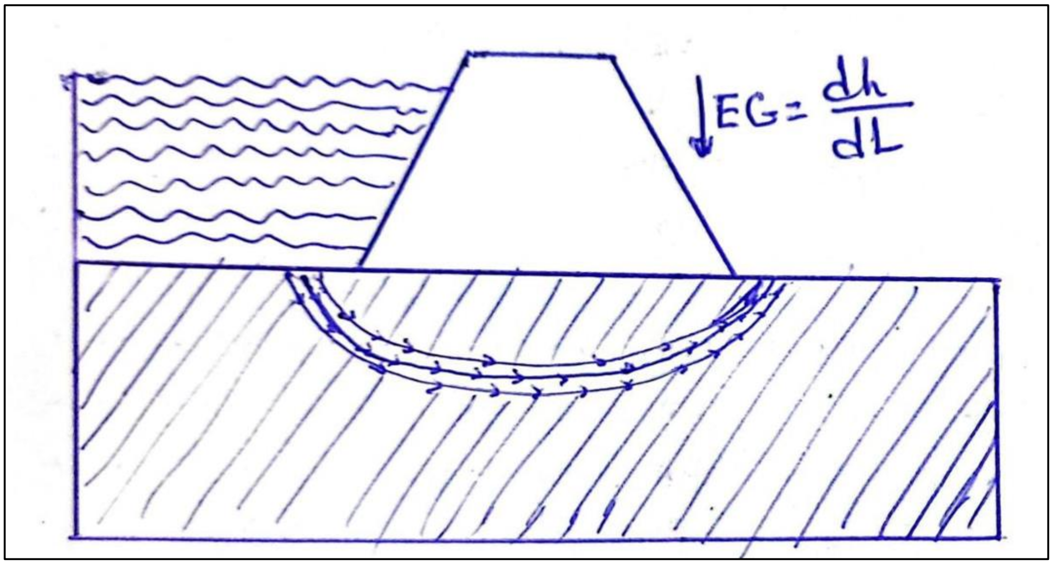

Figure 2. 6 Techniques to extend the flow path by enlarging the dam's base width

2.7.2 Cutoffs

There are two types of Cutoff Control methods. The first one is Complete Cutoff (compacted backfill trench, slurry trench, or concrete wall, see Figure 2.2), and the other is Partial Cutoff (U/S impervious blanket, D/S seepage berm, toe trench drain, or relief walls). It may be recommended when the dam foundation is made of a relatively thick deposit of previous alluvium.

According to Sherard (1968), the following factors should be taken into account when choosing the sort of under-seepage control measures:

1) A cost-benefit analysis of the potential loss of water versus the price of the complete cutoff
2) A complete cutoff is preferable to the foundation, which has layers of fine sand or cohesionless silt, especially if these soils are exposed on the surface of the valley floor when compared with the foundation, which is mostly made of gravel or coarse sand. In fine cohesionless soils, even a small concentrated leak that emerges below the dam might be harmful; however, if a substantial leak occurs in coarse alluvium, backward erosion is probably protected.
3) When the amount of silt and clay-sized particles suspended in river water increases over time, a reservoir tends to silt up and seepage capacity tends to decrease gradually.

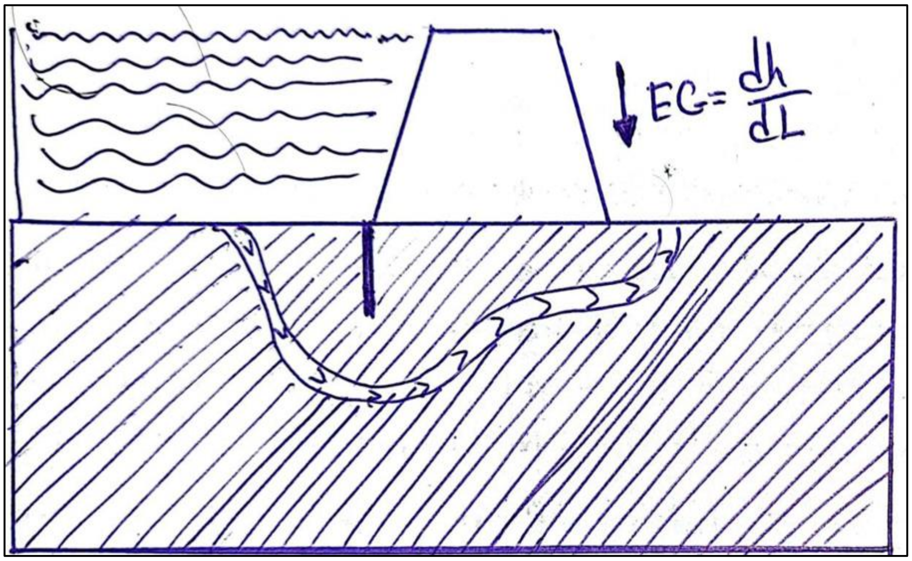

Figure 2. 7 Techniques of the cutoff option

2.7.3 Compacted Backfill Trench

The most efficient method for controlling under-seepage is to excavate a trench through the existing foundation layers and then backfill it with compacted, impermeable material.

2.7.4 Upstream Blanket fill

The upstream (U/S) blanket fill is an impervious layer placed on the dam's upstream side to prevent seepage erosion and piping. Made of low-permeability materials like clay, it increases the flow path, stabilizes the foundation, and reduces the risk of internal erosion. Proper placement and compaction are crucial for its effectiveness.

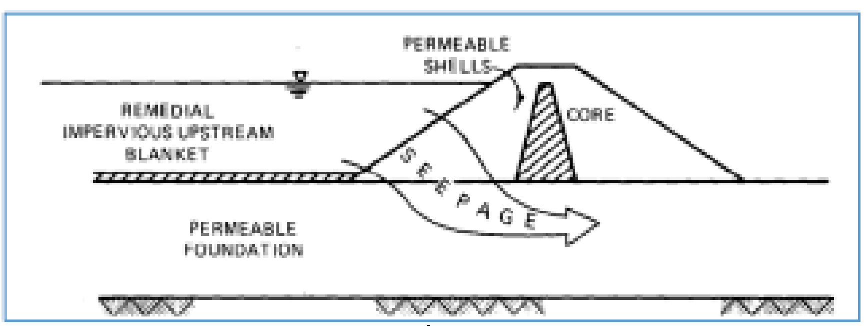

Figure 2. 8 Remedial impervious u/s blanket (prepared by WES, EM 1110-2-1901, Page 12-5)

2.7.5 Slurry Trench Cutoff

A slurry trench cutoff is an effective and practical method for preventing underground seepage when constructing traditional compacted barriers is too costly or difficult, especially in deep or high-dewatering situations. It involves excavating a continuous trench supported by a water-bentonite slurry, then backfilling it with soil containing fines to create a semi-impermeable barrier. Variations include adding cement to produce a stronger, grout-like wall. These cutoffs are typically 1-3 meters wide and can reach depths up to 25 meters, depending on excavation methods. Historically used since 1945, they are common in the US for seepage control, with soil-bentonite walls favored for their flexibility and cost-effectiveness when groundwater is below ground level. Their effectiveness depends on proper design, especially the depth of penetration into the foundation and the interaction with the core, foundation, and groundwater conditions. Laboratory testing of soil-bentonite mixtures helps optimize properties like strength and permeability, sometimes requiring additives. Overall, slurry trench cutoffs are a widely adopted, adaptable, and cost-effective technique for controlling seepage in earth dams and levees.

2.8 Effects of Clay Blanket

Embankment dams are constructed on alluvial layers with high permeability, and therefore controlling the seepage at the foundation of the dam and calculating the discharge of water are very important. If the seepage at the foundation of embankment dams is not controlled, besides wasting the water, in the long term use, piping might occur at the foundation, causing irreversible damage to the dam. Therefore, controlling the seepage is necessary to restrict the amount of seepage, maintain the stability of the downstream backfill and prevent the corrosion of small particles underneath the foundation.

In order to control and prevent the seepage at the foundation of embankment dams, several techniques can be employed. Construction of a clay trench, impermeable upstream blanket, injection curtain, and concrete diagrams are among these methods, any of which have their own practical and technical limitations. For instance, the maximum depth of excavation for a clay trench is 20m (Fell et al. 2000). Therefore, if the foundation is too deep, a clay trench with a maximum depth of 20m cannot control the seepage very well. Considering the practical limitations and condition of foundation, using any of the sealing systems or a combination of them can be right approach for controlling the seepage in the foundation of embankment dams.

Seepage analysis is one of the most substantial stages in the design process of an embankment dam. In recent years, various research methods have been applied to the study of the seepage problem in dams and levees. In order to calculate the amount of seepage passing through the foundation of embankment dams, a limited number of studies have been carried out by various researchers.

2.9 Methods to compute internal erosion and piping

Piping and internal erosion pose significant risks to the safety and stability of embankment dams. Detecting and assessing these potential failures requires rigorous methods and approaches that combine field observations, laboratory testing, and computational modeling. This discussion explores various methods used to compute and predict piping and internal erosion in embankment dams, supported by relevant references (ICOLD, 2019). Effective computation and prediction of piping and internal erosion in embankment dams require a multidisciplinary approach that integrates field investigations, laboratory testing, and advanced computational modeling techniques. By combining these methods, engineers and dam safety professionals can enhance their understanding of potential failure mechanisms and implement proactive measures to mitigate risks and ensure the long-term safety and stability of embankment dams (USSD, 2018).

2.9.1 Field Investigations and Observations

Field investigations are essential for understanding the conditions within and around the dam that could lead to piping and internal erosion. Key aspects of field assessments include:

Piezometric Data: Monitoring water pressures and levels within and around the dam provides insights into potential hydraulic gradients that could drive seepage and erosion processes.

Seepage Monitoring: Observing seepage patterns and rates can indicate locations where erosion may be occurring or where seepage control measures are inadequate.

Geomorphological Surveys: Assessing the topography and geology of the dam foundation and abutments helps in identifying potential pathways for seepage and erosion.

Instrumentation: Installing instrumentation such as piezometers, seepage meters, and settlement gauges allows for continuous monitoring of dam behavior and performance over time.

2.9.2 Laboratory Testing

Laboratory tests are conducted to assess the erodibility of dam materials and the effectiveness of erosion control measures. These tests include:

Erosion Potential Tests: Determining the soil's susceptibility to erosion through tests such as the Jet Erosion Test (JET) or the Erosion Function Apparatus (EFA).

Permeability Tests: Measuring the hydraulic conductivity of soils to understand how water flows through different materials and their potential for piping.

Filter Compatibility Tests: Evaluating the compatibility and effectiveness of filter materials in preventing fine particles from being washed away during seepage events.

2.9.3 Numerical Methods for Modeling Piping in Dam Foundations

Computational modeling plays a crucial role in predicting and assessing the likelihood of piping and internal erosion in embankment dams. Various approaches include: **Seepage Analysis:** Using numerical methods such as finite element analysis (FEA) or finite difference methods (FDM) to simulate groundwater flow and seepage patterns within the dam.

Modeling piping in dam foundations involves simulating the process where water seepage through the foundation material erodes soil particles, potentially leading to the failure of the dam. Numerical software and analysis methods play a crucial role in predicting and mitigating this phenomenon. This theory explores the various numerical tools and methodologies used for modeling piping in dam foundations, with references to established practices and software applications. Piping in dam foundations is a critical issue that can compromise the structural integrity of dams. Numerical modeling helps engineers to understand the underlying mechanisms and to design effective mitigation measures. This paper discusses key numerical software and methods used in this field, highlighting their applications, advantages, and limitations. Numerical software and analysis methods are essential for understanding and mitigating the risks of piping in dam foundations. Tools like GeoStudio, FLAC, and PLAXIS provide robust platforms for simulating seepage, erosion, and stability, enabling engineers to make informed decisions. Continued advancements in numerical modeling will further enhance the ability to predict and prevent piping failures in dam foundations (Chowdhury, R., Sarker, A., 2014).

Several numerical software packages are commonly used for simulating piping in dam foundations. These include, but are not limited to: GeoStudio (SEEP/W and SLOPE/W), FLAC (Fast Lagrangian Analysis of Continua), and PLAXIS.

i. GeoStudio: SEEP/W and SLOPE/W

GeoStudio, developed by Geo-Slope International, offers a suite of tools for geotechnical modeling. SEEP/W is used for analyzing groundwater seepage and pore-water pressure distribution, which are critical for understanding the potential for piping. SLOPE/W can be integrated to evaluate the stability of slopes and embankments under varying seepage conditions (GeoStudio 2022).

ii. FLAC (Fast Lagrangian Analysis of Continua)

FLAC, developed by Itasca Consulting Group, is a numerical modeling software for geotechnical engineering problems. It employs finite difference methods to simulate the behavior of soil and rock, making it suitable for complex piping analyses (Itasca C. Group, Inc. 2019

iii. PLAXIS

PLAXIS, a product of Bentley Systems, is a finite element software specifically designed for the analysis of deformation and stability in geotechnical engineering. It is widely used for simulating seepage and piping phenomena in dam foundations (Bentley Systems, Inc. 2020).

Numerical methods for analyzing piping in dam foundations typically involve the following steps:

2.9.4 Seepage Analysis

The first step is to perform a seepage analysis to determine the flow of water through the dam foundation. This involves solving the governing equations of fluid flow, such as Darcy's law, using numerical methods like finite element or finite difference.

With GeoStudio SEEP/W, seepage analysis involves creating a finite element mesh of the dam foundation and assigning hydraulic properties to different materials. Boundary conditions are set to simulate water levels, and the software calculates the pore-water pressure distribution.

The final step is to evaluate the stability of the dam foundation under the predicted piping conditions. This includes analyzing the potential for slope failure or overall structural collapse.

SLOPE/W can be used in conjunction with SEEP/W to perform stability analysis, considering the pore-water pressures calculated from the seepage analysis.

2.9.5 Case Studies

To illustrate the application of these numerical tools and methods, several case studies can be referenced:

Case Study 1: Karnafuli Dam, Bangladesh: This study utilized GeoStudio (SEEP/W and SLOPE/W) to model seepage and piping risks in the dam foundation, helping engineers to design appropriate remedial measures.

Case Study 2: Wolf Creek Dam, USA: This study employed FLAC to simulate seepage and potential piping in the dam's karstic foundation, providing insights into the complex interactions between water flow and soil erosion.

3 METHODOLOGY

3.1 General

This chapter outlines the systematic approaches and methodologies adopted to evaluate the gravelly clay blanket foundation treatment and remedial measures for the Kalid Dijo Dam. The methodology comprises an overview of the research methods and materials; integration of data collection, review and processing; establishing input data/evaluation parameters; developing numerical modeling using GeoStudio 2022 software; and analysis methods/guidelines adopted for the study.

The overall goal is to assess the effectiveness of foundation treatments in controlling seepage, preventing piping, and ensuring the stability of the dam's foundation.

3.2 Research Approach and Framework

The research adopts a multidisciplinary approach combining geotechnical, geological, geophysical, and numerical analysis methods. The approach begins with an extensive review of existing data, followed by targeted field investigations to fill data gaps and validate prior findings.

Laboratory tests provide critical parameters needed for precise modeling.

Numerical simulation using GeoStudio 2022 allows for a detailed assessment of seepage behavior, slope stability under static and seismic conditions, and the performance of different foundation treatment scenarios.

The overall research process on "Evaluation of Gravelly Clay Blanket Foundation Treatment and Remedial Measures for Piping Control in Embankment Dam: A Case Study of Kalid Dijo Dam " followed the research activities described in Table 3.1 below.

Table 3. 1. The research methodology's activities

<table>
<tr><th>No.</th><th>Stages</th><th>Used data/tools</th><th colspan="2">Descriptions of the purpose of used data/tools used</th></tr>
<tr><td rowspan="3">1</td><td rowspan="3">Desk Study</td><td rowspan="3">Secondary Data</td><td>Geological Investigations</td><td rowspan="3">For the analysis of identified problem</td></tr>
<tr><td>Geotechnical Investigations</td></tr>
<tr><td>Hydrological Investigations</td></tr>
<tr><td>2</td><td>Problem Identification</td><td>Piping</td><td colspan="2">The susceptible problems of the dam's foundation</td></tr>
<tr><td rowspan="2">4</td><td rowspan="2">Data Identification</td><td>In-situ test</td><td colspan="2" rowspan="2">Data compilation and integration for analyzing the problem, such as SPT test, Permeability, Specific Gravity, Unit Weight, borehole log, Shear Strength(c' and Ø), and other standards.</td></tr>
<tr><td>Laboratory test</td></tr>
<tr><td rowspan="3">`5</td><td rowspan="3">Selection of methodology or software</td><td>GeoStudio/ 2022</td><td colspan="2">An all-inclusive tool for modeling soil structures and performing geological engineering tasks is GEOSLOPE Geo-Studio 2022. A series of CAD-integrated software tools is provided, combining many analyses performed with various products into a single package. It makes use of Finite Element Analysis and includes 8 models, including Seep/W and Quake/W. SEEP/W to analyze seepage and piping. QUAK/W to analyze Liquefaction.
The limitations are discussed as follows;
Geo-Studio represents soil and rock behavior using simplified material models. These models may not fully convey the complexity of real-world materials, even though they can offer accurate approximations. Certain hardware combinations or operating systems may not be compatible with Geo-Studio. Users may experience issues with the software's installation or operation on their particular PCs. It is also sensitive to antivirus software.</td></tr>
<tr><td>Auto CAD 2022</td><td colspan="2">To prepare the geometry for importing into Geo-Studio</td></tr>
<tr><td>MS Excel,2013</td><td colspan="2">It is going to be used to analyze some output data, like safety factors.</td></tr>
</table>

No.	Stages	Used data/tools	Descriptions of the purpose of used data/tools used
6	**Data analysis**	Using software	To find out the actual problem and provide results for interpretation
7	**Interpretation**	Standards	To set remedial measures and recommendations

3.3 Data Collection and Processing

In this study, a detailed and systematic method was used to collect, review, and synthesize data. Information was carefully obtained from secondary sources to ensure the necessary breadth and depth to fulfill the research objectives. Geological, geotechnical, and hydrological data pertaining to the Kalid Dijo Dam Project were collected from the office of the former Ethiopian Construction Design & Supervision Works Corporation (EEC), now called Ethiopian Engineering Corporation (EEC), thoroughly examined and incorporated into the analysis..

3.3.1 Secondary Data Collection

(a) Relevant Data Collected for the Study

The secondary data collection for the Kalid Dijo Dam involved gathering and analyzing relevant information from the design consultant (EEC, 2019), including geometric data, geophysical surveys, geotechnical investigations, and engineering geological reports. These sources provided valuable insights into the subsurface geological conditions along the planned Kalid Dijo Dam foundation. Laboratory test results, conducted on soil and rock samples, were also utilized to supplement the secondary data. The specific gravity, grain size analysis, Atterberg limits, direct shear, unconfined compressive strength, bulk unit weight, moisture content, point load, and pinhole tests were performed on soil samples. Test results on rock samples for specific gravity, unit weight, water absorption, and uniaxial compressive strength were also utilized in this study.

All laboratory tests were conducted at the EEC's laboratory facilities on samples collected during fieldwork. The laboratory test findings were used to create the dam's final design report together with the foundation boreholes (EEC, 2019). The types of laboratory tests conducted on soil samples include Specific gravity, Grain Size Analysis, Atterberg Limit, Direct Shear, UCS, Bulk Unit Weight, NMC, Free Swell, Water Absorption, Point Load, Pinhole, Organic Content, Sulfate, and

Chloride. Similarly, rock samples are tested for specific gravity, unit weight, water absorption, and uniaxial compressive strength.

(b) Integration of Engineering Secondary Data

The integration of engineering secondary data involves collecting and applying existing geological, geotechnical, and hydrological information to support dam foundation design. This approach improves analysis accuracy, validates assumptions, and aligns with industry standards, while saving time and resources by reducing redundant investigations. Overall, it helps develop reliable, evidence-based solutions and enhances project confidence.

The respective studies, analyses, and results concerning engineering geological, geotechnical, and hydrological conditions have been integrated to meet the objective of the present study.

3.3.2 Geometric Data

The geometric data, as collected from EEC (2019), comprises the site layouts, engineering plans, and drawings for the Kalid Dijo Dam.

3.3.3 Geological / Geotechnical Data

3.3.3.1. Regional and Local Geology

(a) Regional Geology:

As per the EEC study (2019), the project area lies on the western escarpment of the Main Ethiopian Rift (MER), particularly in its central segment. Thus, the regional geological setup of the MER and, particularly, the Central Main Ethiopian Rift is worthy of explaining the regional geology of the project site.

The regional geology of the study area is composed of: Pre-Tertiary sediments and crystalline basement; Oligocene(32-29 Ma) & lower Miocene(12-8) plateau volcanics; Miocene-Pliocene rift-shoulder trachytic-rhyolitic volcanics & pyroclastic layers; Plio-Pleistocene rift floor; Quaternary central volcanics & basaltic lava flows, associated scoria cones and phreato-magmatic deposits; and Quaternary lacustrine sediments & interbedded pyroclastics.

(b) Local Geology:

As per the EEC study (2019), field mapping at the dam project site/reservoir and surrounding areas at a scale of 1:10000 outlined major stratigraphic successions of Ignimbrite flow units and unconsolidated pyroclastic deposits (Tuff and Volcanic ash). Three types of lithologic units: Ignimbrite, Tuff and Volcanic Ash are outlined during the geological/geotechnical investigations at the captioned scale and their details are briefly presented below:

(a) Ignimbrite (Qi)

Brief descriptions of the geological features of the Ignimbrite flow layers in the Kalid Dijo Dam project area are as follows:

Location and Topography:

- The ignimbrite flow layers are mainly found in the central west and northwestern parts of the project area.
- These areas tend to have flat to gently sloping terrain.

Relationship with Other Layers:

- The ignimbrite flows are usually overlain by thick sequences of volcanic ash, indicating they are older layers beneath the ash deposits.

Stratigraphy and Thickness:

- Stratigraphically, the ignimbrite units are the oldest in this region.
- They form relatively thick, up to one meter, layered sheets of hardened volcanic rock.
- These layers are sub-horizontal, meaning they are mostly flat and level.

Physical Characteristics:

- About 10-15% of these ignimbrite layers are irregularly shaped and poorly sorted.
- They are of various compositions, but compositionally, these rocks are felsic (rich in silica, lighter-colored volcanic rocks).

In summary:

- The oldest volcanic layers, called ignimbrite flows, are found mainly in the central west and northwest areas near the dams.

- They form relatively thick, flat sheets of hardened volcanic rock, often covered by thick volcanic ash layers.
- These rocks are felsic, irregularly shaped, and make up a small portion of the volcanic deposits in the area.

This information helps in understanding the geological foundation and stability considerations for the dam sites.

a) Columbary jointed Ignimbrite flow layers.

b) Angular lithic fragments in light grey crushed volcanic ash.

c) Alternating layers of trachytic and obsidian volcanic flows.

Figure 3. 1 Volcanic Flow Unit Outcrop Nature

(b) Tuff (Qt)

Brief descriptions of the geological features of the Pyroclastic Deposits near Kalid and Dijo dams are as follows:

Main Deposits:

The river beds and banks of the Dijo and Kalid rivers, along with their tributaries, are mainly covered by:

- Unconsolidated to relatively consolidated massive volcanic pyroclastic deposits (deposits from explosive volcanic eruptions).
- These deposits are often overlain by loose volcanic ashes that are unconsolidated.

Cracks and Erosional Features:

- In many areas, the unconsolidated volcanic deposits have developed wide cracks ranging from 9.4 to 10 meters in width, and relatively deep cracks up to 20 meters.
- Over time, erosion has widened these cracks into large gullies.
- Importantly, these cracks are mostly found in the upper unconsolidated tuff layer and do not extend into the more solid, consolidated tuff or other stronger rocks beneath.
- This suggests that the cracks are likely caused by dewatering (loss of water from soft, loose material) rather than tectonic (fault-related) activity.

Erosional Surfaces:

- The area also shows irregular, networked erosional surfaces caused by selective dissolution (chemical weathering where parts of the material dissolve away).

Jointing and Fractures:

- The deposits are cut by two sets of systematic, penetrative, and tight sub-vertical joints.
- The joint sets run parallel to the rift system and transverse (perpendicular) to it.
- These joints influence the stability and erosion patterns of the volcanic deposits.

In summary:

- The river beds near Kalid and Dijo are mainly covered by loose, volcanic pyroclastic deposits, with some more solid, consolidated layers underneath.

- Wide cracks and gullies in the loose deposits are mostly due to water removal, not tectonic movement.
- The area shows signs of chemical erosion and is fractured by systematic joint patterns, affecting its geological stability.

This understanding helps in assessing the stability and potential erosion risks around the dams and river areas.

a) Relatively consolidated tuffaceous deposit, lithic fragments within crushed light yellow groundmass (volcanic ash),

b) Close view picture of the top left picture

c) Relatively welded tuff with coarse lithic fragments of compositionally varying rocks,

d) Voluminous unconsolidated tuff deposit, 20-30% lithic fragments, some coarse obsidian nodules.

Figure 3. 2 Outcrop nature of tuffaceous pyroclastic deposits (c) Volcanic Ash (Qva)

The geological features of the volcanic ash deposits in the area near Kalid and Dijo dams are briefly described below:

Main Deposits:

Most of the area is covered by thick volcanic ash deposits. These deposits are often hidden beneath thick topsoil or have been eroded laterally, exposing the underlying ash.

Eroded Ash Hills:

- Upstream of the dam reservoirs, especially near the Kalid and Dijo rivers, eroded volcanic ash hills are common.
- Some of these hills are capped with horizontally layered sandy tuff deposits or thick black cotton soil.

Variation in Ash Outcrops:

- Thin Ash Layers:
  - In some places, especially along the dam axis on the Kalid River, volcanic ash appears as thin, layered deposits up to 6 meters thick.
  - These thin layers are usually covered by sandy tuffs, indicating they are farther from the volcanic vent.
- Thick Ash Deposits:
  - Near the Dijo River reservoir, large amounts of ash have fallen, creating small, eroded hills.
  - These hills are often found beneath ignimbrite layers (a type of volcanic deposit), suggesting they are closer to the volcanic vent.

In summary:

- The area contains both thin, distant ash layers and thick, nearby ash deposits.
- The thin ash layers, especially at the Kalid River dam site, suggest a location farther from the volcano.
- The thicker ash deposits near the Dijo River indicate proximity to the volcanic source.
- Eroded ash hills, sometimes capped with sandy tuffs or black soil, are common features upstream of the dams.

This understanding helps in assessing volcanic hazards and geological conditions around the Kalid and Dijo dams.

a) Distinct ash layers as a result of separate ash fall events, 410917/866172 UTM location

b) Eroded ash hills

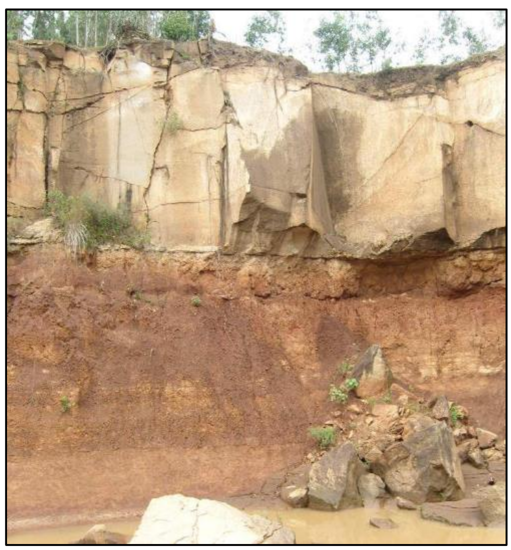

c) Water-lain loose sandy tuff (top light colored layer) overlaying thick stratified volcanic ash deposit (bottom brownish layer)

Figure 3. 3 Outcrop nature of volcanic ash falls

(d) Quaternary Superficial Deposits

River Channel Deposits (Q1): River channel deposit comprising sandy to cobble-sized rock fragments of various compositions covers a few parts of the Dijo and Kalid river channels. Major parts of the river channel are outcropped by tuff and ignimbrites.

Flood Plain Deposits (Q2): Flood plain deposits of sand-silt size fraction sediments are mapped, forming flat plains in some parts of the dam site/reservoir option areas, following banks of Dijo and Kalid Rivers.

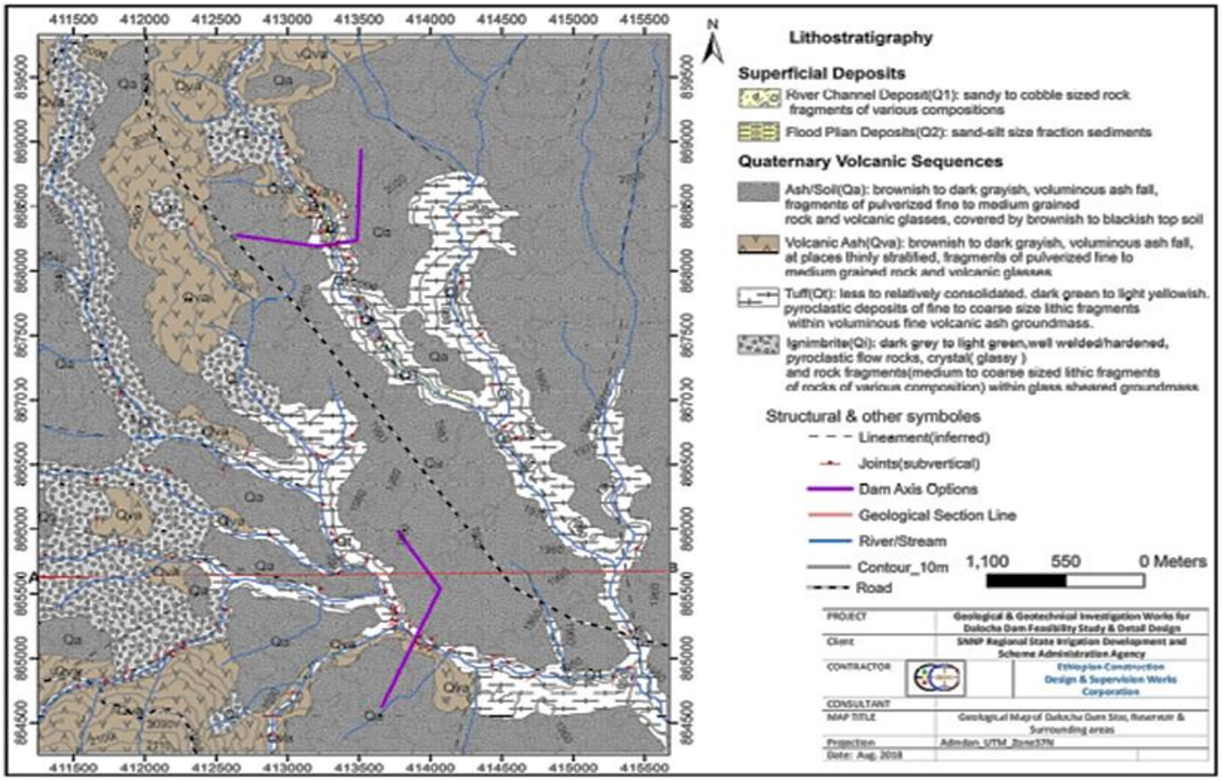

Figure 3. 4 Geological map of Kalid Dijo dam site and its surroundings (EEC, 2019)

Field mapping at the dam option project site/reservoir and surrounding areas at a scale of 1:10,000 identified major stratigraphic successions of Ignimbrite flow units and unconsolidated pyroclastic deposits (Tuff and Volcanic ash).

Exposures of Ignimbrite flow layers were mapped at the central west and northwestern part of the project area, forming flat to gently sloping topography, commonly overlain by thick volcanic ash sequences.

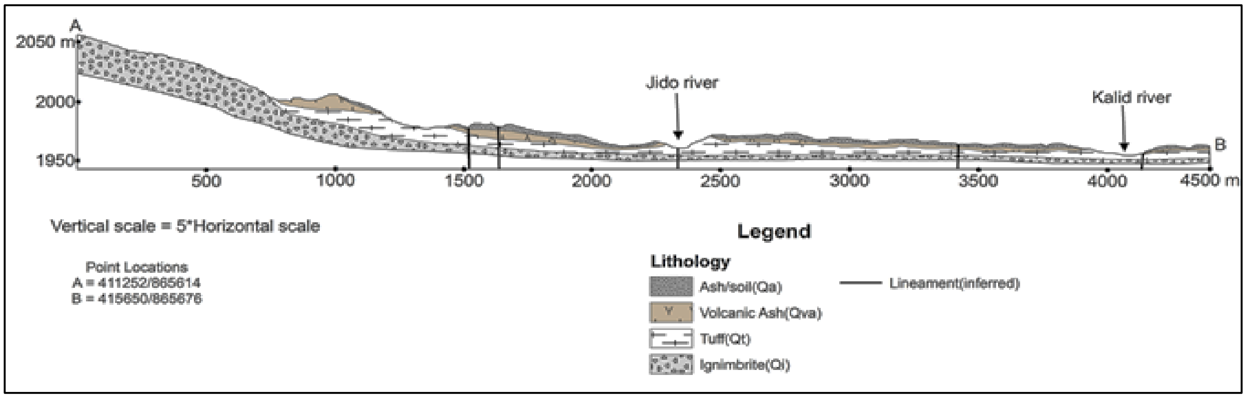

Figure 3. 5 Geological cross-section map along profile Ab (EEC, 2019)

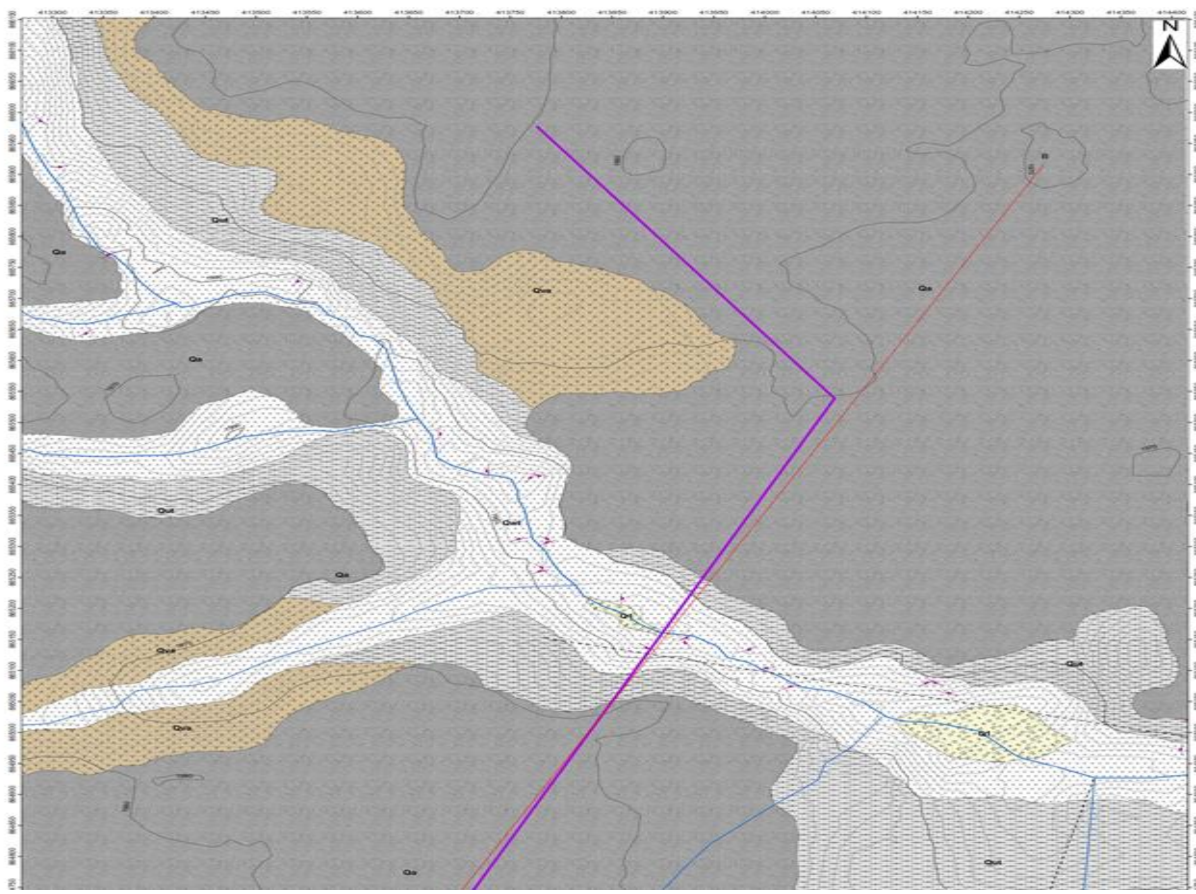

Figure 3. 6 Geological map of Dijo Dam site area (EEC, 2019)

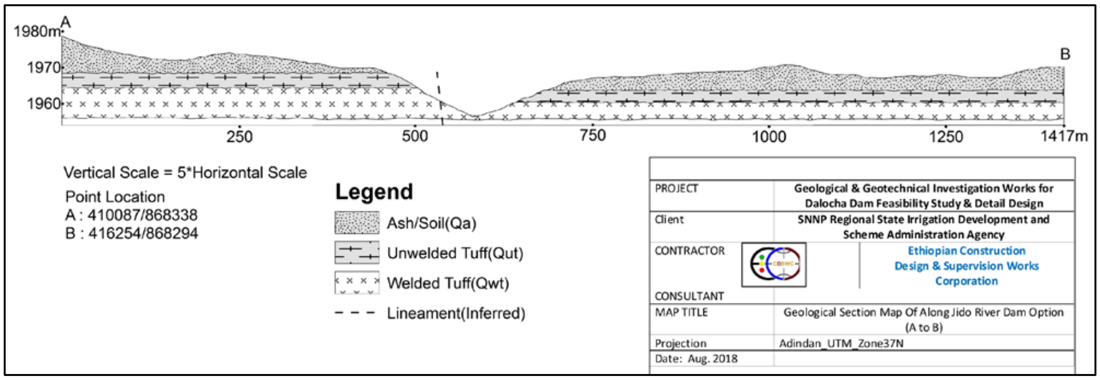

Figure 3. 7 Geological cross-section map along profile Ab (Dijo Dam axis) (EEC, 2019)

3.3.3.2.Geotechnical Engineering Data

As per the EEC study (2019), the geotechnical engineering data were collected from geophysical investigations and geotechnical investigations using core drilling.

(a) Geophysical Investigation Data

Vertical Electrical Sounding (VES) and 2D imaging resistivity methods were employed to confirm continuity and uniformity in the subsurface materials of the dam site area. On the basis of previous geological mapping information, 6 resistivity imaging survey lines with a total length of 4539m and investigation depth of 48m, and 6 VES points with the maximum current electrode separation of AB/2 = 100 m was conducted to characterize the geological features of foundations for the dam site.

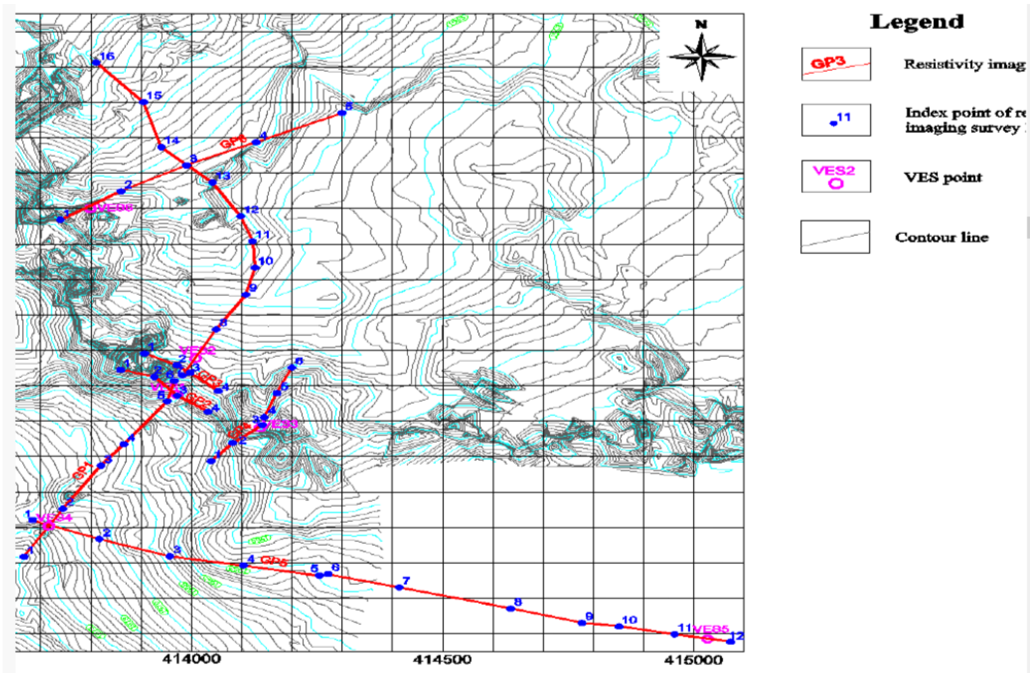

Figure 3. 8 Arrangement of resistivity imaging survey lines and VES points (EEC, 2019)

(b) Geotechnical investigation using the core drilling technique

As per the EEC study (2019), the geotechnical investigation was carried out by employing rotary core drilling, in situ tests in boreholes (water permeability testing, standard penetration testing), excavation of test pits, collection of representative samples from core drilling and excavated test pits, and performing laboratory testing on collected samples to determine parameters for classification and engineering characterization purposes.

A total of 13 boreholes were proposed: 2 boreholes for the construction material and 11 boreholes at the dam site. The location of the borehole sites was decided based on the geophysical investigation result and surface geological and structural map previously done during the prefeasibility study. Hand handheld GPS was used to set out the borehole locations at the site with an accuracy of within 3.0 m.

Core drilling was completed on nine boreholes (identified as DDBH-02, DDBH-02A, DDBH-03, DDBH-04, DDBH-05, DDBH-06, DDBH-06A, DDBH-07, and DDBH-08), for a total depth of 160.50m, at the dam site. From those boreholes, DDBH-01, which is located at the left abutment, was changed to a test pit (DDTP-01) of 5.00m depth and DDBH-04A at the river bed downstream was not done. In all the drilling operations of the current investigation, the core samples were obtained with single and double-tube core barrels, and proper precautions in place to avoid or minimize core sample disturbance. The locations and other details of drilled bore holes are tabulated in Table 3-5. `

(c) Test Pit Excavation

This method was used at the left abutment of the dam foundation to describe the soil material in situ, take samples for classification tests, and calibrate the data with what is obtained by the geophysical resistivity methods.

One test pit (Table 3-5) to a depth of 5m below the bottom of the original ground was performed at the end of the left abutment of the proposed dam foundation of the dam site. The size of the pit was 1.5m by 1.5m, and it was backfilled after completion of the investigation work at the site.

(d) Tests in Geotechnical Investigations

There are two types of tests conducted during geotechnical investigation - laboratory tests and in-situ tests – as summarized below.

Table3. 2. Tests executed in the geotechnical investigation

	Test category	Test Type	Description
i.	**Laboratory Tests**	Direct Shear Test	Suitable only for measuring the strength parameters.
		Triaxial Compression Test	Suitable for measuring both strength parameters and stress-strain properties.
		Unconfined Compression Test	For measurement of compressive strength of rocks and fine-grained soils(sufficient cohesion).
ii.	**In-Situ Tests**	SPT, CPT, Falling Head and Packer Permeability Test	For measurement of resistance of a soil to penetration as an indication of the shearing strength.

[Source: EEC, 2019]

Table 3. 3. Summarized data of bore holes drilled at the project site

BH-ID	Coordinate in UTM /ADINDAN			Location	Drilled Depth (m)	In-Situ Tests				Samples	
	Easting	Northing	Elev (m)			SPT	Packer	Falling Head	Cons Head	Soil	Rock
DDTP – 01	413823	865962	1979	Left Abutment	5.00					2	0
DDBH – 02	414003	865716	1976	Outlet	16.00	5	0	3		2	1
DDBH - 02A	414086	865758	1969	Outlet Downstream Control Room	10.00	5	0	2		1	0
DDBH – 03	413965	865275	1958	Upstream of the dam	22.00	3	2	2		2	2
DDBH – 04	413954	865110	1960	River Bed right foot	27.00	7	3	3		3	2
DDBH - 04A	414016	865092		River Bed downstream							
DDBH – 05	413835	864893	1975	Mid height of right abutment	15.00	6	0	2	1	2	0
DDBH – 06	413723	864705	1975	Spillway	15.00	8	0	3		2	0
DDBH - 06A	413931	864653	1969	Spillway Stilling Basin	10.00	6	0	2		2	0
DDBH – 07	414135	865511	1973	Mid height of left abutment	20.50	9	0	4		2	1
DDBH – 08	414004	865179	1953	Left side near river (on weak zone)	20.00	5	2	2		2	1
Total drilled depth					**160.50**	**54**	**7**	**23**	**1**	**20**	**7**

[Source: EEC, 2019]

(e) In situ Testing

Standard Penetration Test, falling head and constant head permeability tests and packer permeability tests were conducted in the drilled boreholes, where appropriate.

Table 3. 4. Summary table for standard penetration test data

BH-ID	Location	Test No.	Depth (m)	SPT Value (N)				Soil Type Description
				0-15 cm	15-30 cm	30-45 cm	N	
DDBH-02	Outlet	1	1.50 -1.95	3	4	6	10	Silt CLAY
		2	4.50-4.95	8	16	20	36	Clay sandy SILT
		3	7.50-7.95	10	14	20	34	Clay sandy SILT
		4	10.50-10.95	8	12	18	30	Clay sandy SILT
		5	13.50-13.95	9	13	17	30	Clay sandy SILT
DDBH-02A	Outlet Downstream Control Room	1	1.50 -1.95	9	11	15	26	Silt CLAY
		2	3.00-3.45	16	32	R	R	Clay sandy SILT
		3	4.50-4.95	17	29	41	70	Clay sandy SILT
		4	6.00-6.45	19	27	38	65	Clay sandy SILT
		5	9.00-9.45	11	15	21	36	Clay sandy SILT
DDBH-03A	Upstream of the dam	1	1.50 -1.95	6	11	13	24	Clay Sandy SILT
		2	3.00-3.45	6	10	11	21	Clay Sandy SILT
		3	4.50-4.95	6	15	18	33	Clay Sandy SILT
DDBH-04	River Bed right foot	1	1.50 -1.95	6	13	13	26	Sandy SILT
		2	3.00-3.45	8	11	12	23	Sandy SILT
		3	4.50-4.95	9	11	15	26	Sandy SILT

[Source: EEC, 2019]

BH-ID	Location	Test No.	Depth (m)	SPT Value (N)				Soil Type Description
				0-15 cm	15-30 cm	30-45 cm	N	
		4	6.00-6.45	11	14	17	31	Sandy SILT
		5	7.50-7.95	14	17	20	37	Sandy SILT
		6	9.00-9.45	13	15	17	32	Sandy SILT
		7	10.50-10.95	11	13	16	29	Sandy SILT
DDBH-05	Mid height of right abutment	1	1.50 -1.95	3	8	14	22	Silty CLAY
		2	3.00-3.45	8	14	14	28	Silty CLAY
		3	4.50-4.95	9	13	15	28	Sandy Clay SILT
		4	6.00-6.45	6	14	17	31	Sandy Clay SILT
		5	7.50-7.95	7	15	18	33	Sandy SILT with Gravel
		6	9.00-9.45	7	9	11	20	Sandy SILT with Gravel
DDBH-06	Spillway	1	1.50 -1.95	4	9	14	23	Silt Clay
		2	3.00-3.45	11	25	36	61	Clay Sandy SILT
		3	4.50-4.95	13	24	38	62	Clay Sandy SILT
		4	6.00-6.45	20	34	R	R	Clay Sandy SILT
		5	7.50-7.95	17	31	45	76	Clay Sandy SILT
		6	9.00-9.45	15	29	38	67	Clay Sandy SILT
		7	12.00-12.45	16	19	23	42	Sandy SILT
		8	13.50-13.95	15	17	21	38	Sandy SILT
DDBH-06A	Spillway Stilling Basin	1	1.50 -1.95	3	5	6	11	Silty CLAY
		2	3.00-3.45	7	11	17	28	Sandy Clay SILT
		3	4.50-4.95	8	10	14	24	Sandy Clay SILT
		4	6.00-6.45	8	11	13	24	Clay Sandy SILT
		5	7.50-7.95	11	14	21	35	Clay Sandy SILT
		6	9.00-9.45	12	15	20	35	Clay Sandy SILT
DDBH-07	Mid height of left abutment	1	1.50 -1.95	6	9	10	19	Silty Clay
		2	3.00-3.45	10	16	20	36	Silty Clay
		3	4.50-4.95	7	11	15	26	Clay Sandy SILT
		4	6.00-6.45	11	15	14	29	Clay Sandy SILT
		5	7.50-7.95	8	10	12	22	Clay Sandy SILT
		6	9.00-9.45	6	7	6	13	Sandy SILT
		7	11.40-11.85	7	9	12	21	Sandy SILT
		8	13.00-13.45	7	9	8	17	Sandy SILT
		9	14.50-14.95	6	7	8	15	Sandy SILT
DDBH-08	Left side near river (on weak zone)	1	1.50 -1.95	5	9	14	23	Silty CLAY
		2	3.00-3.45	6	10	12	22	Silty CLAY
		3	4.50-4.95	5	7	10	17	Silty CLAY
		4	6.00-6.45	5	8	12	20	Sandy Clay SILT
		5	7.50-7.95	4	10	12	22	Sandy Clay SILT

[Source: EEC, 2019]

(f) Permeability Tests

(i) Falling Head Permeability

A total of 23 falling head permeability tests were carried out in geotechnical boreholes where appropriate. The falling head borehole permeability tests were conducted on soil layers and/or highly weathered and intensively fractured rock zones. The test procedures were undertaken in accordance with the British Code of Practice for site investigation BS5930 (1999) and U.S. Bureau of Reclamation Procedures.

The collected information was therefore analyzed for the determination of the tested section permeability value:

(ii) Constant Head Permeability Test

A total of 1 constant head permeability test was carried out in geotechnical boreholes where appropriate. The constant head borehole permeability tests were conducted on coarse-grained soil layers and/or highly weathered and intensively fractured rock zones.

Accordingly, the constant head tests were conducted in one borehole (DDBH-05). The constant head test results are annexed.

(iii) Packer Permeability Test

A total of 7 Packer permeability tests were carried out in boreholes where appropriate. Single packer permeability tests were conducted for rock mass sections of the drilled boreholes.

The standard practice of the test procedure and plant arrangement was applied for the testing operation:

Table 3. 5. Summary of borehole permeability test

BH-ID.	BH Location	Test Type	Test Section (m)	Permeability (k in cm/s)	Remark
DDBH-02	Outlet	Falling Head	0.00-5.00	1.09E-05	
			5.00-10.00	1.97E-04	
			10.00-16.00	2.13E-04	
DDBH-02A	Outlet Downstream Control Room	Falling Head	0.00-5.00	1.30E-05	
			5.00-10.00	3.30E-04	
DDBH-03	Upstream of the dam	Falling Head	0.00-5.00	9.00E-05	
			5.00-10.00	8.26E-05	
		Packer	11.00-16.00	2.10E-04	Washout
			15.00-20.00	1.31E-05	Laminar
DDBH-04	River Bed right foot	Falling Head	0.00-5.00	4.49E-05	
			5.00-10.00	4.65E-04	
			10.00-15.00	3.95E-04	
		Packer	15.00-20.00	6.55E-05	Dilation
			20.00-25.00	1.31E-05	Dilation
			24.00-27.00	2.62E-05	Dilation
DDBH-05	Mid height of right abutment	Falling Head	0.00-5.00	1.34E-06	
			5.00-10.00	6.37E-05	
		Constant Head	10.00-15.00	8.80E-04	
DDBH-06	Spillway	Falling Head	0.00-5.00	8.90E-05	
			5.00-10.00	5.42E-05	
			10.00-15.00	3.30E-04	
DDBH-06A	Spillway Stilling Basin	Falling Head	0.00-5.00	4.68E-05	
			5.00-10.00	1.64E-05	
DDBH-07	Mid height of left abutment	Falling Head	0.00-5.00	3.94E-05	
			5.00-10.00	2.52E-04	
			10.00-15.00	3.53E-04	
			15.00-20.50	8.63E-05	
DDBH-08	Left side near river (on weak zone)	Falling Head	0.00-5.00	8.16E-06	
			5.00-10.00	4.78E-05	
		Packer	10.00-15.00	1.31E-05	Dilation
			15.00-20.50	1.57E-04	Dilation

[Source: EEC, 2019]

(g) Piezometer Installation and Groundwater Level Monitoring

To construct observation well piezometers are planned at two selected boreholes located along the dam axis near the river bank, DDBH-08 and DDBH-04, but the site conditions have not permitted to installation of piezometers, for the reason that of a false indication of the water level, but not the actual groundwater, has been obtained due to water used for drilling activity.

(h) Sampling and Laboratory Analysis

Representative rock and soil samples were collected from core drilling recovery and excavated test pits. The required laboratory tests of these samples were analyzed based on the corresponding ASTM and BS standards.

(i) Tests on Rock samples

The intact rock samples were studied in the laboratory for the determination of index and engineering properties.

Such tests are performed to determine Index and engineering properties of intact rock samples: specific gravity, water absorption, bulk unit weight and strength (uniaxial compressive strength (UCS)) of rock specimen. The details of collected rock samples, the type of laboratory tests conducted, and corresponding laboratory test results summary is presented in Table 3.8.

Table3. 6. List of rock core samples collected from boreholes at the dam axis and summary of corresponding laboratory results

BH-ID	Sample Id	Sample depth(m)	Rock Description	Specific Gravity	Water Absorption (%)	Unit weight (g/cc)	UCS (Mpa)
DDBH-02	DDBH-02/RS-1	15.65-16.00	Welded Tuff	1.45	40	1.15	4.58
DDBH-03	DDBH-03/RS-1	12.12-12.30	Welded Tuff	1.42	44.16	1.05	2.03
	DDBH-03/RS-2	16.10-16.32	Welded Tuff	1.42	39	1.02	3.23
DDBH-04	DDBH-04/RS-1	15.20-15.45	Welded Tuff	1.43	40	1.1	6.56
	DDBH-04/RS-2	19.50-20.00	Welded Tuff	1.54	39	1.36	13.7
DDBH-07	DDBH-07/RS-1	19.70-20.00	Welded Tuff	1.43	47	1.08	5.51
DDBH-08	DDBH-08/RS-1	11.40-11.75	Welded Tuff	1.4	41.85	1	2.89

[Source: EEC, 2019]

(ii) Tests on Soil Samples

A total of twenty soil samples were obtained from boreholes recovered and test pits excavated at the foundation area. Silt or Clay Soils SPT and undisturbed and disturbed soil core samples were mixed; and undisturbed (rolled by aluminum foil) and disturbed small (plastic bag) samples were taken from the foundation site upper soil strata. As well as for construction material from shell borrow, natural sand borrow and dam impervious core material source area a total of six bulk soil samples were collected. They were sent for classification and chemical tests in the laboratory.

The laboratory tests performed included: grain size analysis (sieve and hydrometer), Atterberg limits, bulk unit weight, specific gravity, natural moisture content, free swell, standard and modified compaction/proctor, direct shear, consolidation (odometer), unconfined compressive strength, dispersion (double hydrometer), and permeability. All tests were carried out at the Ethiopian Engineering Corporation, Geotechnical Laboratory. Tabulated summary of tested samples information, laboratory test types and results obtained are presented herein (Tables 3-7)

Table 3. 7. Summary of laboratory results of soil samples taken from boreholes

BH-ID	Sample ID	Depth (m)	Grain size analysis (%)				Sp.gr	Unit Wt	Atterberg limit			FS	Moisture Content (%)	Dispersion
			Clay	Silt	Sand	Gravel			LL	PL	PI			
DDBH-02	DDBH-02/SS-3	4.30-5.00	3.22	70.25	25.63	0.9	2.4	1.34	33.84	Non-PL		37.5	3.46	D
	DDBH-02/SS-5	10.25-11.00	9.47	66.86	22.43	1.24	2.39	1.31	34.3	29.17	5.13	40	1.19	ID
DDBH-02A	DDBH-02A/SS-4	6.00-6.65	11.39	66.86	21.75	0	2.43	1.42	38.6	35.99	2.61	32.5	2.48	ID
DDBH-03	DDBH-03/SS-4	4.00-4.30	22.74	50.91	26.28	0.08	2.19	1.26	60.15	49.22	10.93	62.5	10.89	ID
	DDBH-03/SS-6	7.70-8.30	5.99	68.13	25.76	0.11	2.43	1.2	37.16	35.75	1.41	20.25	1.47	ID
DDBH-04	DDBH-04/SS-5	6.00-6.70	3.85	65.55	29.68	0.92	2.38	1.21	32	Non-PL	_	20	1.53	D
	DDBH-04/SS-7	9.00-9.80	6.02	66.9	26.58	0.5	2.37	1.24	40.96	36.94	4.02	20	2.24	ID
	DDBH-04/SS-9	12.00-12.40	9.28	56.8	33.46	0.47	2.55	1.32	29.6	Non-PL	_	50	6.79	ID
DDBH-05	DDBH-05/SS-6	6.00-6.80	20.4	61.13	15.83	2.64	2.33	1.28	45.7	35.68	10.02	50	8.14	ID
	DDBH-05/SS-8	9.00-9.75	0	68.2	25.58	6.22	2.56	1.15	28.85	Non-PL	_	30.25	12.97	D
DDBH-06	DDBH-06/SS-6	7.20-8.00	11.14	70.15	18.35	0.35	2.45	1.83	40	27.78	12.22	45	3.83	ID
	DDBH-06/SS-8	11.60-12.70	7.99	66.09	24.66	1.26	2.39	1.51	34.3	Non-PL	_	40	2.98	ID
DDBH-06A	DDBH-06A/SS-6	5.40-5.65	20.08	56.52	19.25	4.15	2.41	1.54	51.9	34.32	17.58	50	26.65	ND
	DDBH-06A/SS-8	7.25-8.00	10.94	55.79	31.42	1.85	2.51	1.66	35.25	Non-PL	_	50	3.19	ID
DDBH-07	DDBH-07/SS-5	5.85-6.55	15.07	53.9	30.85	0.19	2.42	1.74	36.5	Non-PL	_	50	1.62	ID
	DDBH-07/SS-9	13.00-13.70	5.86	68.9	27.89	0.35	2.45	1.63	33.5	Non-PL	_	30	0.53	D
DDBH-08	DDBH-08/SS-5	4.50-5.15	43.06	42	14.29	0.65	2.52	2.13	57.82	29.74	28.08	60	4.85	ND
	DDBH-08/SS-9	8.00-8.25	26.23	59.12	14.45	0.21	2.54	1.92	52.5	34.79	17.71	55	17.3	ND
DDTP-01	DDTP-01/SS-1	1.30-2.20	54.3	35.72	7.66	2.32	2.63	2.17	59.5	36.9	22.6	60	7.02	ND
	DDTP-01/SS-2	2.50-4.20	8.95	57.71	24.87	8.47	2.6	1.52	35.9	Non-PL	_	35	7.04	ND

[Source: EEC, 2019]

(i) Foundation Soil

Engineering Soil Classifications

One major engineering geological soil units have been identified in the area, and described below, i.e., the Black Cotton & reddish brown Clay (is considered only as Top Soil). On the other hand, engineering classification of soils was made using the Unified Soil Classification System (USCS) of the soils. The grain size percentage of the laboratory test results shows that the foundation soil has a high percentage of Silt, followed by Minor sand and trace clay (sandy SILT with minor clay) percentages and it is regarded as cohesive soil; therefore plasticity chart has been used to classify the soil type.

Further characteristics of fine soils and fine soil fractions in coarse and medium grain soils of the residual and Ash & decomposed tuff soils have been made using standard terms for description of plasticity index classes.

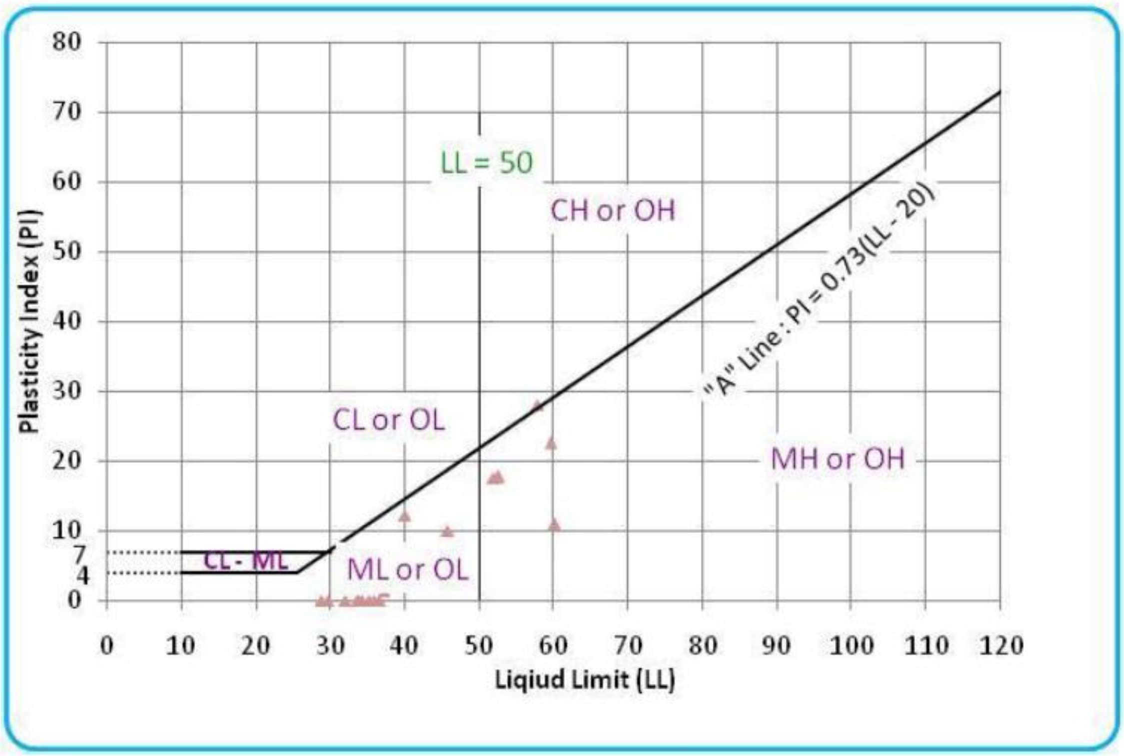

Figure 3. 9 Unified soil classification system (USCS) of the foundation soils (EEC, 2019)

Resistance to Erosion

The resistance of the embankment or foundation to piping depends on:

1. Plasticity of the soil
2. The gradation
3. The degree of compactness

Since the site soil is cohesive soil, its piping resistance is evaluated based on its plasticity as presented in the following table.

Table3. 8. Plasticity and gradation test results for foundation soil

Resistance controlled by	Suitability	Property
Plasticity of the soil	Suitable Poor	PI = 15 – 20% PI < 12% , PI > 30%
Gradation	Suitable Poor	Well graded Uniformly graded

[Source: EEC, 2019]

(j) Foundation Rocks

Rock Mass Classification

The Geomechanics Classification (Rock Mass Rating System) was used for classifying and interpreting for quality of the foundation rocks of the proposed dam site. Typical of classifications are those published by Bieniawski (1973, 1974) and by Barton, Lien and Lunde (1974).

The following six parameters were used to classify a rock mass using the RMR system; they were collected in the field and from laboratory test results.

1. UCS of rock material
2. Rock Quality Designation (RQD)
3. Spacing of discontinuities
4. Condition of discontinuities
5. Groundwater condition
6. Orientation of discontinuities

The dam foundation rock mass was first divided into two (2) geotechnical domains, based on geophysical VES sections, geophysical 2D imaging profiles and fracture density and evenness as displayed by weighted RQD. These regions are assumed to be more or less uniform in certain geotechnical features. Because the resistivity values can be affected by the rock type and rock mineralogy, other than rock mass properties, calibration was made to the geotechnical parameters of the drilled cores.

Table3. 9. Rock mass classification, based on geomechanics classification method (Biniawski 1973)

Item	UCS (MPa)	RQD (%)	Spacing of Discontinuities(mm)	Condition of Discontinuities	Ground Water	Total	Rock mass Class Number
Zone-1	3	Fragmented	Fragmented	>5mm thich soft gouge	Dry		IV
Ratings	1	3	5	0	15	24	
Zone-2	7	70	1000mm	<1mm separation, Slightly rough surfaces	None		II
Ratings	2	17	15	25	15	74	

Therefore, the rock mass of the dam is classified into three zones of different rock mass qualities. These are:

- Rock Mass Class II: Good Rock, and
- Rock Mass Class IV: Poor Rock

Rock Mass Permeability and Seepage Potential

Summary of Permeability test results are given in Table 3-5. Interpretations and hydraulic domain classifications were made based on the permeability classification of rocks given by Lashkaripour and Ghafoori, 2002: i.e.:

- Impervious, if Lugeon Value is 0-3,
- Low permeability, if the Lugeon Value is 3-10,
- Medium permeability, if the Lugeon Value is 10-30,
- High permeability, if the Lugeon Value is 30-60,
- Very high permeability, if Lugeon Value is >60,

According to Table 3.5, the foundation rock mass units are of low permeability.

Rock Mass Modulus

A number of empirical methods have been developed that correlate various rock quality indices or classification systems to in-situ modulus. The more commonly used include correlations between RQD, RMR and Q.

A more recent correlation between in-situ modulus of deformation and the RMR Classification system was developed by Serafim and Pereira (1983), which included an earlier correlation by Bieniawski (1978), for RMR values ranging from approximately 25 to 85.

Table 3. 10. Modulus of deformation of rock mass classes (based on Serafim and Pereira, 1983)

Structure Class	RMR average	Ed	Deformability
II	74	16 GPa	Moderate
IV	24	3.5GPa	High

The Geomechanics classification application has a prime importance to have knowledge of deformability of rock mass, for foundations. It is proved to be a useful method for in-situ deformability of the rock mass (Bieniawski, 1978).

$$Ed=2RMR-100 \qquad \text{Eq.4.1}$$

Where Ed is modulus of deformation in GPa, and RMR >50

Table3. 11. Situ modulus of deformation of rock masses according to Bieniawski, 1978

Structural Class	RMR average	Ed	Classification
II	74	48 GPa	Low

Accordingly, the identified two foundation geotechnical rock mass units are characterized as follows:

Rock Class IV (Poor Quality Rock Mass, RMR value = 24):

It lies below the foundation from DDBH-02 to DDBH-08 in the left abutment and from DDBH-04 to DDBH-06 in the right abutment. It is mainly consists of loose, soft, unconsolidated, friable and highly weathered, very closely jointed to fragmented, weak, pervious, unwelded to welded tuff with high deformability. Volcanic ash seams and crushed welded tuff rocks have been found intermingled with this layer, in DDBH-08 and DDBH-03, as a mixture of highly fragmented rock and soft volcanic soils, and they are expected to have resulted from partially disintegrated rock or physically grounded rock mass in contact zones. A possible fault at the left side of the river bank site forms a shattered zone that extends up to 19 & 20m in DDBH-08 & DDBH-07, respectively.

Rock Class II (Good Quality Rock Mass, RMR value= 74):

This rock mass is found in the whole part of the foundation constituting the lower position in the investigated depths. The material type is relatively more consolidated pyroclastic deposit (welded tuff), and it is exposed at the surface covering a 60 to 100m span of the dam axis section in the river channel. This rock mass is fresh to faintly weathered, soft, friable, weak, semi-pervious to impervious, moderately deformable and is systematically jointed by at least two main tectonic extensional tight joints sub-vertically trending NNW to NS and E-W. Along water courses, at places, selective dissolution of soft materials developed open, irregularly sized cavities/caves on river bed/bank exposures. It is encountered in the left abutment boreholes, such as in DDBH-02 (in 13.90-16.00m depth range), in DDBH-07 (in 19.00-20.50m depth range), in DDBH-08 (in 11.40-15.00m depth range); and in right abutment DDBH-04 (17.85-27.00m) underlying the highly weathered and fractured/jointed to fragmented Rock Class IV rock mass. Unexpectedly, in DDBH-08, the rock mass (Rock Class IV) comes next to the Rock Class II rock mass in depth of 15.00 to 20.00m.

3.4 Evaluation/Analysis Methodology

The research work on the Evaluation of Gravelly Clay Blanket Foundation Treatment and Remedial measures for Kalid Dijo Dam was carried out in accordance with the approaches and methodologies as explained in the following sections.

3.4.1 Review/Update of Dam Design Geometry

To conduct this research, the researcher has chosen five representative cross-sections based on the geological profile at the changes of 0+520, 0+770,1+123, 1+228, and 1+670. To analyze the problems of each layer, based on the geotechnical investigation report, the foundation’s soil layers should be characterized and identified in detail. The following drawings have been adjusted.

Figure 3.1 below shows the typical cross-sectional drawing at the chainage of 1+123, prepared by the engineering design team of EEC (2019) as the final detail design typical drawing for Kalid Dijo Dam construction. However, for this thesis work in the next chapter, there are going to be some modifications to some extent, and some adjustments with explanations.

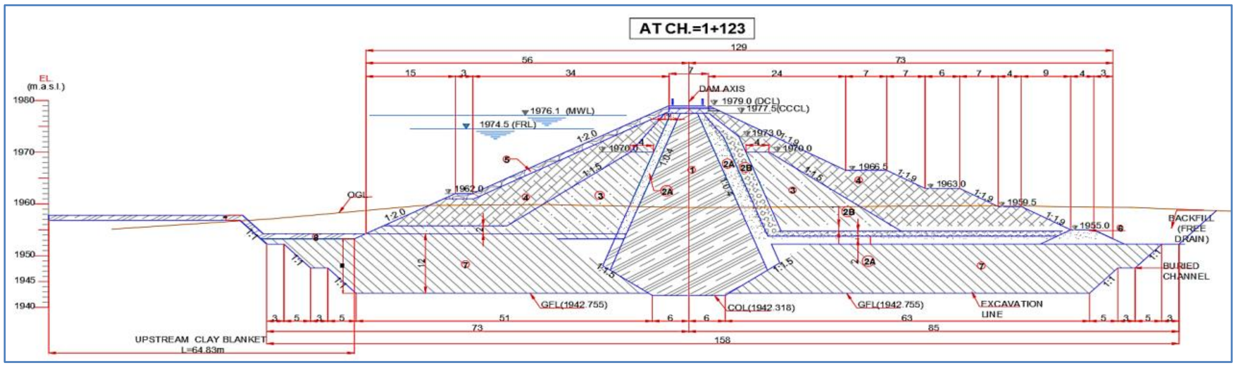

Figure 3. 10 Previous typical cross-section of Kalid Dijo dam at 1+123

The sections of the dam body that make up the zoned cross-section are;

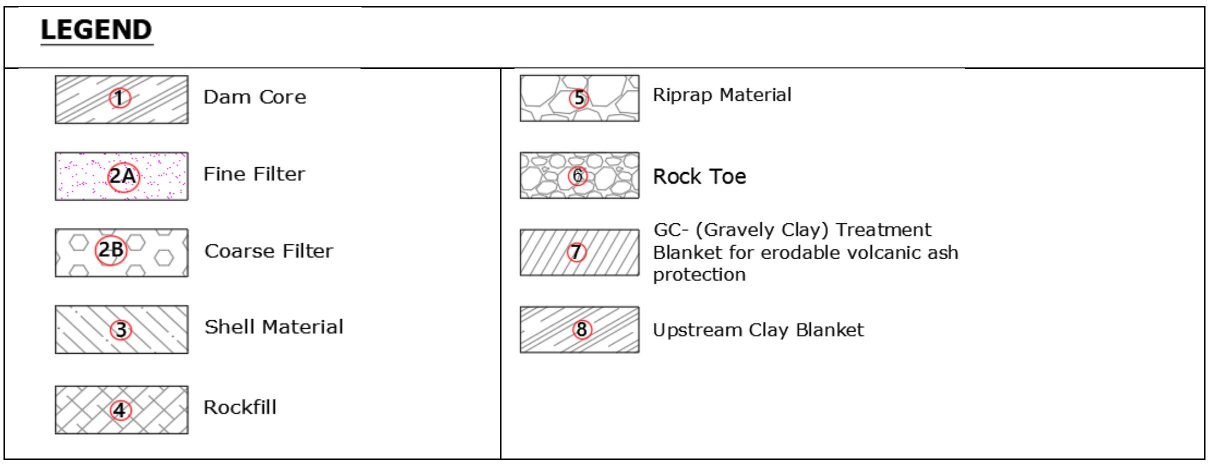

Figure 3. 11 Zoned dam bodies' cross-section descriptions

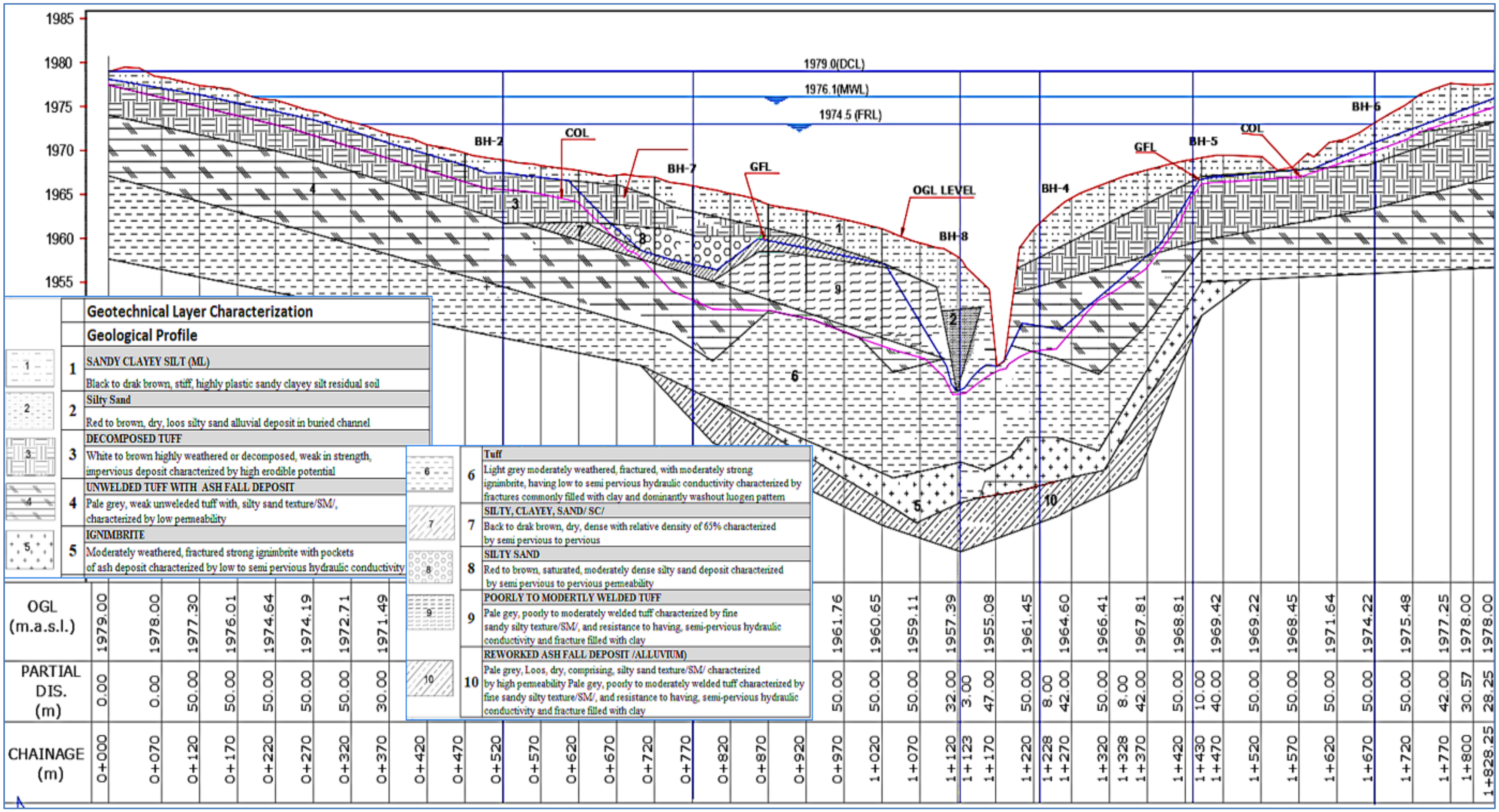

Figure 3. 12 Geological profile and profile with borehole Pattern (RRC, 2019)

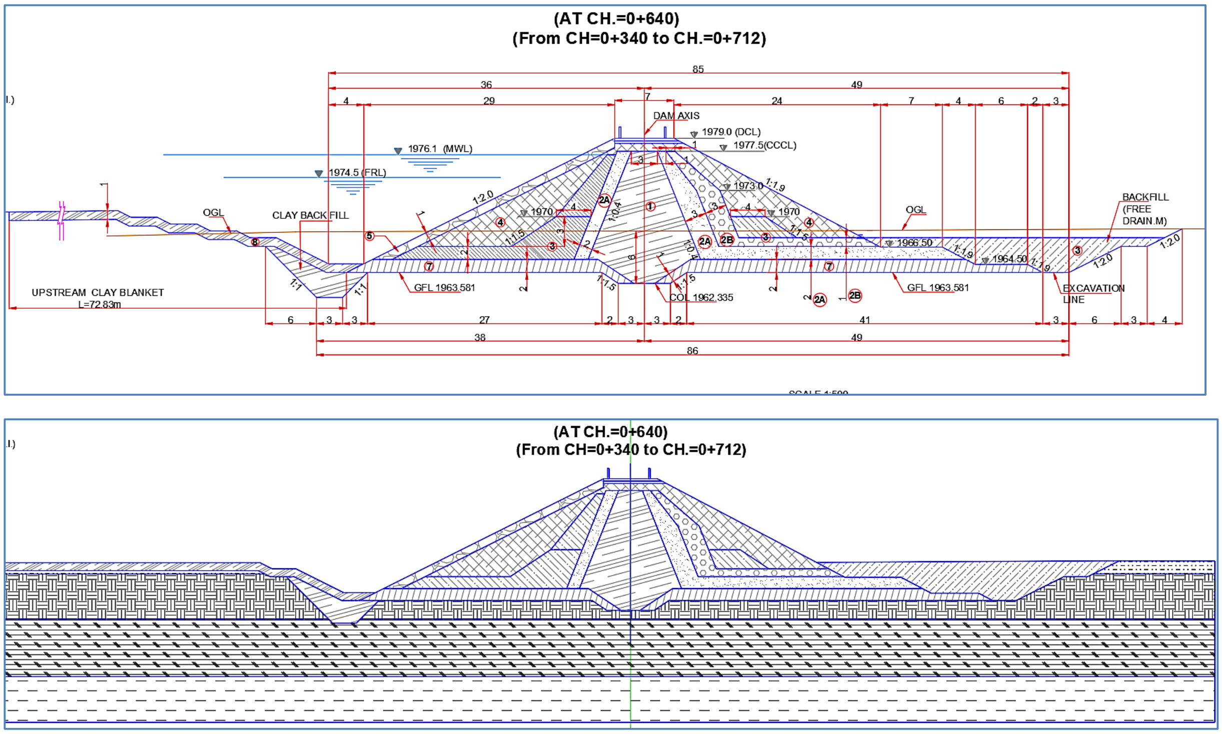

Figure 3. 13 Adjusted cross-section profile for BH2

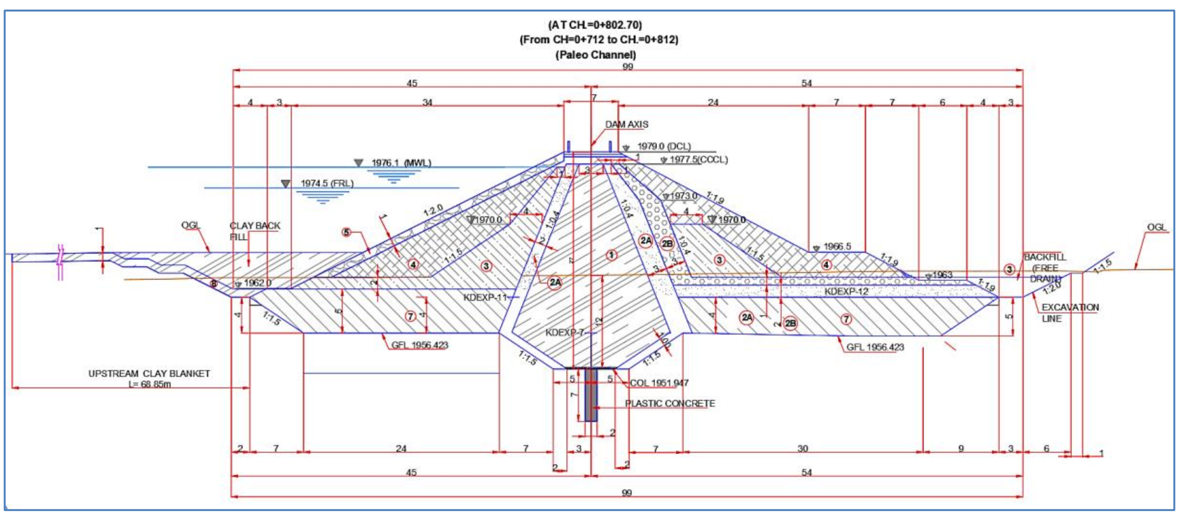

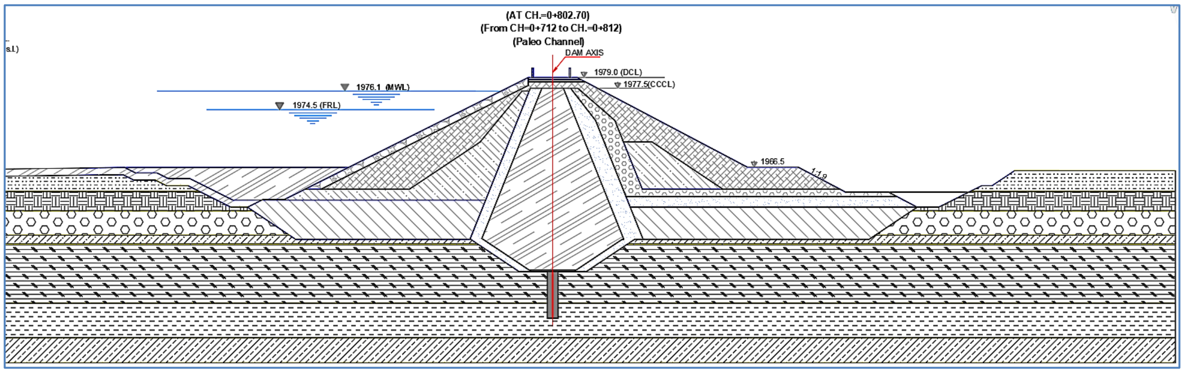

Figure 3. 14 Adjusted cross-section profile for BH7

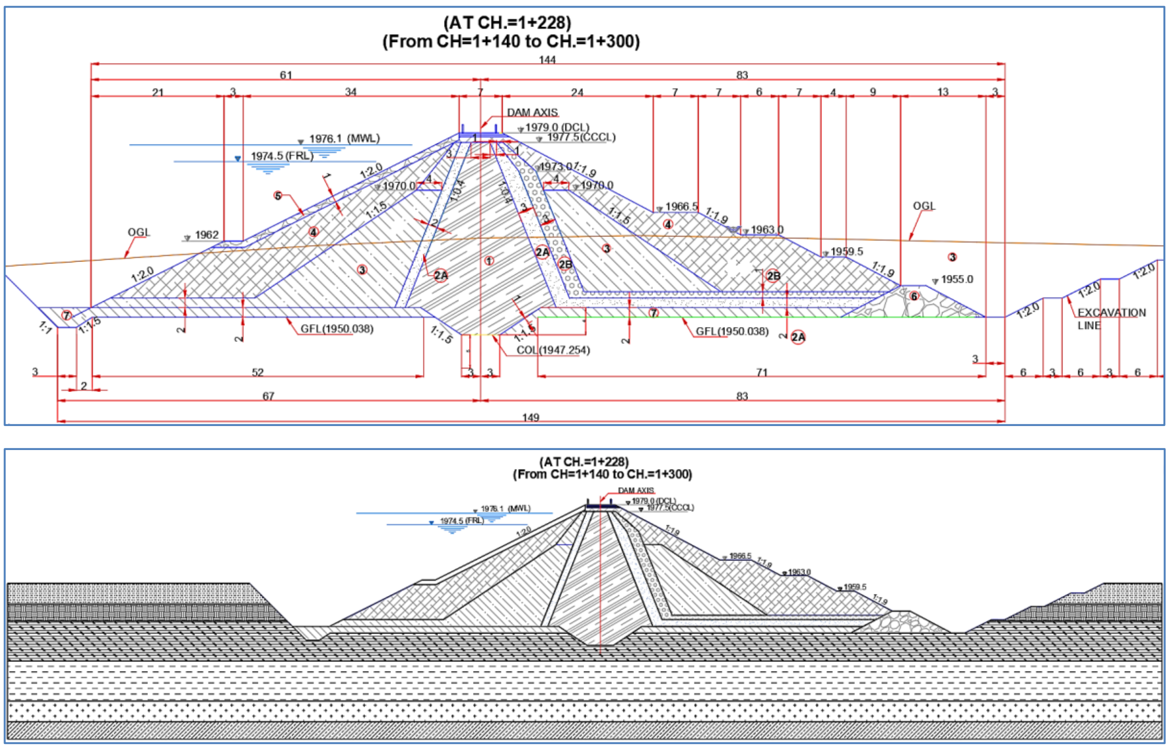

Figure 3. 15 Adjusted cross-section profile for BH8

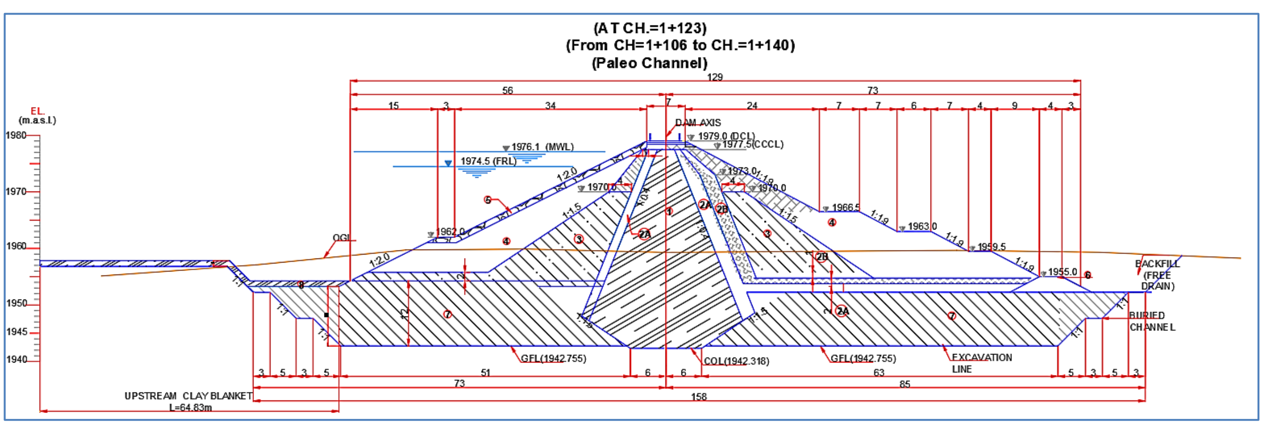

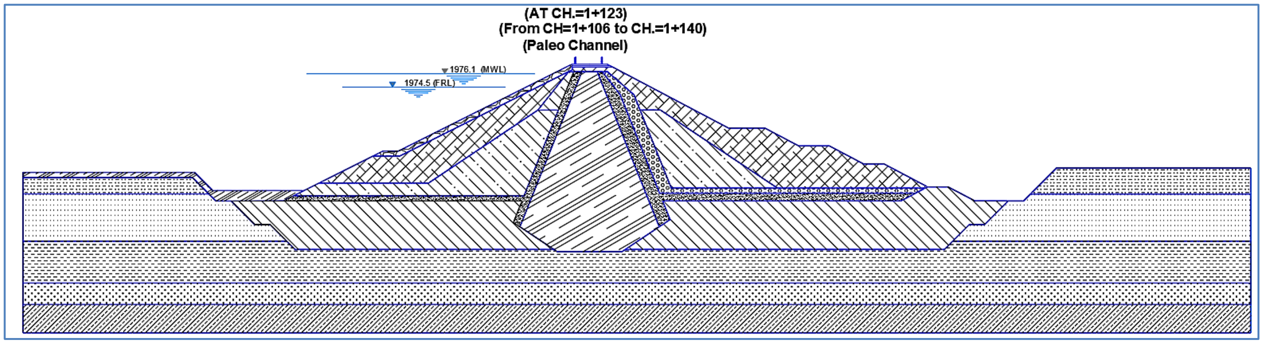

Figure 3. 16 Adjusted cross-section profile for BH4

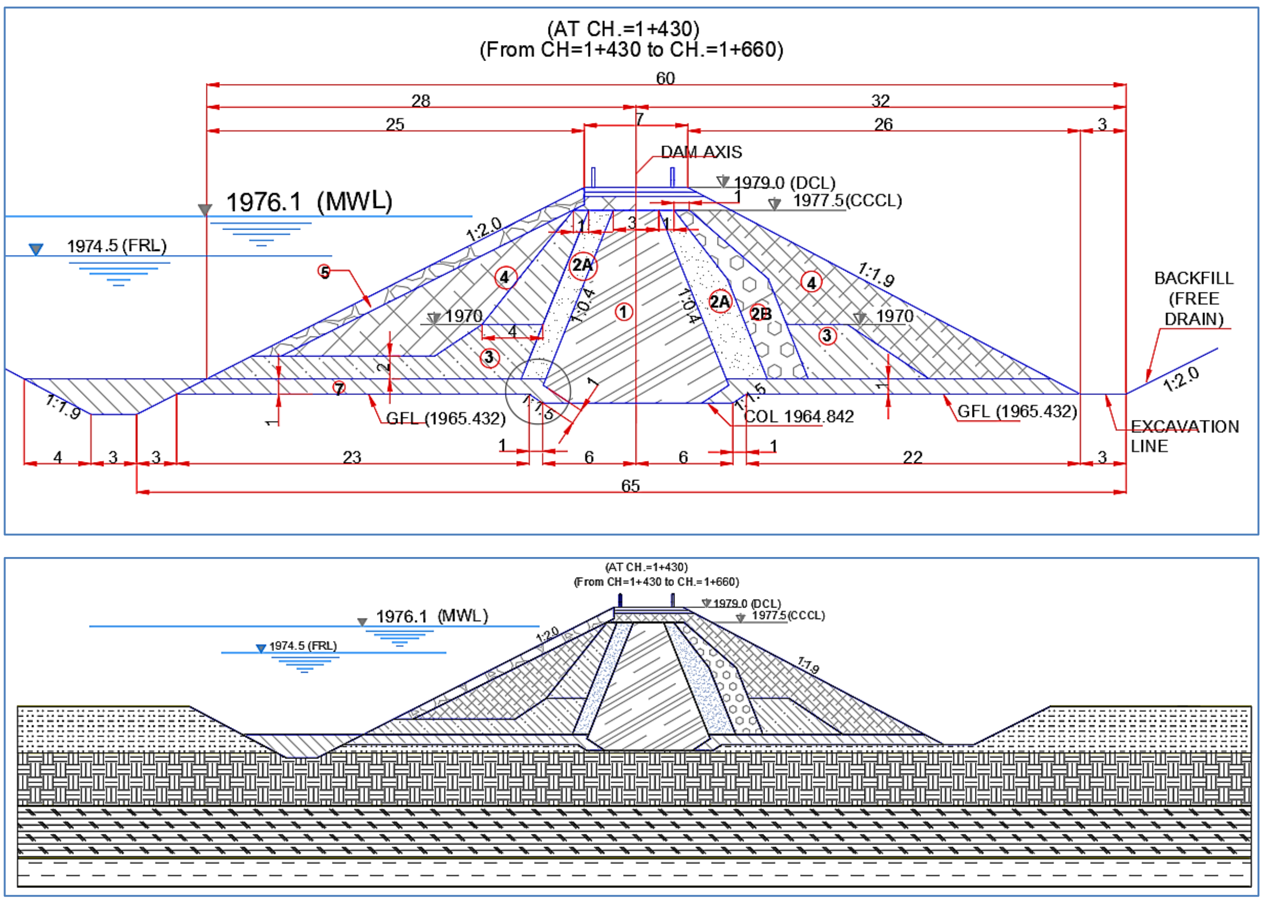

Figure 3. 17 Adjusted cross-section profile for BH

3.4.2 Establish Seepage Control Options for Viable Foundation Treatment

The evaluation of procedures or methods used for the analysis of the Kalid Dijo dam has been presented using the software of Geo-Studio 2022, as follows.

The Evaluation of Gravelly Clay Blanket Foundation Treatment and remedial measure for Kalid Dijo Dam was carried out by considering different options of treatment methods at different sections of the dam for seepage control in accordance with the details provided in the table below.

Table3. 12. Proposed options of treatment methods at different sections of the dam for seepage control

Borehole Ref.No.	Chain age	Seepage Control Options	Description
2	0+520	Option-1	This option has been regarded as the original design of the dam.
		Option-2	This designation includes a 7-meter cut-off slurry wall and a 1.9-meter increase in the clay core depth to improve seepage control and water retention.
		Option-3:	This design option features a 7-meter cut-off slurry wall and a 1.9-meter increase in the clay core depth. The upstream backfill cut-off, which was originally filled with clay, has also been eliminated from the design.
7	0+770	Option-1	This option has been regarded as the original design of the dam.
		Option-2	In this option, the design is modified to eliminate the filter material that was originally placed in the foundation, covering the clay core in the key trench.
8	1+123	Option-1	This option has been regarded as the original design of the Kalid Dijo Dam.
		Option-2	This adjustment involved reducing the original design thickness by 8 meters and incorporating an additional 7 meters of cutoff slurry made from plastic concrete.
		Option-3	This adjustment involved reducing the original design thickness by 7 meters and incorporating an additional 7 meters of cutoff slurry made from plastic concrete.

Borehole Ref.No.	Chain age	Seepage Control Options	Description
4	1+228	Option-1	This option has been regarded as the original design of the Kalid Dijo Dam.
		Option-2	In this design option, a 2.8-meter layer of GC material and a 5-meter cutoff slurry layer of plastic concrete are added.
6	1+670	Option-1	This option has been regarded as the original design of the Kalid Dijo Dam.
		Option-2	To address potential issues related to internal erosion and piping, a 1-meter layer of Gravel Clay (GC) was introduced immediately beneath the dam body.

3.4.3 Numerical Modelling and Analysis

The procedures or methods used for developing the model and analyzing the proposed options of treatments for the Kalid Dijo dam have been done using the geotechnical analysis software Geo-Studio 2022 - Seep\W and Quake\W.

GeoStudio 2022 is a comprehensive suite of geotechnical software tools designed for the analysis and design of geotechnical problems such as slope stability, soil settlement, seepage, and retaining wall stability. Developed by Geo-Slope International Ltd., GeoStudio 2022 integrates various modules—including SLOPE/W, SEEP/W, SIGMA/W, and others—allowing engineers and researchers to perform detailed numerical analyses of complex geotechnical systems within a user-friendly interface.

At its core, GeoStudio 2022 employs fundamental principles of soil mechanics and fluid flow, utilizing well-established mathematical models to simulate real-world behaviors. The primary formulas used in these analyses are derived from classical soil mechanics equations, including Terzaghi's principles of effective stress and Darcy's law for seepage. For instance, slope stability analyses often rely on the limit equilibrium method, which involves calculating the factor of safety (FoS) based on shear strength parameters and the geometry of the slope.

A basic formula frequently used in GeoStudio's slope stability analysis is the limit equilibrium equation:

FoS=Resisting Forces Driving ForcesFoS = \frac{\text{Resisting Forces}}{\text{Driving Forces}}

$$FoS = \frac{\text{Driving Forces}}{\text{Resisting Forces}}$$

Where the resisting forces are primarily governed by the soil's shear strength parameters (cohesion ccc and internal friction angle ϕ\phiϕ), and the driving forces are due to the weight of the soil mass and any external loads.

In seepage analysis, Darcy's law plays a pivotal role in modeling the flow of water through porous media. Darcy's law states that the flow velocity qqq is proportional to the hydraulic gradient

$$q=-K\nabla h \qquad \text{Eq4.2}$$

where q is the Darcy flux (flow per unit area), K is the hydraulic conductivity of the soil, and

∇ nabla h∇h is the hydraulic gradient.

This fundamental law allows GeoStudio's SEEP/W module to simulate water seepage accurately, which is critical for assessing pore pressure distributions, seepage paths, and potential failure zones in geotechnical systems.

Furthermore, GeoStudio employs the finite element method (FEM) for advanced numerical analysis in modules such as SIGMA/W and others. FEM discretizes the soil domain into a mesh of elements, enabling the solution of complex differential equations governing stress, deformation, and seepage with high precision. This approach allows for the modeling of non-linear behaviors, heterogeneous materials, and boundary conditions that are representative of real-world conditions, making GeoStudio a powerful tool for comprehensive geotechnical analysis.

In summary, GeoStudio 2022 integrates classical formulas like the limit equilibrium method and Darcy's law within a robust finite element framework, providing detailed insights into geotechnical stability and fluid flow phenomena essential for safe and effective engineering design.

3.4.4 Comparison of Options of Treatments

The essential considerations while choosing a treatment method are the quantity of seepage, hydraulic gradient, safety factor, and cost. It appears that using a cutoff wall rather than a GC blanket is the better method of waterproofing the dam. The finite element technique and the Seep/W software were used to accomplish this aim. Using the numerical analysis approach, the Seep/W software is a finite element program that can theoretically simulate seepage (Krahn, 2009).

The best alternative for the foundation treatment is the type of treatment that is effective in mitigating potential internal erosion and ensuring long-term stability. This assessment underscores the importance of optimizing foundation treatments in dam design to achieve both safety and durability.

4 ANALYSIS RESULTS AND DISCUSSIONS

4.1 SEEP/W Analysis

4.1.1 Geometry Importing

Data from geological engineering inquiries have been gathered for the current study through methodical field investigations. A broad overview of all the geological site conditions is provided by a geological map of some kind. Additionally, the map can be utilized to identify potential problems or positive features of the project site (Daniel Gebremichael, 2017). The engineering characterization of the rock mass and soils present at the site served as the basis for the engineering geological mapping of the Kalid Dijo dam foundation and the surrounding area. Based on geotechnical characteristics established during a thorough design study (EEC, 2019), the soils of the dam site area were mapped.

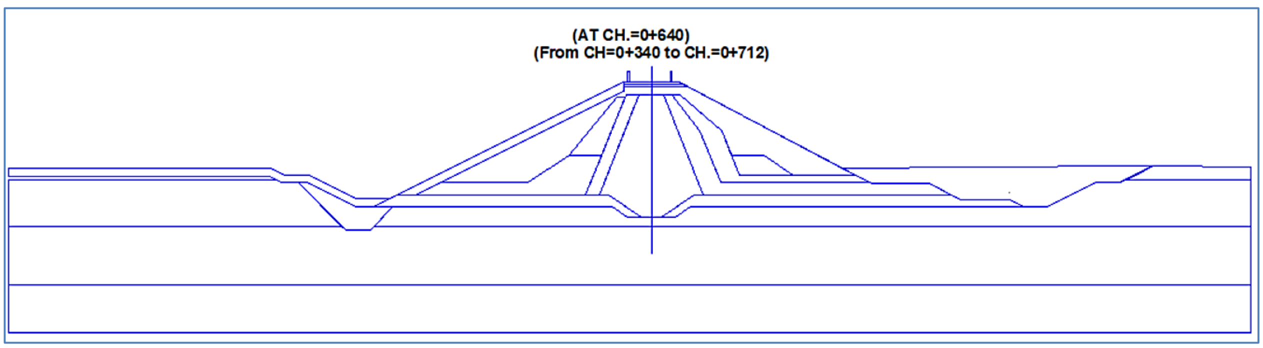

a) Adjusted geometry cross-section at chainage 0+640

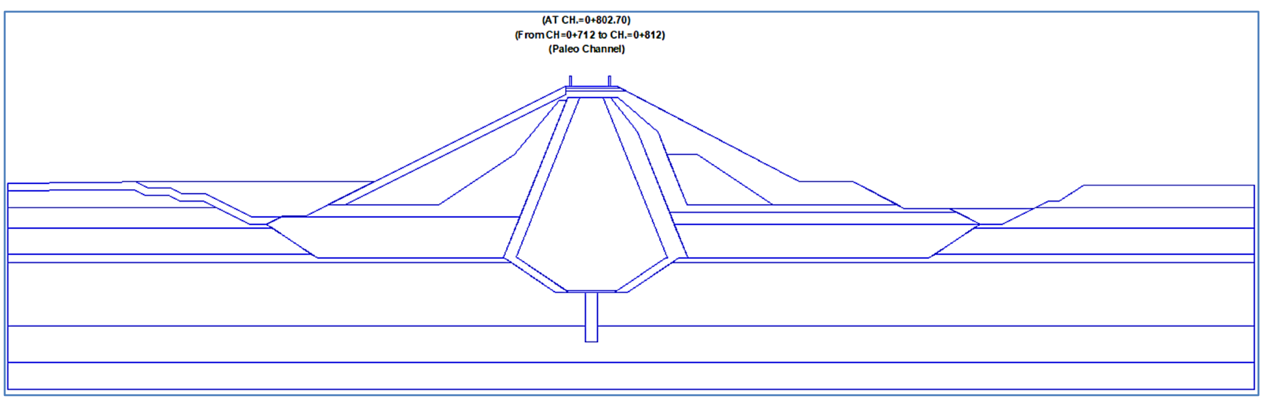

b) Adjusted geometry cross-section at chainage 0+802.7

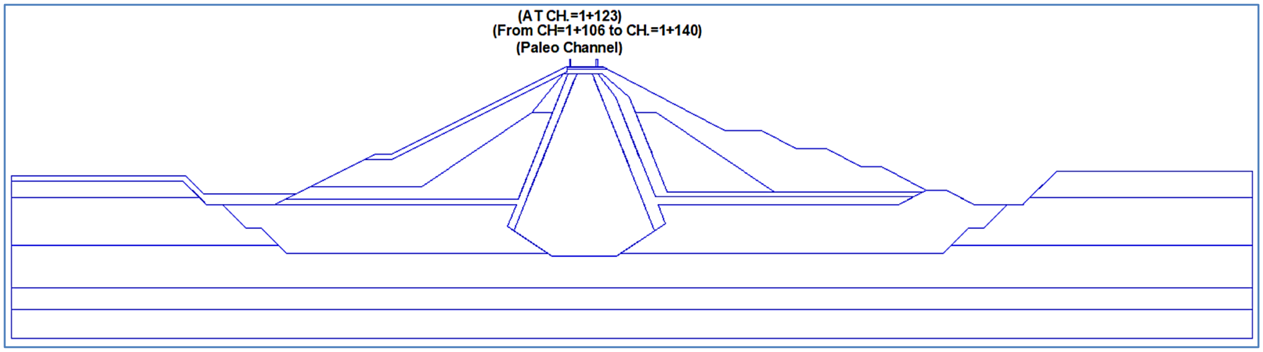

c) Adjusted geometry cross-section at chainage 1+140

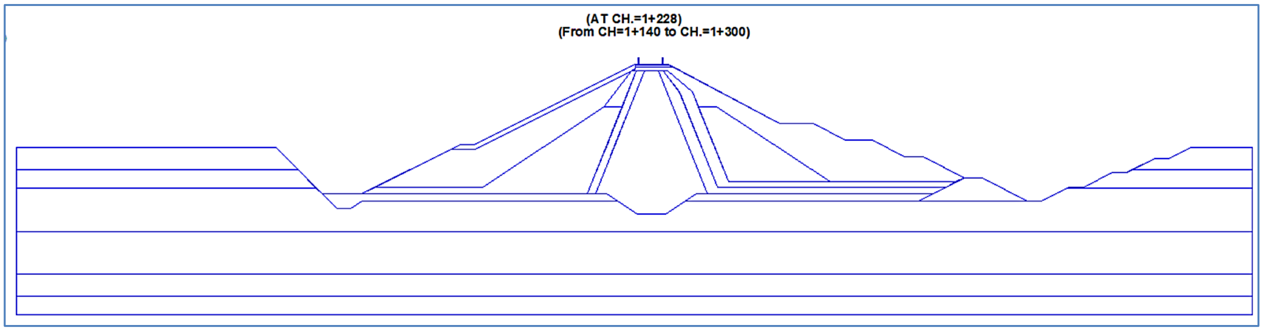

d) Adjusted geometry cross-section at chainage 1+300

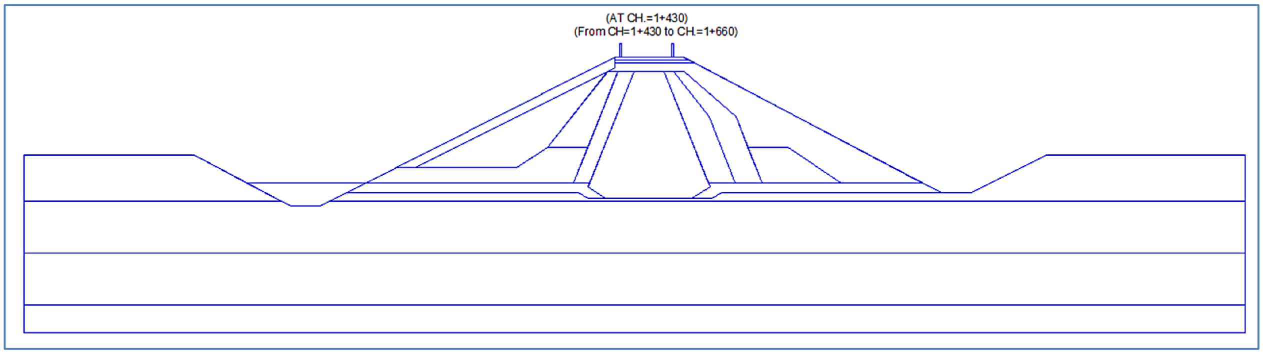

e) Adjusted geometry cross-section at chainage 1+43

Figure 4. 1 Adjusted design drawings for importing into GeoStudio 2022 work

4.1.2 Defining Materials

Each material has been allocated to its corresponding area. Those filled dam materials and the layered foundation materials would be given distinct engineering characteristics in this stage, and each material would be distinguished by color, as seen in the dialog box that follows. Each area would be allocated a material attribute and a material model. The study would employ the unit weight, angle of friction, and cohesiveness of the material as input factors.

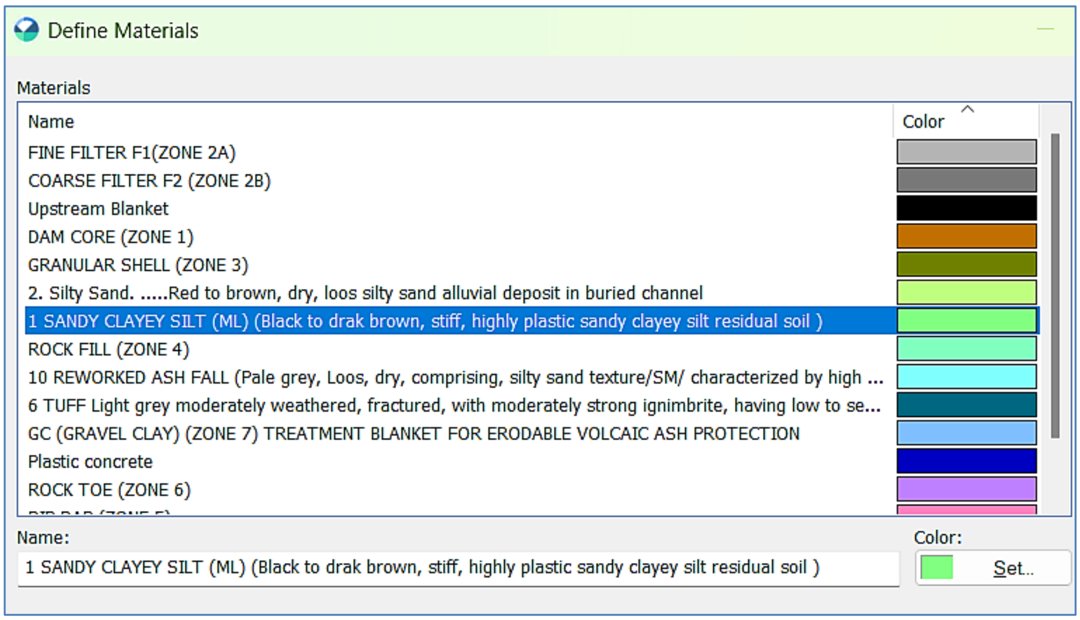

Figure 4. 2 Defined materials

4.1.3 Parameters Used for Seepage Analysis.

The coefficient of permeability for the foundation and embankment materials was taken from the Kalid Dijo Dam final design report and prepared according to EEC (2019), as well as a few other standards. In this investigation, pore water has been extracted from the Seep/w result. After the issue was resolved, the findings were examined and discussed.

Table 4. 1. Summary of embankment fill and foundation material characteristics used in seepage and stability analysis

Function	Unit Weight (KN/m^3)	Permeability (m/s)	C'(KPa)	ϕ'(o)
Core	18.0	$3.56x10^{-8}$	90	18
Fine filter	20.0	$1x10^{-4}$	0.0	30
Coarse filter	20.0	$1x10^{-3}$	0.0	32
Granular shell	18.0	$5.2x10^{-5}$	5.0	30.0
Rock fill	22.0	$1x10^{-2}$	0.0	40.0
Riprap	22.0	$1x10^{-2}$	0.0	42.0
Rock Toe	20.0	$1x10^{-3}$	0.0	38.0
Sandy Clayey Silt	16.0	$1x10^{-7}$	80.0	18.0
Foundation Rock class IV	20.0	$2.1x10^{-6}$	50.0	20.0
Foundation Rock class II	Bed rock impenetrable	$2.62x10^{-7}$	Bed rock impenetrable	

4.1.4 Porosity (e)

The typical values of Porosity (e) are described by Domenico and Schwartz (1997). Values of Porosity for Gravel (0.24-0.38), Coarse Sand (0.31-0.46), and Fine Sand (0.26-0.53). However, the grain size in itself does not affect the value of porosity, as well-rounded, similarly packed sediments, notwithstanding their particle size, will maintain similar porosities.

4.1.5 Anisotropy (KH/KV)

According to the Design Standards, Embankment Dams /DS-13(8)-4.1(2014), the following permeability of various embankment materials has been listed.

Table 4. 2. Permeability of various embankment materials

Material	K_H/K_V Range	Reference
Embankment core	4 to 9	Cedergent, H.R. 1977., U.S. Army Corps of Engineers,1986. EM 1110-2-1901., Casagrande, A. 1940., Esmiol, E.E., 1977., Hirschfeld, R.C.1973.
Nonstandard placement	9 to 36	
Hydraulic fill	64 to 225	
Embankment shell	4 to 9	
Embankment shell	1 to 4	
Anisotropy (K_H/K_V) of embankment materials, K_H/K_V increases with placement water content		

4.1.6 Pore-Water Pressure Ratio (Ru)

A pore-water pressure ratio (Ru) value has been utilized to connect the overburden stress to pore water pressure during the computation of slope stability for stage construction and end of construction. The Ru value for non-free drained material is displayed in Table 4.3 and was taken from the project's design report (EEC, 2019).

Table 4.3. Pore-pressure ratio (EEC's Kalid Dijo dam design Report (2019)

Material zone	Pore-water pressure ratio Ru during of construction	Pore-water pressure ratio Ru at end of construction
Impervious Core (Zone 1)	0.40	0.35
Filter and Transition (Zone 2)	--	--
Granular Shell (Zone 3)	0.25	0.20
Rock Fill (Zone 4)	--	--
Riprap (Zone 5)	--	--
Toe Rock	--	--
Clay Blanket	0.40	0.35
Sandy Silty Clay	0.35	0.30
Foundation Rock	0.30--	0.25

4.1.7 Boundary Condition (BC)

Boundary conditions are essential for any analysis, including susceptible seepage problems on Seep/W. These conditions provide information about the behavior of the system at its boundaries, which is crucial for determining the solutions. In the case of seepage problems, the boundary conditions specify the hydraulic total head difference between two points or the specified flow rate into or out of the system. These conditions serve as the driving force behind the seepage flow, determining the direction and magnitude of the flow. Without these boundary conditions, it would be impossible to obtain a solution for the seepage problem. The behavior of the system would remain unknown, and there would be no way to predict or analyze the seepage flow. Therefore, specifying boundary conditions is crucial in the analysis of susceptible seepage problems on Seep/W. These conditions are the key factors that provide the necessary information for determining the solutions to these problems.

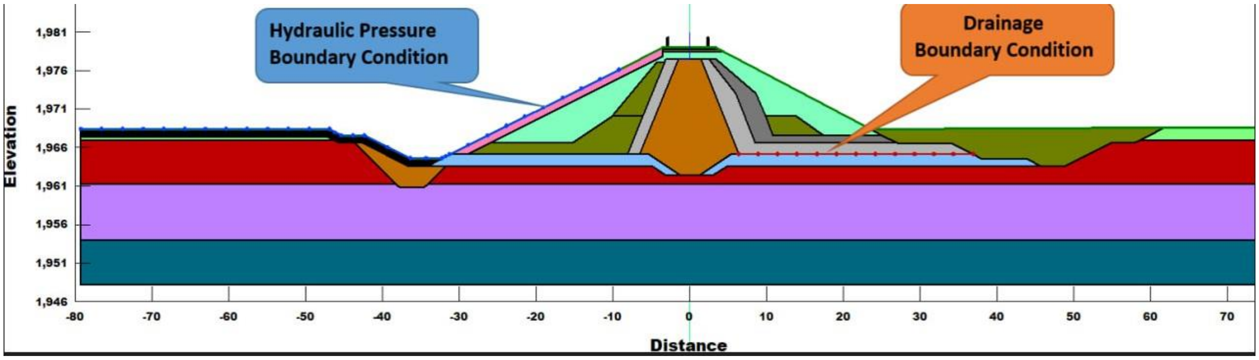

Figure 4. 3. Boundary condition during seepage analysis

4.2 Determining the Seepage Protection Options

According to EM 1110-2-1901, even though choosing a cutoff can be challenging and expensive, using a flow net system can help compare various under-seepage control techniques for a dam and its foundation. This allows engineers to assess the relative advantages and efficacy of each technique, aiding in the selection of the most suitable one. The flow nets system helps in understanding the flow patterns and potential areas of under-seepage, enabling a more informed decision-making process regarding the choice of under-seepage control measures. Therefore, it is important to analyze the steady seepage to understand the amount of water flowing through the embankment's foundation. This will help in calculating the pore water pressure within the foundation, which is crucial for the piping analysis. The steady seepage analysis will be conducted at five specific chainages - 0+640, 0+802.5, 1+123, 1+228, and 1+430.. These chainages were selected based on the geological profile of the foundation, which indicates the presence of multiple alluvial deposited layers with varying thicknesses. The presence of these layers increases the likelihood of abnormal seepage, which can lead to concentrated leakage and ultimately result in piping issues. Therefore, it is crucial to analyze the steady seepage to assess the potential seepage flow and pore water pressure within the foundation. By conducting these analyses, we can better understand the potential issues related to seepage and piping in the embankment's foundation. This information will be valuable for designing appropriate measures to address these problems and ensure the stability and integrity of the Kalid Dijo Dam.

According to the geological profile (Figure 3.12), the dam's foundation is highly exposed to abnormal seepage that is capable of passing large amounts of water. The seepage examination will determine the flux through the dam body and foundation, and the distribution of pore water pressure is crucial for a steady-state seepage study. The author provides five options other than the original designs for regulating seepage without piping, allowing for comparison, analysis, and selection of the minimum risk remedial measure.

The essential considerations while choosing a treatment method are the quantity of seepage, hydraulic gradient, safety factor, and cost. It appears that using a cutoff wall rather than a GC blanket is the better method of waterproofing the dam. The finite element technique and the Seep/W software were used to accomplish this aim. Using the numerical analysis approach, the Seep/W software is a finite element program that can theoretically simulate seepage (Krahn, 2009).

4.2.1 Seepage Control Options at Chainage 0+520 (At Borehole 2)

4.2.1.1. Option 1: Base Case

This option has been regarded as the base case or original design of the Kalid Dijo Dam. According to the geotechnical investigation, it has been recognized that the selected dam foundation has presented significant geotechnical challenges, rendering it susceptible to risks such as piping and erosion. These vulnerabilities have raised critical concerns regarding the foundation's stability and the overall safety of the dam.

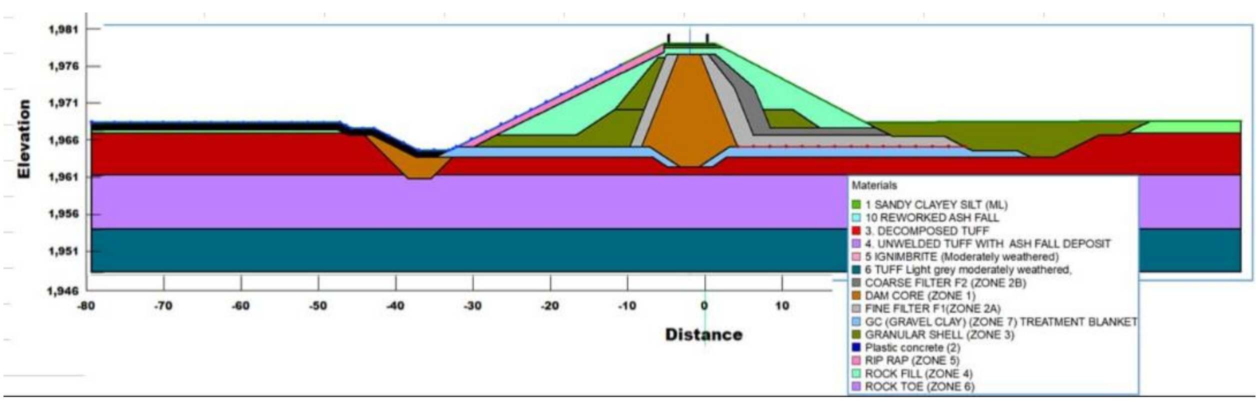

Figure 4. 4. Material defined at chainage 0+520 (Option 1:-Base Case)

The foundation, considered in the original design, is expected to undergo a thorough evaluation to better understand its performance and identify potential weaknesses. Further analysis has become necessary to address these geotechnical issues and assess their implications for water flow management.

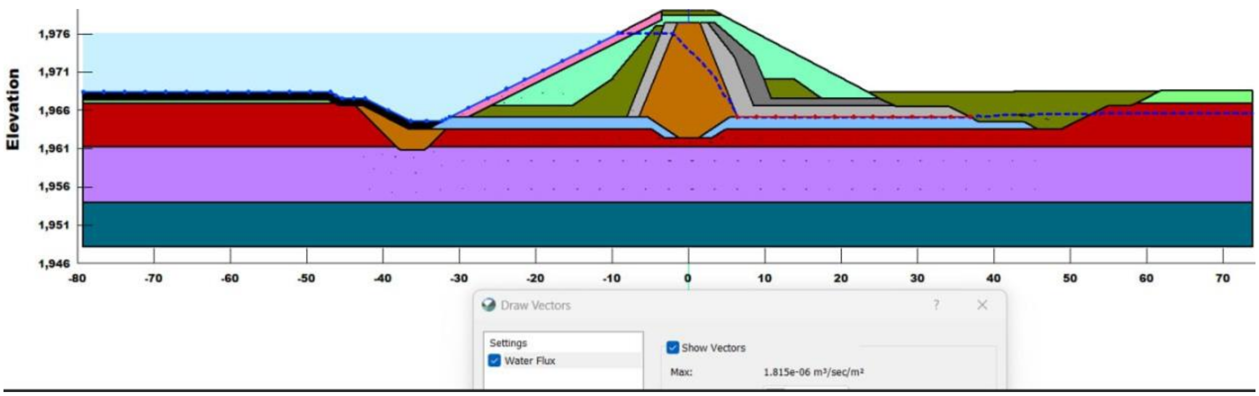

Figure 4. 5. Maximum water flux value at chainage 0+520 (Option 1:-Base Case)

As a result of the original design parameters, the calculated maximum water flux has been approximately 1.815 x 10^-6 m³/sec/m². This value serves as an important benchmark for understanding the hydraulic behavior of the dam, providing a reference point for any future modifications that may be required. The insights gained from this analysis will play a crucial role in informing subsequent design improvements aimed at ensuring the dam's long-term integrity and safety in light of the identified challenges.

4.2.1.2.Option 2

In this design option for the Kalid Dijo Dam, a cut-off slurry wall with a depth of 7 meters has been incorporated to improve the dam's effectiveness in controlling seepage. Additionally, the depth of the clay core has been increased by 1.9 meters, enhancing the dam's ability to retain water and reduce permeability. This modification aims to strengthen the overall structural integrity of the dam while minimizing the risk of water leakage. As a result of these design modifications, the calculated maximum water flux is approximately 3.6687 x 10^-7 m³/sec/m².

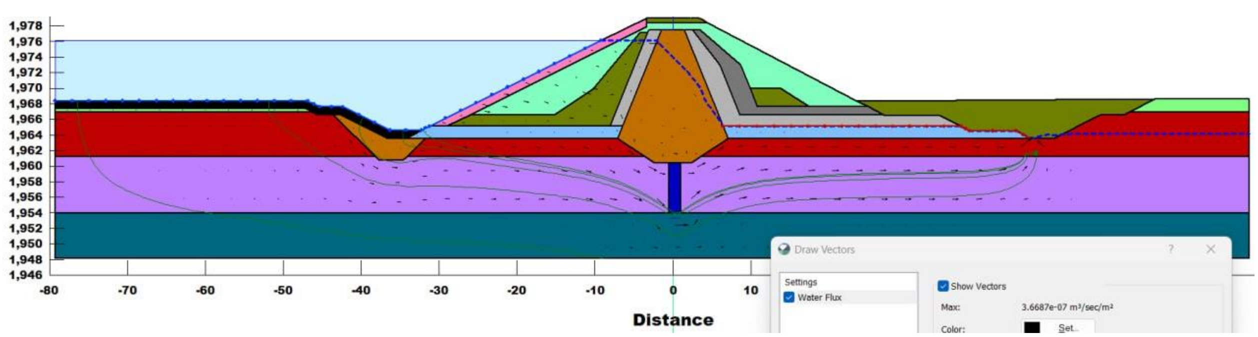

Figure 4. 6. Seepage control options at chainage 0+520 (Option 2)

4.2.1.3.Option 3

In this design option for the Kalid Dijo Dam, a cut-off slurry wall with a depth of 7 meters has been incorporated to enhance the dam's impermeability. Additionally, the depth of the clay core has been increased by 1.9 meters to further strengthen the dam's water retention capabilities. However, the upstream backfill cut-off, which was originally filled with clay, has been eliminated from the design. This decision was made based on the assessment that it did not result in a significant reduction in water flux discharge. Following these modifications, the calculated maximum water flux is approximately 3.68 x 10^-7 m³/sec/m². This value is crucial for understanding the hydraulic performance of the dam and ensuring its stability and efficiency in managing water flow. Optimizing the water flux is essential for maintaining the dam's stability and efficiency in managing reservoir levels.

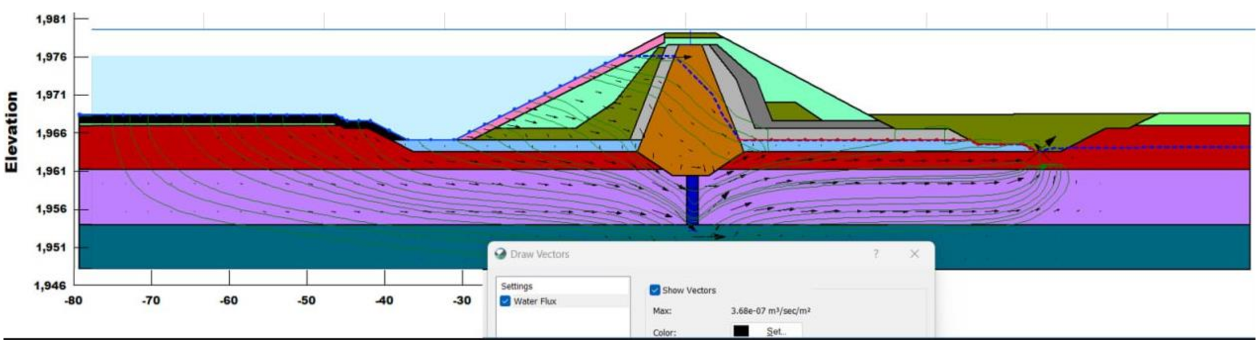

Figure 4. 7. Seepage control options at chainage 0+520 (Option 3)

4.2.2 Seepage Control Options at Chainage 0+770, (At Borehole-7)

4.2.2.1. Option 1: Base Case

This option represents the base case design of the Kalid Dijo dam at chainage 0+770 and borehole-7. It has been analyzed and has yielded a calculated maximum water flux of approximately 1.5566 x 10^-5 m³/sec/m². This assessment is intended to inform future modifications aimed at enhancing the dam's performance and safety.

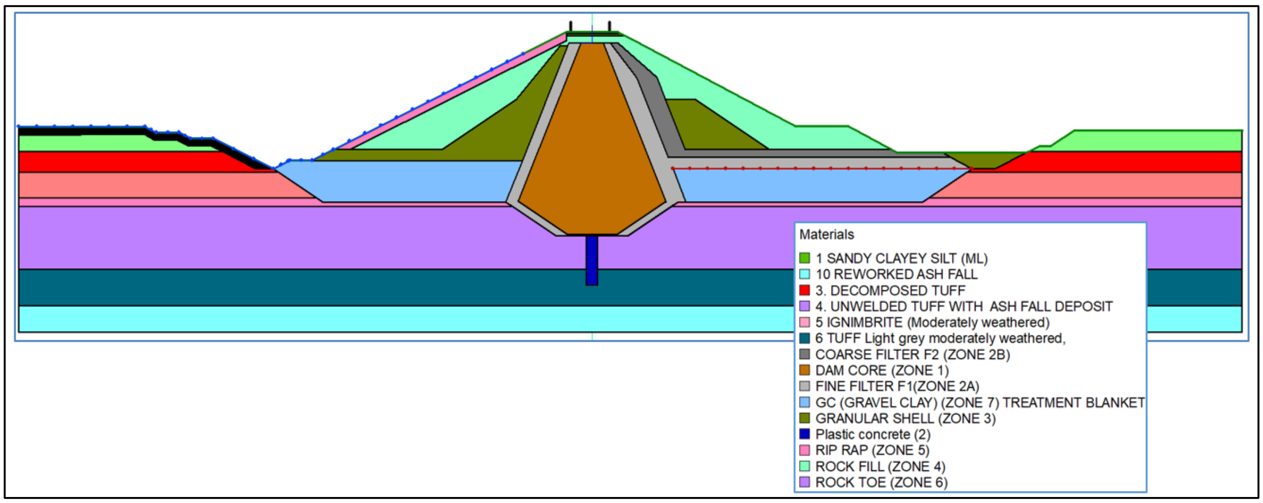

Figure 4. 8. Material defined at chainage 0+770 (Option 1:-Base Case)

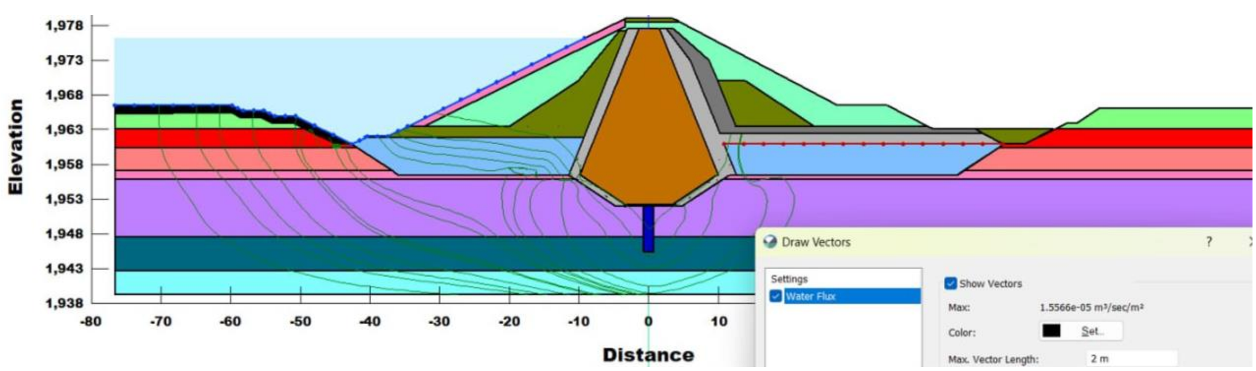

Figure 4. 9. Maximum water flux value at flux chainage 0+770 (Option 1:-Base Case)

Additionally, in this study and research, the design will undergo a detailed assessment to identify and address various geotechnical challenges, including the potential risks of piping and erosion. A thorough evaluation and further analysis of the original foundation design are anticipated to ensure the stability and integrity of the dam in light of these concerns.

4.2.2.2.Option 2

In this option, specifically at the chainage of 0+750 and borehole-7, the analysis has revealed that the maximum water flux discharge has become approximately 6.56 x 10^-7 m^3/sec/m^2. This outcome has been achieved by modifying the design to remove the filter material that was initially present in the foundation, which covered the clay core in the key trench.

This modification has been particularly significant given that the selected dam foundation presents geotechnical challenges, rendering it susceptible to risks such as piping and erosion. By addressing these issues through the removal of filter material, the design aims to enhance the stability and integrity of the foundation, ultimately improving the dam's overall performance in managing water flow. Future assessments will continue to focus on ensuring the foundation's resilience against the identified geotechnical risks.

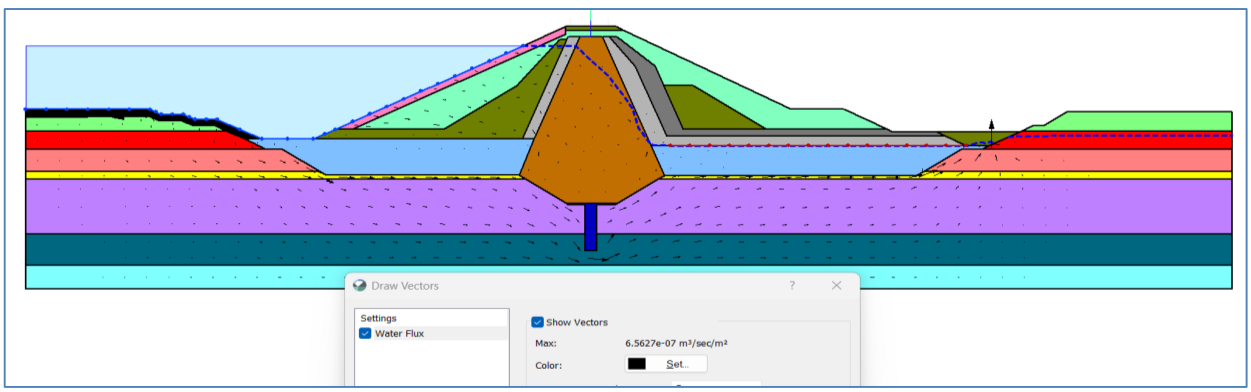

Figure 4. 10. Maximum water flux value at chainage 0+770 (Option 2)

4.2.3 Seepage Control Options at chainage 1+123 (At Borehole-8)

4.2.3.1. Option 1: Base Case/ Original design

As a foundational case in the evaluation and analysis process of the Kalid Dijo Dam design, the original design parameters were thoroughly reviewed to assess their performance. The resulting output for the maximum water flux discharge from this initial assessment was quantified at 5.2841 x 10^-7 m^3/sec/m^2.

This value represents the rate at which water can flow through the dam's foundation material, serving as a critical indicator of its permeability. Analyzing the maximum water flux is essential in determining the potential for seepage and the risk of internal erosion, both of which pose significant threats to the structural integrity of the dam.

By establishing this baseline measurement, subsequent design modifications and treatment evaluations can be effectively compared. Understanding the implications of this discharge rate forms the basis for identifying necessary improvements that ensure enhanced stability and safety of the dam over its operational lifespan.

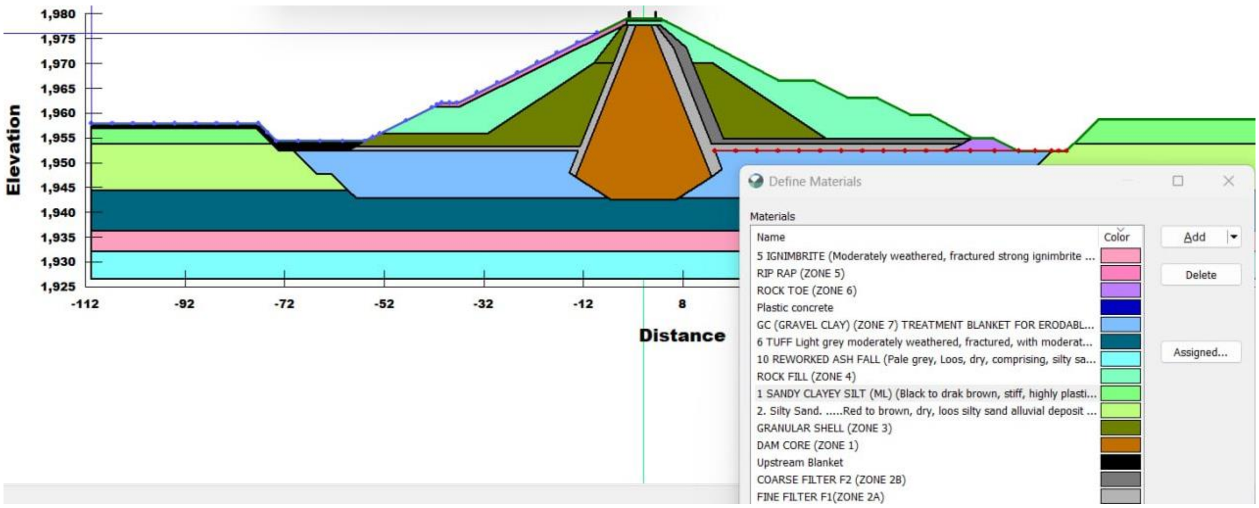

Figure 4. 11. Material define at chainage 1+123 (Option 1:-Base Case)

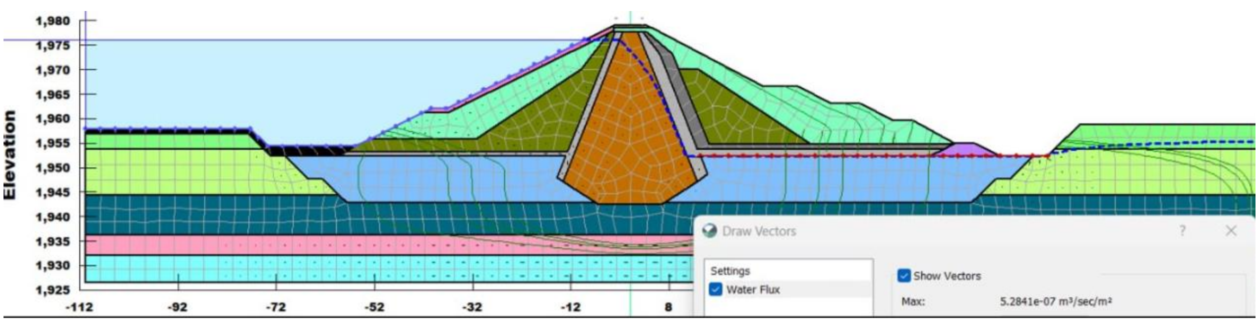

Figure 4. 12. Maximum water flux value at chainage 1+123 (Option 1:-Base Case)

4.2.3.2.Option 2

In this option, at a chainage of 1+123, the gravelly clay (GC) material has been modified to a thickness of 2 meters. This adjustment involved reducing the original design thickness by 8 meters and incorporating an additional 7 meters of cutoff slurry made from plastic concrete. The results of the seepage analysis indicate that the maximum water flux discharge is 5.6917 x 10^-7 $m^3/sec/m^2$.

This modification to the design aims to enhance the performance of the structure concerning water retention and seepage control. By reducing the thickness of the GC material, material usage is optimized while still achieving the necessary structural integrity and waterproofing. The introduction of the plastic concrete cutoff slurry serves to further mitigate potential seepage, creating a barrier that effectively reduces water flow through the structure.

The seepage analysis results are critical, providing insights into the efficacy of these modifications. A maximum water flux discharge of 5.6917 x 10^-7 $m^3/sec/m^2$ suggests that, under the given conditions, the sealing effect of the modified GC material and the added cutoff slurry is functioning well to limit water movement. These findings can inform future design decisions and adjustments, ensuring that the structure meets the required performance standards in its operational environment.

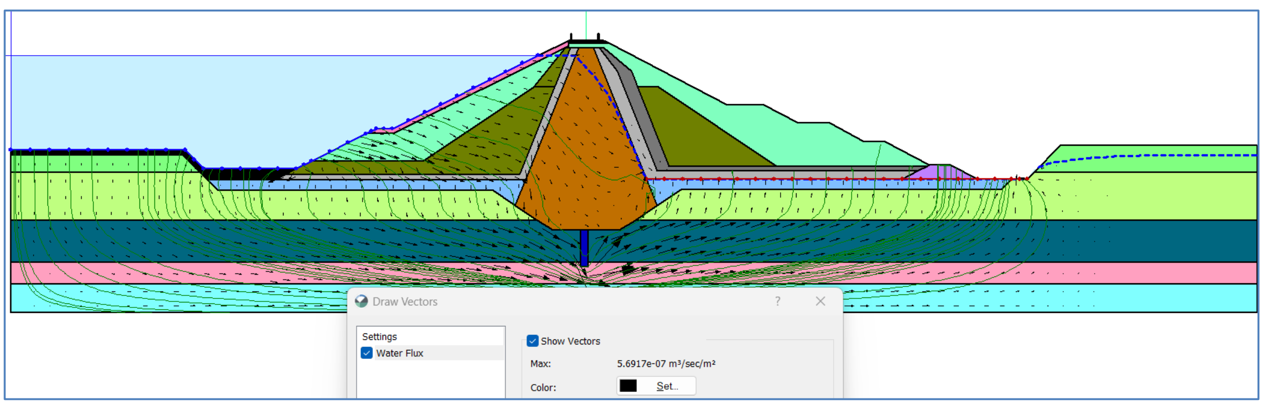

Figure 4. 13. Maximum water flux value at chainage 1+123 (Option 2)

4.2.3.3.Option 3

In the evaluation of the foundation treatment for the Kalid Dijo Dam, an additional 1-meter thickness of Clay Grave (GC) material has been incorporated into Option 2, which originally featured a 2-meter thickness. This modification elevates the total depth of the GC material to 3 meters.

As a result of this increased thickness, the calculated maximum water flux has been determined to be 5.075 x 10^-7 m³/sec/m². This measure is critical, as it reflects the permeability of the dam's foundation treatment and its ability to manage water flow effectively.

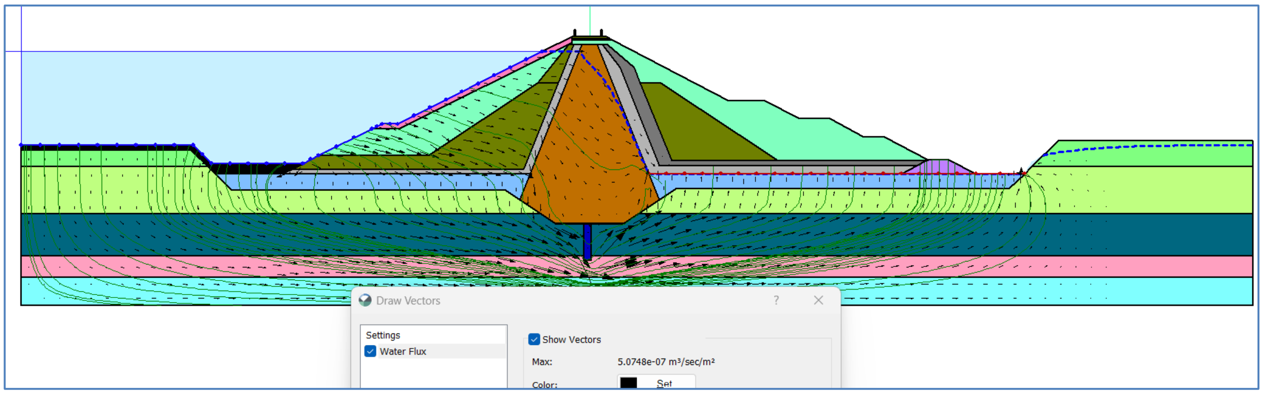

Figure 4. 14. Maximum water flux value at chainage 1+123 (Option 3)

4.2.3.4.Comparison of the Seepage Control Options-1, -2 and -3 at Chainage 1+123

When comparing the water flux outputs among all three design options, the discharge values are as follows:

Option 1: 5.2841 x 10^-7 m³/sec/m²

Option 2: 5.6917 x 10^-7 m³/sec/m²

Option 3: 5.075 x 10^-7 m³/sec/m²

From this comparison, it is evident that Option 3 exhibits the lowest water flux rate of 5.075 x 10^-7 m³/sec/m². This reduced flux indicates enhanced performance in terms of containment against internal erosion and piping—a critical concern in dam design. Lower water flux values are typically associated with improved structural integrity and reduced risk of seepage or failure.

Consequently, Option 3 is identified as the safest alternative for the dam due to its effectiveness in mitigating potential internal erosion and ensuring long-term stability. This assessment underscores the importance of optimizing foundation treatments in dam design to achieve both safety and durability.

4.2.4 Seepage Control Options at Chainage 1+228 (At Borehole-4)

4.2.4.1. Option 1:-Base Case/ Original design

In Option 1, during the evaluation of the original design's foundation treatment blanket utilizing Clay Gravel (GC), at chainage 1+228 and borehole 4, the calculated water flux was determined to be 3.221 x 10^-6 m³/sec/m².

This output result is instrumental for the research, as it provides a baseline for comparing subsequent proactive options aimed at enhancing the foundation's safety and stability. By analyzing the water flux, the study can effectively assess risks associated with internal erodibility and piping, which are critical factors in ensuring the structural integrity of the dam.

Overall, the findings from this evaluation will inform decisions regarding potential improvements to the foundation treatment, ultimately contributing to the long-term reliability of the Kalid Dijo Dam.

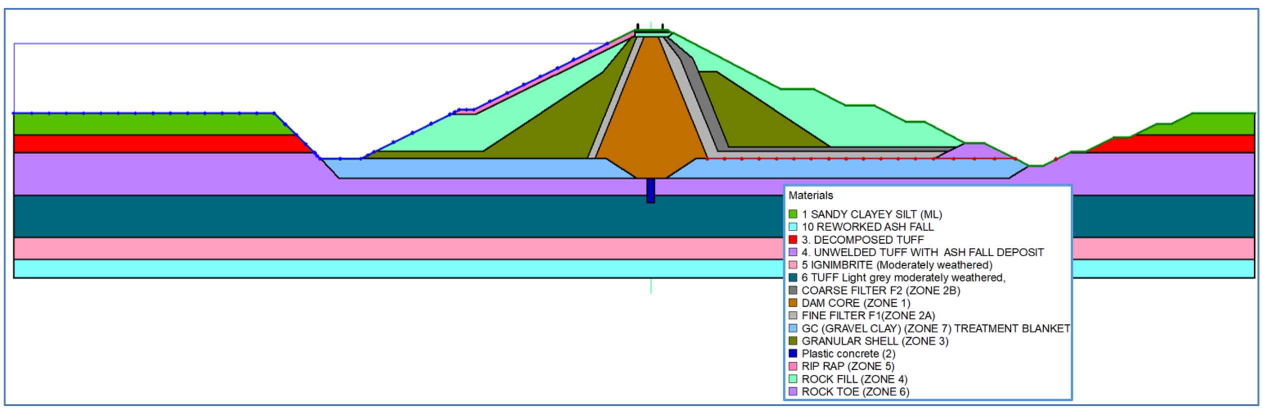

Figure 4. 15. Material defined at chainage 1+123 (Option 1:-Base Case)

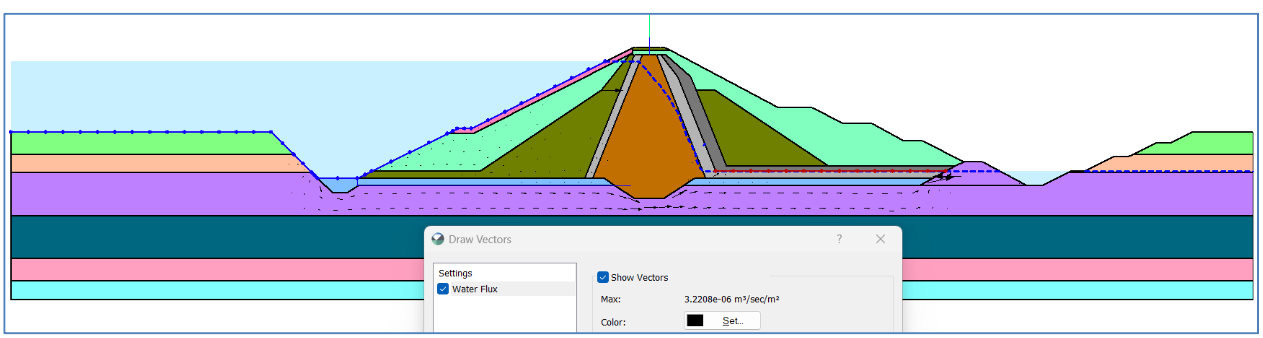

Figure 4. 16. Maximum water flux value at chainage 1+228, (Option 1:-Base Case)

4.2.4.2.Option 2:-

In this proactive study evaluating the foundation treatment for the Kalid Dijo Dam, Option 2 was explored, which incorporates two integrated approaches. The first method involves adding a 2.8 m layer of Gravel Clay (GC) to the original design, resulting in a total GC thickness of 4.28 m. The second approach consists of a 5 m cutoff slurry plastic concrete layer.

Following a comprehensive analysis of the foundation treatment methods, the maximum water flux discharge was determined to be 4.81 x 10^-7 m^3/sec/m^2 for Option 2. This represents a significant improvement in water retention capabilities compared to the original design, which exhibited a maximum discharge rate of 3.2208 x 10^-6 m^3/sec/m^2.

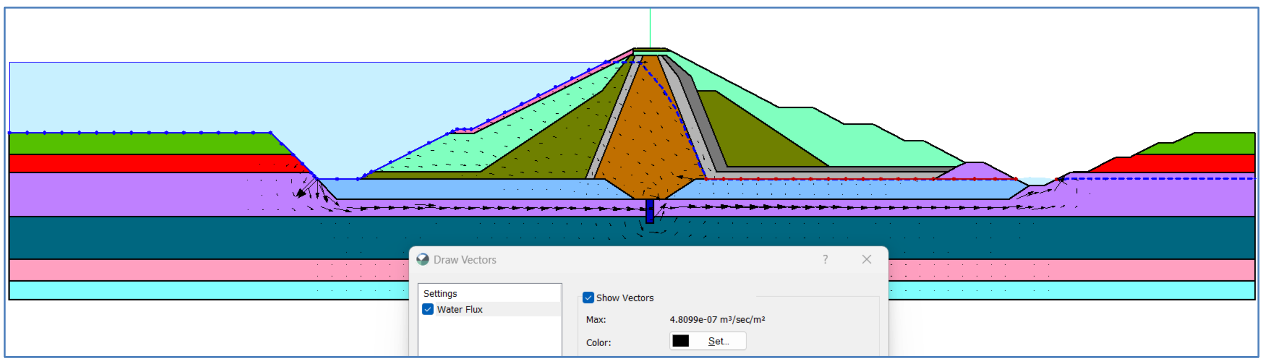

Figure 4. 17. Maximum water flux value at chainage 1+228 (Option 2)

4.2.4.3. Comparison of the Seepage Control Options -1 and -2 at Chainage 1+228

When comparing the water flux outputs among the two options at chainage 1+228, the discharge values are as follows:

Option 1: 3.221 x 10^-6 m^3/sec/m^2

Option 2: 4.81 x 10^-7 m^3/sec/m^2

From this comparison, it is evident that Option 2 exhibits the lowest water flux rate of 4.81 x 10^-7 m^3/sec/m^2. Thus, the water flux discharge for Option 2 is considerably safer and more effective than that of the original design.

Based on these findings, Option 2 has been selected as the preferred treatment solution for the foundation of the Kalid Dijo Dam.

4.2.5 Seepage Control Options at Chainage 1+670 (At Borehole-6)

4.2.5.1. Option 1:- Base Case /Original Design/

At chainage 1+670, located at Borehole 6, an evaluation of the original design was conducted to thoroughly assess its structural integrity and capacity to safeguard against internal erosion and piping. This assessment aimed to identify an alternative option that could enhance the foundation's safety and performance.

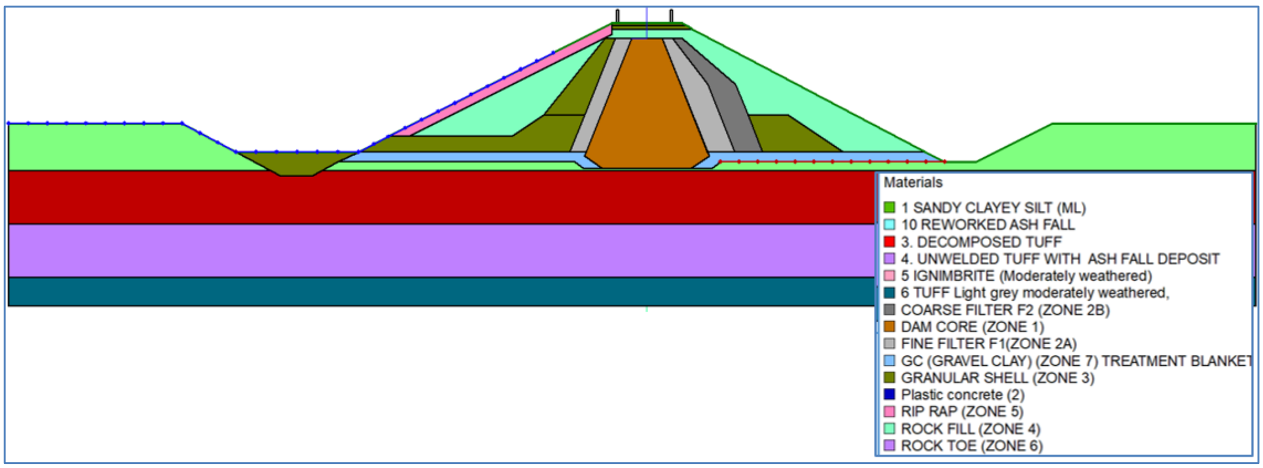

Figure 4. 18. Seepage Control Options at chainage 1+670, (Option 1:-Base Case)

Utilizing Geo-Studio 2022 for the modeling analysis, key performance metrics were obtained. The maximum water flux discharge was determined to **be 6.6949 x 10^-7 m³/sec/m².** This result underscores the need for further investigation and potential modifications to the original design, as high water flux values can indicate susceptibility to internal erosion and diminish the dam's overall stability.

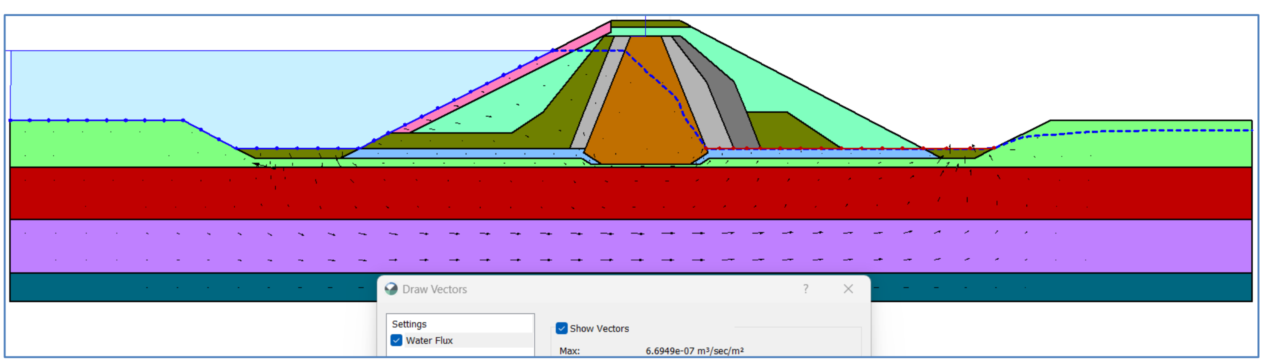

Figure 4. 19. . Seepage Control Options at chainage 1+670,(Option 1:-Base Case)

In light of the above findings based on option 1, exploring additional foundation treatment options is crucial to ensure the long-term effectiveness and safety of the Kalid Dijo Dam.

4.2.5.2.Option 2

In this alternative design for chainage 1+670, the evaluation of the original design, as presented in the preceding research report, indicated the necessity for modifications to enhance the foundation's performance.

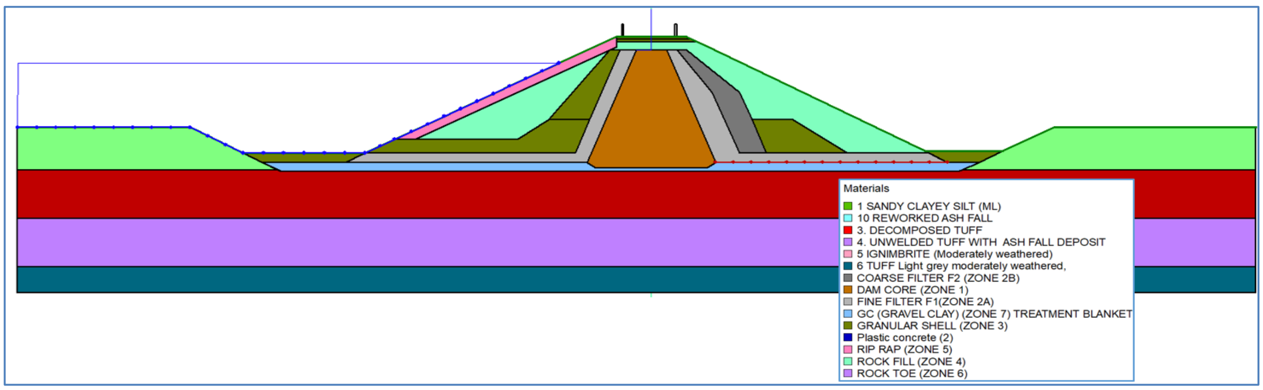

Figure 4. 20. . Material Define at chainage 1+670,(Option 2)

To address potential issues related to internal erosion and piping, a 1-meter layer of Gravel Clay (GC) was introduced immediately beneath the dam body, as depicted in the modified drawings.

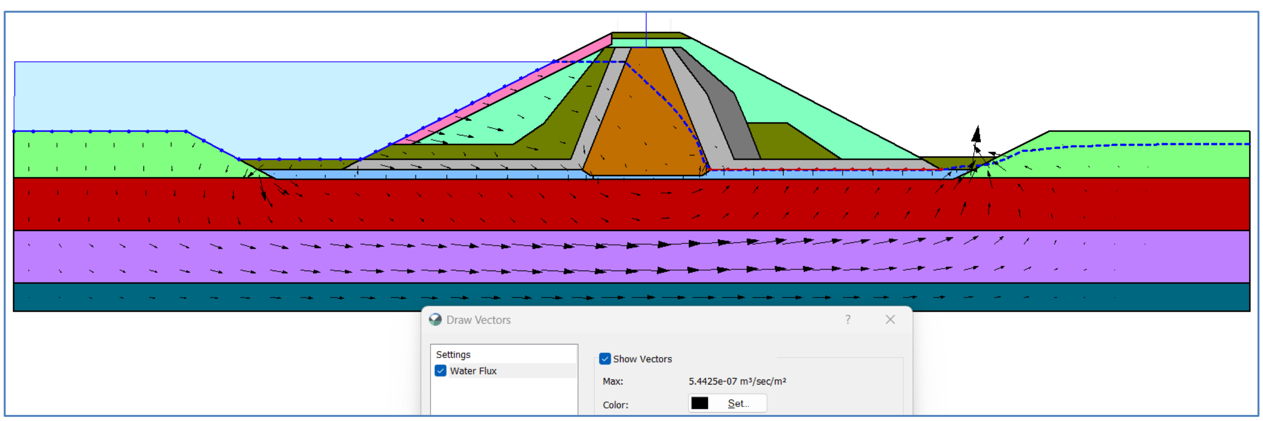

Figure 4. 21 Maximum water flux value at chainage 1+670 (Option 2)

According to the analysis conducted using Geo-Studio 2022, the maximum water flux discharge for this revised design was calculated to be 5.44 x 10^-7 m³/sec/m². This result represents a significant improvement over the original design, which recorded a maximum water flux discharge of 4.003 x 10^-6 $m^3/sec/m^2$.

4.2.5.3.Recommended Treatment Option

It is observed that the proposed design (Option-2) demonstrates a marginal reduction in water flux, with a value of 5.44 x 10^-7 $m^3/sec/m^2$, in comparison to the original design (Option-1), which exhibits a flux of 6.6949 x 10^-7 $m^3/sec/m^2$. Although this indicates a slight improvement, the magnitude of the difference is not sufficiently significant to justify the replacement of the original design. Consequently, it is recommended to maintain the use of the original design (Option 1) in its current form.

4.2.6 Summary of Enhanced Dimensions for Evaluating Foundation Treatment

This research provides a comprehensive summary of the enhanced dimensions developed for evaluating the foundation treatment of the Kalid Dijo dam. The following accompanying drawings (figures 4.21 to 4.25) have been meticulously crafted and compiled to illustrate the finalized cross-sections relevant to the dam's foundation treatment strategy.

These illustrations reflect the recommended remedial measures, which have been carefully derived from the seep/w steady-state analysis performed using Geo-Studio 2022. The analysis output has been reviewed for each selected chainage, ensuring that the proposed cross sections are well-supported by quantitative data and tailored to address specific conditions observed in the dam's foundation.

Furthermore, these finalized drawings are intended to serve as a critical reference for the next phase of the research, which involves the execution of a steady-state assessment of slope stability. This assessment will employ advanced numerical methods to carry out a thorough evaluation of the dam's stability, resilience, and overall performance under varying conditions. The integration of these analytical approaches aims to enhance the understanding of the foundation treatment's effectiveness and to provide actionable insights for potential improvements in the dam's design and maintenance strategy.

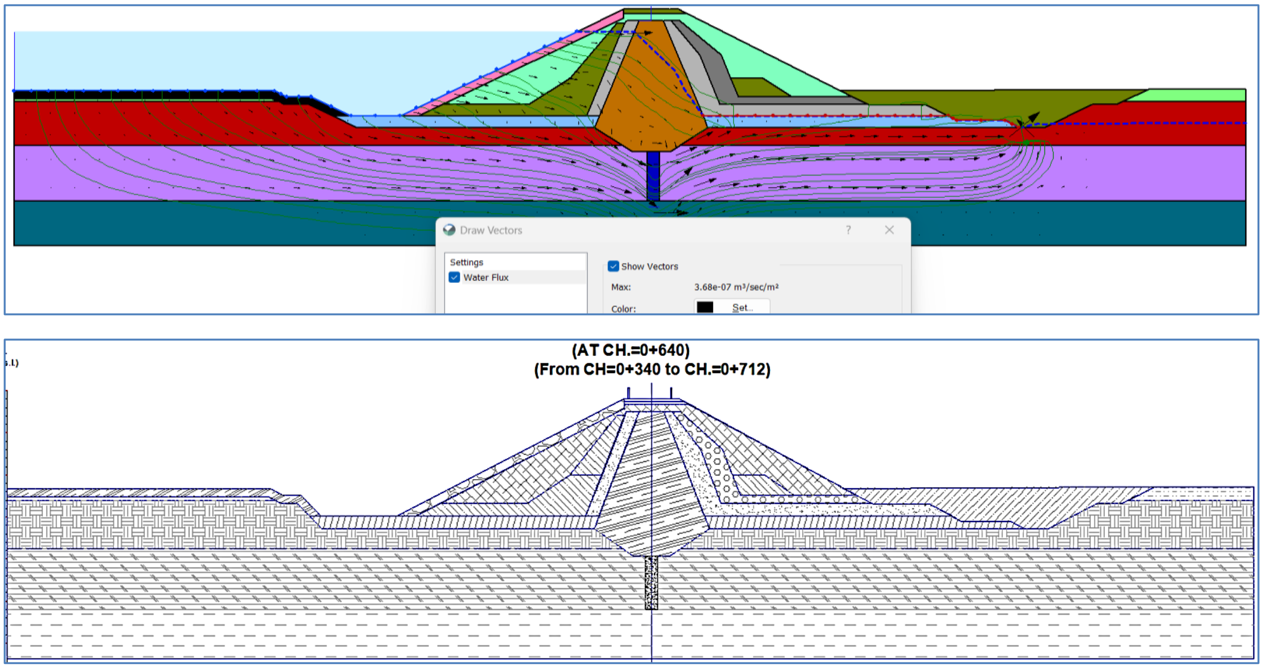

Figure 4. 22. Summary of enhanced dimensions for evaluating foundation treatment of (Borehole 2)

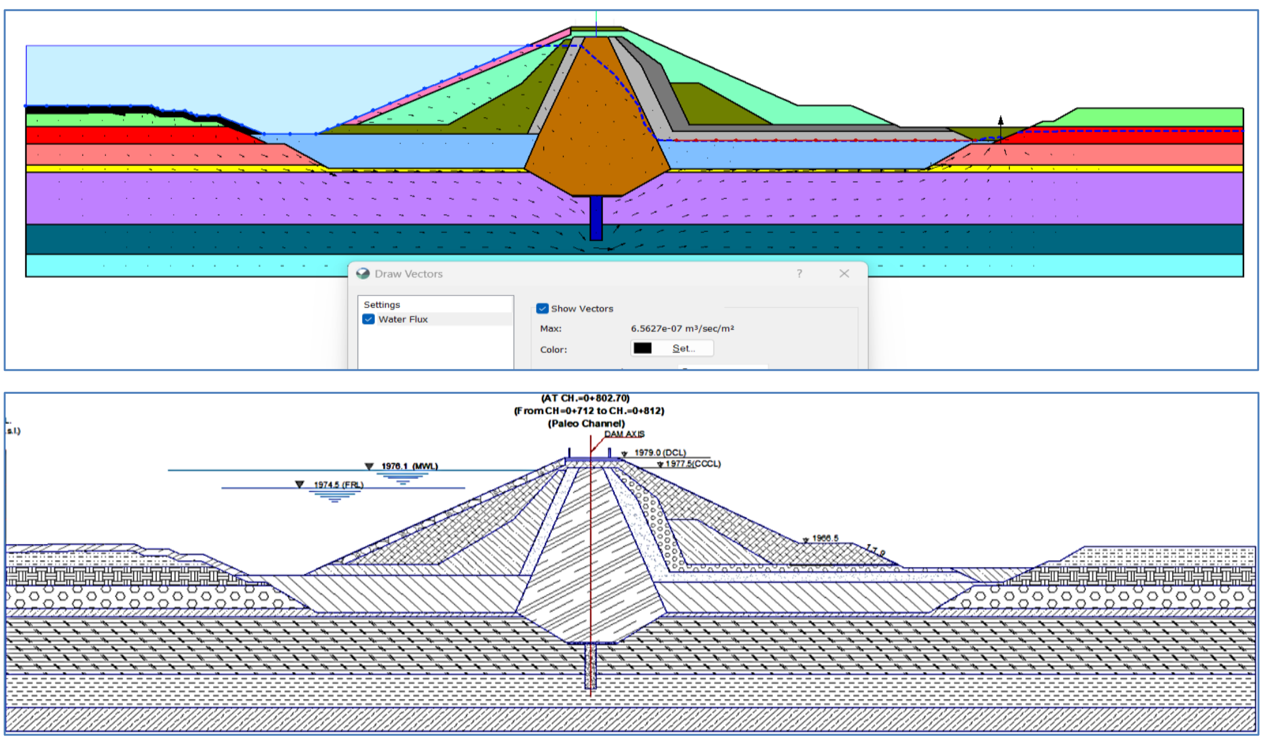

Figure 4. 23. Summary of Enhanced Dimensions for Evaluating Foundation Treatment of (Borehole 7)

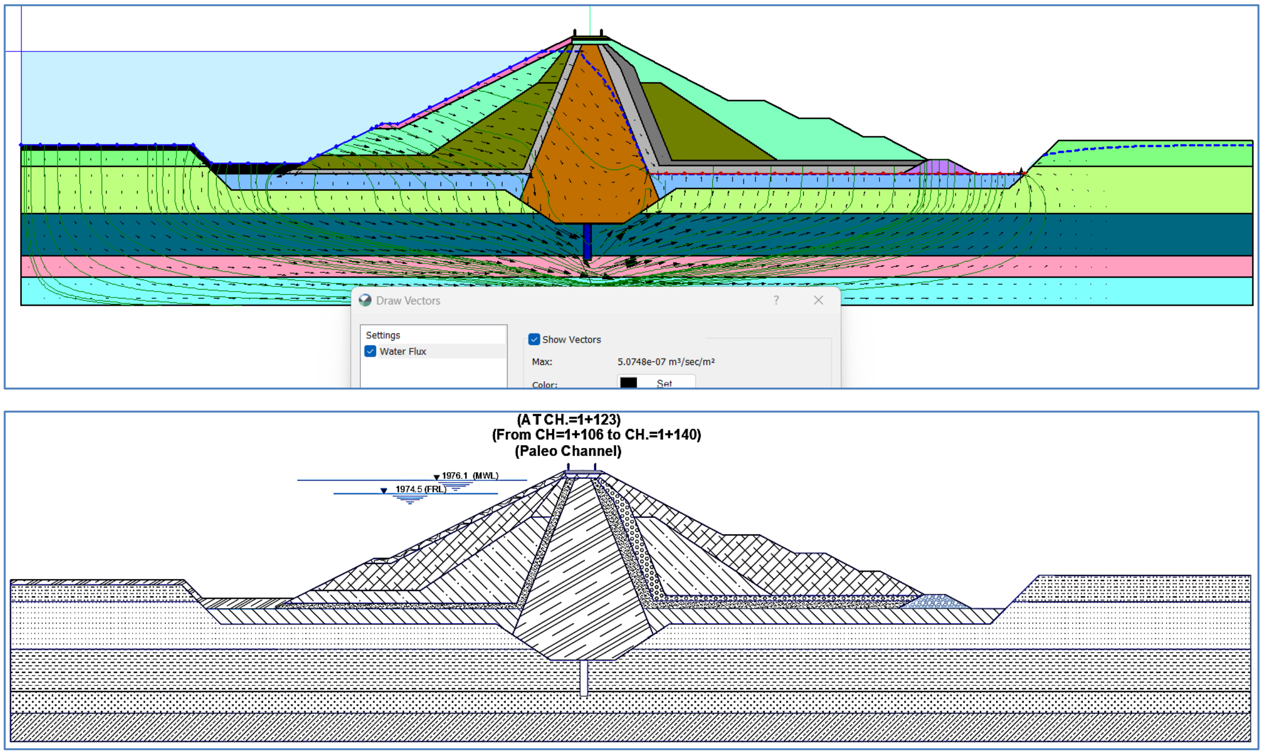

Figure 4. 24. Summary of Enhanced Dimensions for Evaluating Foundation Treatment of (Borehole 8)

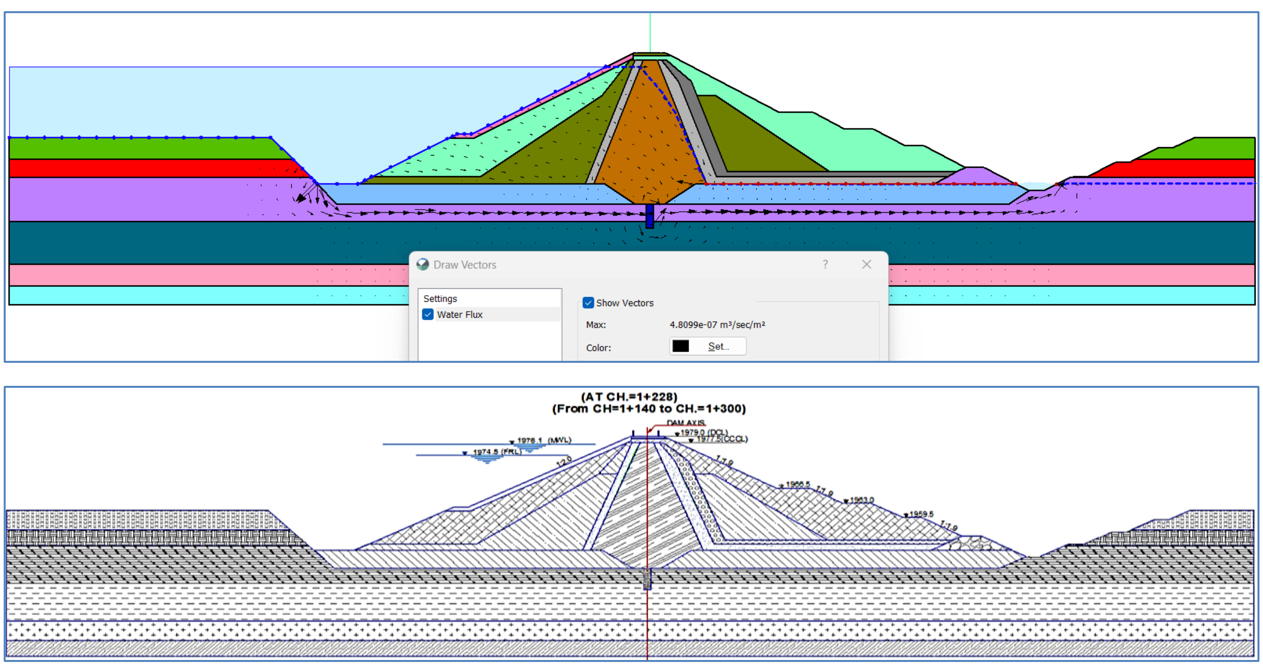

Figure 4. 25. Summary of Enhanced Dimensions for Evaluating Foundation Treatment of Borehole 4

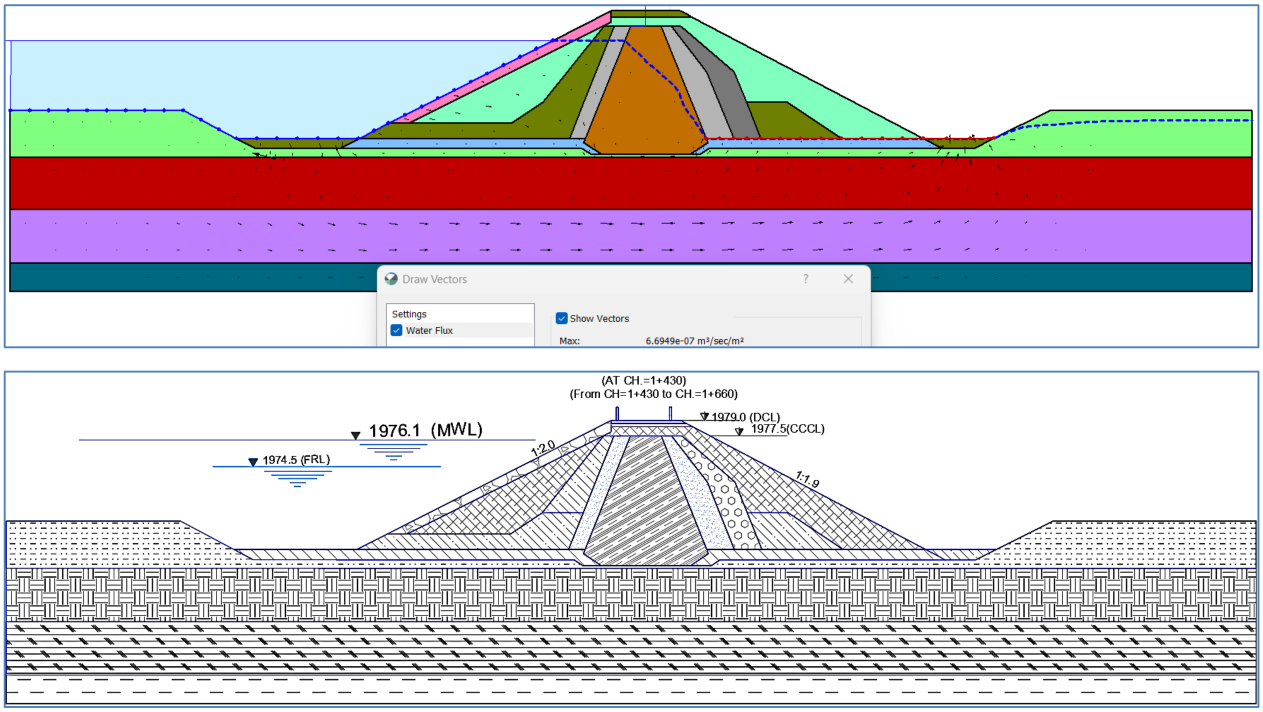

Figure 4. 26. Summary of Enhanced Dimensions for Evaluating Foundation Treatment of Borehole 6

Table 4. 4. Summary of Results

BH	Option	Maximum waterFlux m3/sec/m2	Remark
2	1	1.815 x 10^-6	
	2	3.6687 x 10^-7	
	3	3.68 x 10^-7	Recommended
7	1	1.5566 x 10^-5	
	2	6.56 x 10^-7	Recommended
8	1	5.2841 x 10^-7	
	2	5.6917 x 10^-7	
	3	5.075 x 10^-7	Recommended
4	1	3.2208 x 10^-6	
	2	4.81 x 10^-7	Recommended

4.3 Slope Stability Analysis

4.3.1 Input Data/Parameters Used for Stesdy state Slope stability Analysis

(a) Dam Geometry

When choosing the most vulnerable section for Steady state slope stability analysis, the thickness of the alluvium deposit and section size have to be taken into consideration.

(b) Geotechnical parameters

The following data have been utilized by referring to the EEC Geotechnical report and other standards: cohesion, angle of internal friction, relative density, fines, and unit weight. All of the data that were cited have been listed in the table below.

Table 4.5. Kalid Dijo dam summarized input data/parameters

Function	Unit Weight (KN/m^3)	Permeability (m/s)	C'(KPa)	ϕ'(o)
Core	18.0	3.56×10^{-8}	90	18
Fine filter	20.0	1×10^{-4}	0.0	30
Coarse filter	20.0	1×10^{-3}	0.0	32
Granular shell	18.0	5.2×10^{-5}	5.0	30.0
Rock fill	22.0	1×10^{-2}	0.0	40.0
Riprap	22.0	1×10^{-2}	0.0	42.0
Rock Toe	20.0	1×10^{-3}	0.0	38.0
Sandy Clayey Silt	16.0	1×10^{-7}	80.0	18.0
Foundation Rock class IV	20.0	2.1×10^{-6}	50.0	20.0
Foundation Rock class II	Bed rock impenetrable	2.62×10^{-7}	Bed rock impenetrable	

Table 4.6. Summary of laboratory results of soil samples taken from boreholes

BH-ID	Depth (m)	Grain size analysis (%)				Sp.gr	Unit Wt	Atterberg limit		
		Clay	Silt	Sand	Gravel			LL	PL	PI
DDBH-02	4.30-5.00	3.22	70.25	25.63	0.9	2.4	1.34	33.84	Non-PL	_
	10.25-11.00	9.47	66.86	22.43	1.24	2.39	1.31	34.3	29.17	5.13
DDBH-04	6.00-6.70	3.85	65.55	29.68	0.92	2.38	1.21	32	Non-PL	_
	9.00-9.80	6.02	66.9	26.58	0.5	2.37	1.24	40.96	36.94	4.02
	12.00-12.40	9.28	56.8	33.46	0.47	2.55	1.32	29.6	Non-PL	_
DDBH-06	7.20-8.00	11.14	70.15	18.35	0.35	2.45	1.83	40	27.78	12.22
	11.60-12.70	7.99	66.09	24.66	1.26	2.39	1.51	34.3	Non-PL	_
DDBH-07	5.85-6.55	15.07	53.9	30.85	0.19	2.42	1.74	36.5	Non-PL	_
	13.00-13.70	5.86	68.9	27.89	0.35	2.45	1.63	33.5	Non-PL	_
DDBH-08	4.50-5.15	43.06	42	14.29	0.65	2.52	2.13	57.82	29.74	28.08
	8.00-8.25	26.23	59.12	14.45	0.21	2.54	1.92	52.5	34.79	17.71

4.3.2 Steady State Slope Stability Analysis: Chainage 0+640

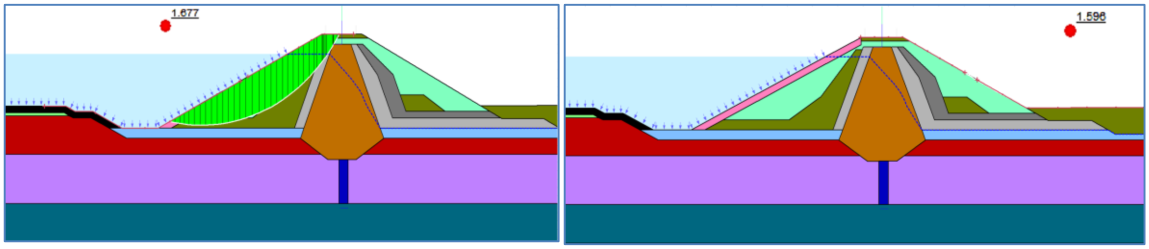

Figure 4. 27. Steady state slope stability for section at chainage of 0+640

The steady-state slope stability analysis conducted at the specific location with a chainage of 0+640 yielded critical safety factor values of 1.677 for the upstream slope and 1.598 for the downstream slope. These safety factors represent the ratio of resisting forces (such as soil shear strength) to driving forces (like gravity) acting on the slopes under static conditions. A safety factor greater than 1.5 indicates that the slopes have sufficient stability to withstand current conditions and are unlikely to experience failure. In this case, both slopes exhibit safety factors significantly above this critical threshold, which suggests that they are in a stable and secure condition at this particular location. The slightly higher safety factor for the upstream slope indicates a marginally greater margin of safety compared to the downstream slope. These results provide confidence that the slopes are structurally sound and capable of resisting potential failure mechanisms such as sliding or collapse under existing static loads. However, it is important to note that these safety margins should be periodically reviewed, especially if environmental factors or loading conditions change over time. Overall, the analysis confirms that the slopes at chainage 0+640 are currently safe, reducing the risk of slope failure and supporting ongoing infrastructure stability in the area.

4.3.3 Steady State Slope Stability Analysis: Chainage 0+802.5 (BH-7)

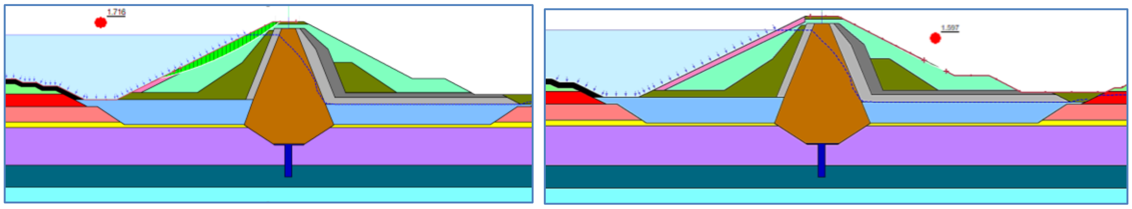

Figure 4. 28. Steady state slope stability for the section at the chainage of 0+802.7

The steady-state slope stability analysis at chainage of 0+802.7 yielded critical safety factor values of 1.716 for the upstream slope and 1.597 for the downstream slope. These safety factors serve as indicators of the slope's ability to withstand gravitational and other forces without failure. Typically, a safety factor greater than 1.5 signifies that the slope is stable under static conditions, with higher values indicating greater stability margins. In this case, both slopes have safety factors significantly above the threshold, suggesting that they are currently stable and pose minimal risk of failure under steady-state conditions. The slightly higher safety factor on the upstream side reflects a marginally greater stability margin compared to the downstream side, but overall, the analysis confirms that the slopes are safe and unlikely to experience instability or failure during normal, static conditions. This stability assessment is crucial for ensuring the long-term safety and integrity of the slope-related structures and the surrounding environment.

4.3.4 Steady State Slope Stability Analysis: Chainage 1+123(BH-8)

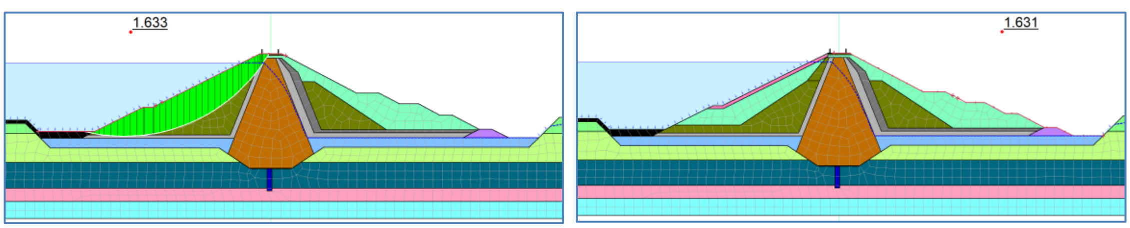

Figure 4. 29. Steady state slope stability for section at the chainage of 1+123

The steady-state slope stability analysis at chainage 1+123 produced critical safety factor values of 1.633 for the upstream slope and 1.631 for the downstream slope. These safety factors serve as key indicators of the slopes' ability to resist failure under static conditions, where the forces acting on the slopes remain constant over time. Typically, a safety factor greater than 1.5 signifies that the slope is stable, with higher values indicating a greater margin of safety. In this case, both slopes have safety factors well above the minimum threshold, suggesting they are reliably stable under current static conditions. The close similarity between the two values indicates that both the upstream and downstream slopes possess comparable stability margins. Overall, these results confirm that the slopes are safe, with a sufficient safety buffer to prevent failure under normal static loads. This assessment provides confidence in the long-term stability and integrity of the slopes, reducing concerns about potential landslides or structural failures that could compromise safety or infrastructure.

4.3.5 Steady State Slope Stability Analysis: Chainage 1+228 (BH-4)

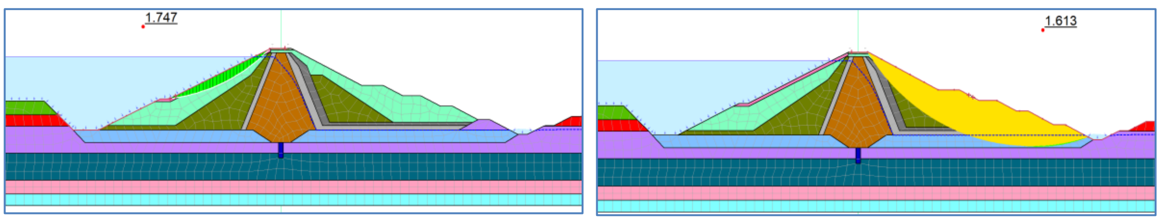

Figure 4. 30. Steady state slope stability for section at the chainage of 1+228

The steady-state slope stability analysis at chainage of 1+228 resulted in critical safety factor values of 1.747 for the upstream slope and 1.613 for the downstream slope. These safety factors are quantitative measures of the slopes' capacity to resist failure under static conditions, where external loads and environmental factors are constant over time. A safety factor greater than 1.5 indicates that the slope has sufficient strength to withstand the forces acting upon it, with higher values reflecting a greater margin of stability. In this case, both the upstream and downstream slopes exhibit values well above the minimum threshold, suggesting they are stable and unlikely to fail under current conditions. Notably, the upstream slope has a slightly higher safety factor, implying it is marginally more stable compared to the downstream slope. Overall, these results confirm that the slopes are safe and possess adequate stability margins to prevent failure under static loading scenarios. This assessment provides confidence that the slopes can maintain their integrity over time, minimizing risks related to landslides or structural instability, and ensuring safety for the surrounding environment and infrastructure.

4.3.6 Steady State Slope Stability Analysis: Chainage 1+430 (BH-6)

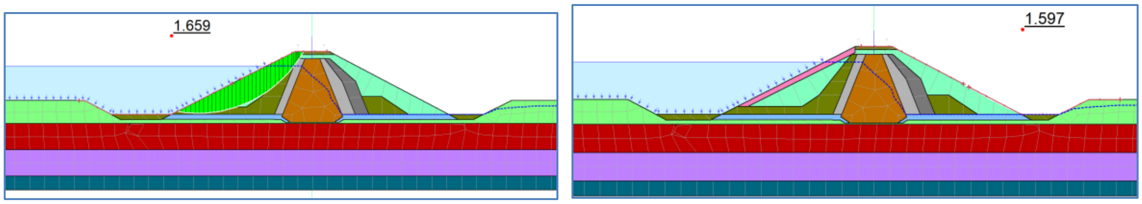

Figure 4. 31. Steady state slope stability for the section at the chainage of 1+430

The steady-state slope stability analysis at chainage of 1+430 produced critical safety factor values of 1.656 for the upstream slope and 1.597 for the downstream slope. These safety factors represent the ratio of resisting forces to driving forces acting on the slopes under static conditions, providing an indication of their overall stability. A safety factor greater than 1.5 signifies that the slopes have sufficient strength to prevent failure when subjected to constant loads and environmental factors. In this case, both the upstream and downstream slopes exhibit safety factors well above this critical threshold, indicating they are stable and unlikely to experience failure under current conditions. The slightly higher safety factor for the upstream slope suggests it has a marginally greater margin of stability compared to the downstream slope. These results confirm that the slopes are in a safe condition, with adequate stability margins to withstand static loads and environmental influences such as rainfall or minor seismic activity. Overall, the analysis provides confidence that the slopes are structurally sound, reducing the risk of landslides or other failure modes. It also underscores the importance of continued monitoring to maintain these safety margins over time and ensure ongoing stability in the face of changing environmental conditions or potential future loads.

4.3.7 Summary of Slope Stability Analysis Results

The static slope stability analyses at multiple locations (chainages 0+640, 0+802.7, 1+123, 1+228, and 1+430) show that both upstream and downstream slopes have safety factors well above the critical threshold of 1.5, indicating stable and secure conditions under current static loads. Generally, the safety factors range from approximately 1.6 to 1.75, with upstream slopes exhibiting slightly higher margins of safety than downstream slopes. These results confirm the slopes are unlikely to fail under static conditions, supporting long-term stability and infrastructure safety. Regular monitoring is recommended to maintain these safety margins amid environmental or load changes.

4.4 Estimation of Hydraulic Gradient and Factor of Safety

The empirical calculation procedures developed by Bligh (1910) and Lane (1935) are, in theory, designed for pipe inspection.

$C = L/h$ Eq.4.1

Where: C = the weighted creep ratio

L is the length of the seepage path, and h represents the overall head loss.

$h = h1 - h2$ Eq.4.2

$i_{cr} = (G_s - 1)(1 - n)$; $n = \frac{e}{1 + e}$; $i_{cr} = \frac{G_s - 1}{1 + e}$; $e = \frac{n}{1 - n}$; $i_e = (h_1 - h_2)/L$; $FS = \frac{i_{cr}}{i_e}$	Eq.4.3
Where; **Gs** = Specific Gravity; **e** = Void Ratio; **n** = Porosity; i_{cr} = Critical Gradient; i_e = Exit Gradient; h_1 = U/S hydraulic head; h_2 = D/S hydraulic head; **L** = Length flow path; **FS** = Factor of Safety	

Specific Gravity from the Report at different depths of KDBH	Porosity from reference for Gravel (0.24-0.38), Coarse Sand (0.31-0.46), and Fine Sand (0.26-0.53).
Table 4.7. G. Specific gravity from EEC's report	*Table 4. 8. n.Porosity from the standard reference*

Average Specific Gravity(G) from Report @ KDBH

BH 2	2.395
BH 7	2.435
BH 8	2.53
BH 4	2.46
BH 6	2.42
Average	**2.448**

Porosity – n (%)

Porosity 1	0.31
Porosity 2	0.39
Porosity 3	0.40
Average	**0.36**

- Using the above tabulated referenced data, a critical gradient has been calculated.

$$\mathbf{icr = (Gs-1)\,(1-n) = (2.448-1)*(1-0.36) = 0.927}$$

- Exit gradient has also been calculated for each flow path, and then, to check the safety of the foundation, the weighted creep ratio(C) has been computed based on the aforementioned formula and as computed in the following tables 4.10, 4.11, 4.12, and 4.13.

4.4.1 Calculation of Factor of Safety

(a) Calculation of Factor of Safety at Chainage 0+640

To determine the factor of safety, essential data were extracted from the Seep/W-Steady State model. Two key parameters were focused on: the flow travel distance and the water flux. These parameters are crucial for understanding the movement of water through the subsurface and assessing the stability of the system.

Using the view button within the model interface, relevant result information was accessed, providing detailed insights into the hydraulic behavior of the system. The flow travel distance indicates how far water has moved through the soil or geological layers, while the water flux measures the rate at which water is passing through a given area.

This step is vital for ensuring and validating the remedial measures and recommended foundation treatment and evaluation that have been done in this research and thesis.

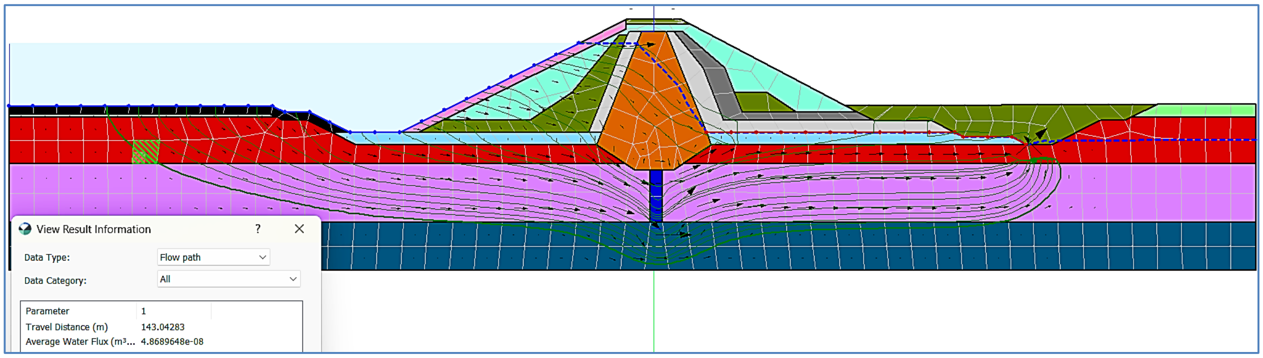

Figure 4. 32. Flow path at chainage of 0+640

Second Step:

Measure the depth of hydraulic head from upstream (h1) and downstream (h2), and then calculate the difference between the two heads, which it became symbolized as H, as shown in the next tabulated table.

Third step:

- Using the above tabulated referenced data (table G and n), a critical gradient has been calculated for each flow path (flow travel distance).

$$\mathbf{icr = (Gs-1)(1-n)}$$

- Exit gradient has also been calculated for each flow path and then, to check the safety of the foundation, the factor of Safety(FS) and the weighted creep ratio(C) have been computed based on the aforementioned formula and as computed in the following Tables 4.7, 4.8,4.9, 4.10, and 4.11.

Table 4.9. Calculation of factor of safety at chainage of 0+640

BH= 2 @ Chainage 0+640							
Flow No.	**Flow Travel Distance (m)**	**Water Flux (m^3/sec/m^2)**	**H**	**iex**	**icr**	**FS**	**C**
1	**143**	**4.87E-08**	11.02	0.08	0.893	**11.6**	**13.0**
2	**133**	**6.72E-08**	11.02	0.08	0.893	**10.8**	**12.1**
3	**124**	**8.74E-08**	8.52	0.07	0.893	**13.0**	**14.5**
4	**112**	**1.14E-07**	7.74	0.07	0.893	**12.9**	**14.5**
5	**96**	**1.16E-07**	7.74	0.08	0.893	**11.1**	**12.4**
AVG						**11.9**	**13.3**

The critical exit hydraulic gradient, the factor of safety, and the weighted creep ratio have been assessed and computed based on the results of the Seep/W flow route distance and water flux discharge. After comparing it to the safety factor value of 11.19, it was discovered that the average weighted creep ratio at chainage 0+640 is 13.31. Consequently, in terms of critical gradient and outflow, seepage beneath the chainage is vulnerable to pipes.

(b) Calculation of Factor of Safety at chainage of 0+802.7

To calculate the factor of safety, first flow travel distance and water flux were provided from the model (Seep/W-Steady State) from view button and result information, as following diagram.

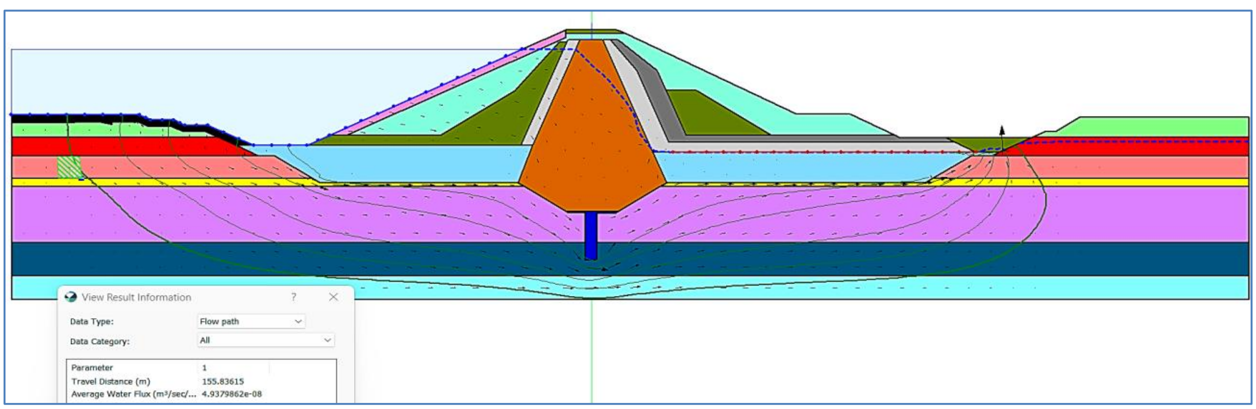

Figure 4. 33. Flow path at chainage of 0+802.7

The second and third steps of the process have been repeated in the same manner as the steps were executed at chainage 0+802.7.

Table 4.10. Calculation of factor of safety at chainage of 0+802.5

BH=7 @ Chainage 0+802.5							
Flow No.	**Flow Travel Distance (m)**	**Water Flux ($m^3/sec/m^2$)**	**H**	**iex**	**icr**	**FS**	**C**
1	**155.8**	**4.94E-08**	9.66	0.06	0.918	**14.8**	**16.1**
2	**137.4**	**6.82E-08**	9.66	0.07	0.918	**13.1**	**14.2**
3	**130.2**	**8.56E-08**	10.42	0.08	0.918	**11.5**	**12.5**
4	**108.2**	**1.04E-07**	14.2	0.13	0.918	**7.0**	**7.6**
5	**92.8**	**1.02E-07**	14.2	0.15	0.918	**6.0**	**6.5**
AVG						**10.5**	**11.4**

The critical exit hydraulic gradient, safety factor, and weighted creep ratio have been evaluated and calculated based on the Seep/W flow path distance and water flux discharge results. Upon comparison with the safety factor of 10.5, it was found that the average weighted creep ratio at chainage 0+802.5 is 11.40. As a result, regarding the critical gradient and water outflow, the seepage beneath this chainage is susceptible to pipe failure. Therefore, in terms of critical gradient and exit, the seepage beneath this segment is resistant to pipe-related issues.

(c) Calculation of Factor of Safety at chainage of 1+123

To calculate the factor of safety first, flow travel distance and water flux were provided from the model (Seep/W-Steady State) from the view button and result information, as the following diagram.

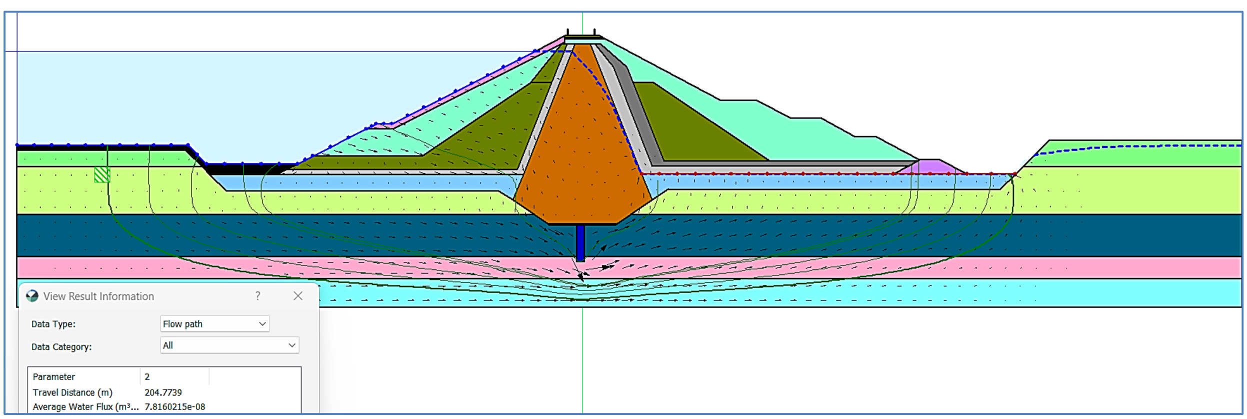

Figure 4. 34. Flow path at chainage of 1+123

The second and third steps of the process have been repeated in the same manner as the steps were executed at chainage 1+123.

Table 4.11. Calculation of the factor of safety at a chainage of 1+123

BH=8 @ Chainage 1+123							
Flow No.	**Flow Travel Distance (m)**	**Water Flux ($m^3/sec/m^2$)**	**H**	**iex**	**icr**	**FS**	**C**
1	**204.8**	**7.82E-08**	18.27	0.09	0.979	**11.0**	**11.2**
2	**188.6**	**8.18E-08**	18.27	0.10	0.979	**10.1**	**10.3**
3	**171.8**	**8.48E-08**	21.87	0.13	0.979	**7.7**	**7.9**
4	**152.4**	**6.12E-08**	21.87	0.14	0.979	**6.8**	**7.0**
5	**148.8**	**6.85E-08**	21.87	0.15	0.979	**6.7**	**6.8**
AVG						**8.5**	**8.6**

Using the Seep/W flow path distance and water flux discharge data, the critical exit hydraulic gradient, safety factor, and weighted creep ratio were computed. At chainage 1+123, the average weighted creep ratio was found to be 8.63 in comparison to the safety factor of 8.5. Water outflow and the crucial gradient make the seepage beneath this chainage vulnerable to pipe failure. Thus, with relation to the critical gradient and exit, seepage in this region is impervious to pipe-related problems.

(d) Calculation of Factor of Safety at chainage of 1+228

To determine the factor of safety, the flow travel distance and water flux were obtained from the Seep/W-Steady State model using the view button and result information, as illustrated in the following diagram.

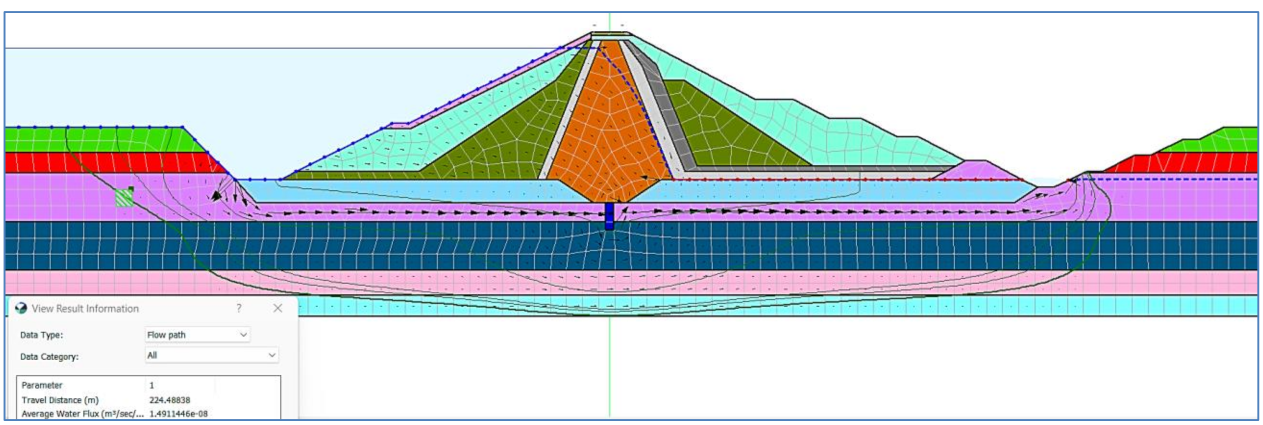

Figure 4. 35. Flow Path at chainage of 1+228

Table 4.12. Calculation of factor of safety at chainage of 1+228

BH=4 @ Chainage 1+228							
Flow No.	**Flow Travel Distance (m)**	**Water Flux ($m^3/sec/m^2$)**	**H**	**iex**	**icr**	**FS**	**C**
1	**224.48838**	**1.49E-08**	14.83	0.07	0.934	**14.1**	**15.1**
2	**207.66136**	**2.01E-08**	14.83	0.07	0.934	**13.1**	**14.0**
3	**199.28325**	**2.36E-08**	14.83	0.07	0.934	**12.6**	**13.4**
4	**175.99753**	**6.26E-08**	24.56	0.14	0.934	**6.7**	**7.2**
5	**117.76278**	**1.80E-16**	24.56	0.21	0.934	**4.5**	**4.8**
AVG						**10.2**	**10.9**

Based on the findings of the Seep/W flow route distance and water flux discharge, the critical exit hydraulic gradient, the factor of safety, and the weighted creep ratio have been evaluated and calculated. The average weighted creep ratio at chainage 1+228 was found to be 10.91 after being compared to the safety factor value of 10.20. Seepage under the chainage is therefore impervious to pipes in terms of critical gradient and discharge. In terms of critical gradient and egress, seepage under the chainage is therefore impenetrable to pipes.

(e) Calculation of Factor of Safety at Chainage of 1+430

To determine the factor of safety, key data were extracted from the Seep/W-Steady State model, focusing on flow travel distance and water flux. These parameters are essential for understanding subsurface water movement and system stability. The model interface provided detailed insights into hydraulic behavior, with flow travel distance indicating how far water has moved through soil layers and water flux measuring the rate of water passage through a specific area. Analyzing these parameters enables an accurate calculation of the factor of safety, which is crucial for evaluating the original foundation treatment, stability, and validating remedial measures and recommended foundation treatments proposed in the research.

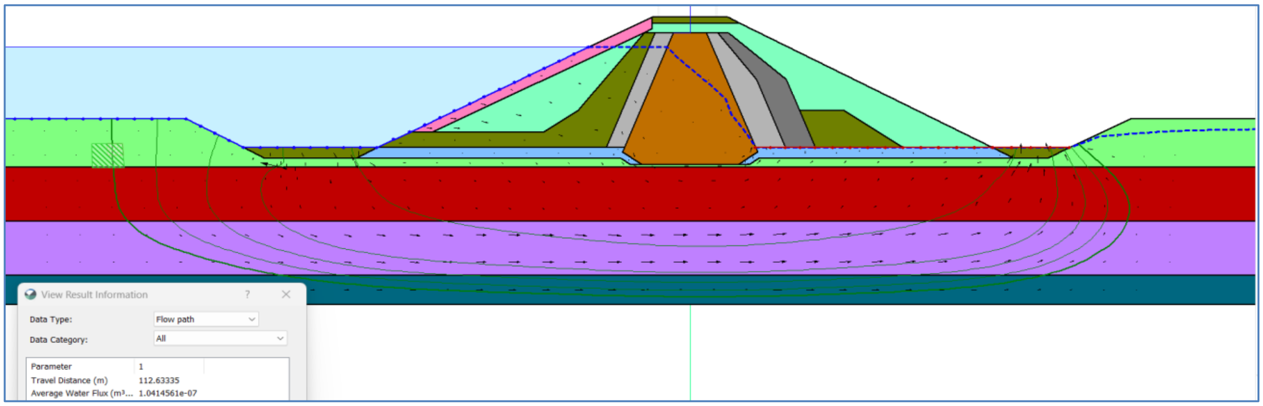

Figure 4. 36. Flow path at chainage of 1+430

Table 4.13. Calculation of factor of safety at chainage of 1+430

BH=6 @ Chainage 1+430							
Flow No.	**Flow Travel Distance**	**Water Flux ($m^3/sec/m^2$)**	**H**	**iex**	**icr**	**FS**	**C**
1	**108.5668**	**1.41E-07**	6.9	0.06	0.909	**14.3**	**15.7**
2	**109.3697**	**1.54E-07**	6.9	0.06	0.909	**14.4**	**15.9**
3	**100.8651**	**1.76E-07**	8.3	0.08	0.909	**11.0**	**12.2**
4	**81.48043**	**1.77E-07**	9.7	0.12	0.909	**7.6**	**8.4**
5	**68.28171**	**1.30E-07**	9.7	0.14	0.909	**6.4**	**7.0**
AVG						**10.8**	**11.8**

The Seep/W flow route distance and water flux discharge values have been used to evaluate and calculate the critical exit hydraulic gradient, the factor of safety, and the weighted creep ratio. It was found that the average weighted creep ratio at chainage 1+430 is 11.80 after comparing it to the safety factor value of 10.80. This makes seepage under the chainage susceptible to pipes in terms of critical gradient and outflow. As a result, seepage beneath the chainage is not susceptible to pipes in terms of exit and critical gradient.

4.4.2 Comparing and Analyzing the Maximum and Individual Water Flux

In this thesis and research that focused on the Kalid Dijo Dam, a comprehensive comparison and analysis of water flux data derived from the Seep/W model was conducted. This analysis serves as a validation of the findings, particularly in relation to the effectiveness of the proposed remedial measures and foundation treatments.

Table 4.14. Individual flow and maximum water flux from draw vectors

BH=2 @ Chainage 0+640

BH= 2 @ Chainage 0+640		
Flow No.	Flow Travel Distance (L)	Water Flux
	m	(m^3/sec/m^2)
1	143	4.87E-08
2	133	6.72E-08
3	124	8.74E-08
4	112	1.14E-07
5	96	1.16E-07

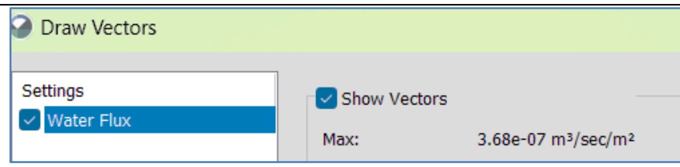

3.68e^{-07} m^3/sec/m^2 is more dischargable than the individual flow paths of water flux that are listed in Table A

BH=7 @ Chainage 0+802.5

BH=7 @ Chainage 0+802.5		
Flow No.	Flow Travel Distance (L)	Water Flux
	m	(m^3/sec/m^2)
1	156	4.94E-08
2	137	6.82E-08
3	130	8.56E-08
4	108	1.04E-07
5	93	1.02E-07

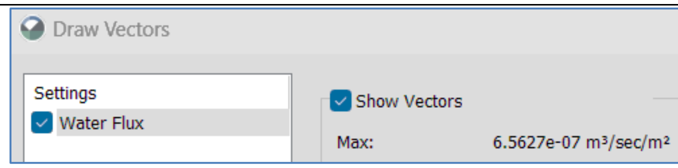

6.5627e^{-07} m^3/sec/m^2 is more dischargable than the individual flow paths of water flux that are listed in Table A

Table-a…..Individual flow path with water flux

Table-b…..Maximum Water Flux from Draw Vectors

BH=8 @ Chainage 1+123

BH=8 @ Chainage 1+123		
Flow No.	Flow Travel Distance (L)	Water Flux
	m	(m^3/sec/m^2)
1	205	7.82E-08
2	189	8.18E-08
3	172	8.48E-08
4	152	6.12E-08
5	149	6.85E-08

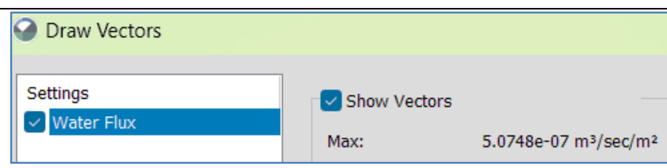

5.0748e^{-07} m^3/sec/m^2 is more dischargable than the individual flow paths of water flux that are listed in Table A

Table-a…..Individual flow path with water flux

Table-b…..Maximum Water Flux from Draw Vectors

BH=4 @ Chainage 1+228

BH=4 @ Chainage 1+228		
Flow No.	Flow Travel Distance (L)	Water Flux
	m	($m^3/sec/m^2$)
1	224	1.49E-08
2	208	2.01E-08
3	199	2.36E-08
4	176	6.26E-08
5	118	1.80E-16

Table-a…..Individual flow path with water flux

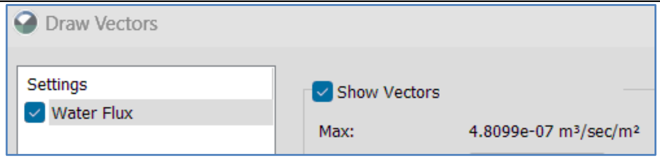

$4.8099e^{-07}$ $m^3/sec/m^2$ is more dischargable than the individual flow paths of water flux that are listed in Table A

Table-b…..Maximum Water Flux from Draw Vectors

BH=6 @ Chainage 1+430		
Flow No.	Flow Travel Distance (L)	Water Flux
	m	($m^3/sec/m^2$)
1	113	1.04E-07
2	105	1.23E-07
3	96	1.56E-07
4	87	2.08E-07
5	67	2.16E-07

Table-a…..Individual flow path with water flux

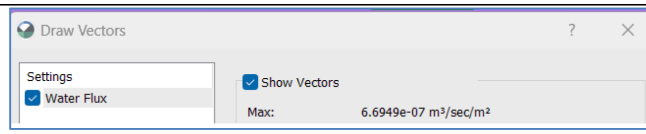

$6.6949e^{-07}$ $m^3/sec/m^2$ is more dischargable than the individual flow paths of water flux that are listed in Table A

Table-b…..Maximum Water Flux from draw Vectors

(a) Validation Through Water Flux Comparison:

The assessment involved examining the modeled maximum water flux from draw vectors and individual water flux values obtained from five distinct flow paths extending from the upstream to the downstream areas of the dam. As illustrated in the attached figures in the above sub-section, the output results clearly indicate that the maximum water flux is significantly higher than the individual water flux values associated with each flow path..

(b) Implications for Remedial Measures:

The observation that the maximum water flux exceeds the values associated with individual flow paths highlights the critical need for the recommended remedial actions. The elevated water flux, which may surpass the maximum flux generated from the draw vectors, indicates potential risks related to soil erosion and piping that could compromise the structural integrity of the dam.

Consequently, after thoroughly evaluating the original design, the proposed remedial measures and foundation treatments in this research are not only appropriate but also represent a proactive strategy for mitigating these risks.

By implementing these solutions, it is anticipated that the dam's resilience against unforeseen soil erosion and piping phenomena will be enhanced. The analysis provides strong evidence that these interventions will contribute to a safer and more stable structure, ultimately minimizing risks associated with groundwater movement and ensuring the long-term functionality of the Kalid Dijo Dam.

In conclusion, this research highlights the significance of thorough hydrological modeling in informing engineering decisions. The validation of the findings through water flux comparisons reinforces confidence in the proposed solutions, which are essential for safeguarding the dam against potential hydraulic failures.

4.4.3 Comparing the Discharge in Percentage

(a) Comparing the Discharge of the Original and Recommended Design at Chainage 0+640

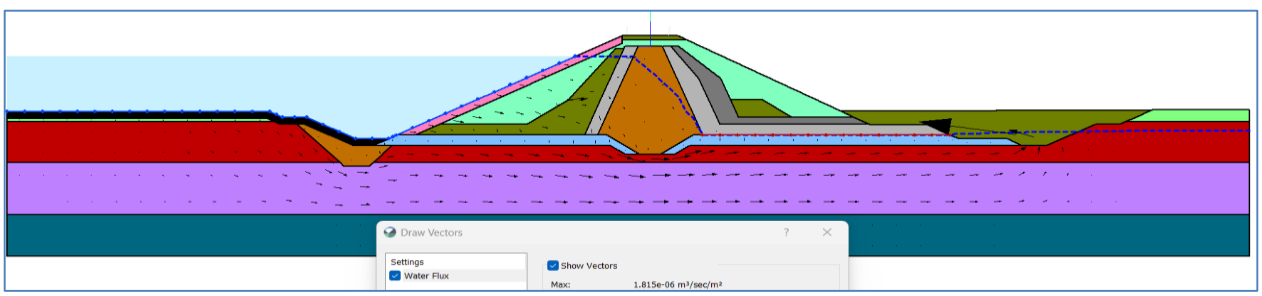

(a) The original design maximum discharge from the model is 1.815e^{-06} m^3/sec/m^2

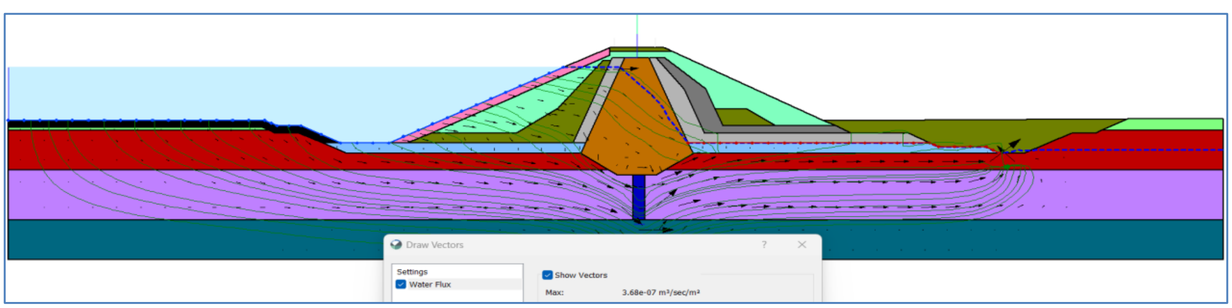

(b) Recommended foundation treatment's maximum discharge from the model is **3.68e^{-07}m^3/sec/m^2**

Figure 4. 37. Comparing the discharge of the original and recommended design at chainage 0+640

Calculate the percentage difference with the updated values.

Find the Difference:

Subtract the output result discharge from the original design discharge to see the reduction:

Difference = 1.815×10−6 m3/sec/m2−3.68×10−7 m3/sec/m2

To perform the subtraction, it's helpful to have the exponents of 10 the same. Let's convert 3.68×10−73.68 \times 10^{-7}3.68×10−7 to have an exponent of −6:

3.68×10−7=0.368×10−6

Now subtract:

Difference = 1.815×10−6 m3/sec/m2−0.368×10−6 m3/sec/m2

Difference = (1.815−0.368)×10−6 m3/sec/m2

Difference = 1.447×10−6 m3/sec/m2

Calculate the Percentage Difference:

Divide the difference by the original design discharge and multiply by 100:

Divide the difference by the original design discharge and multiply by 100:

$$\text{Percentage Difference} = \frac{\text{Difference}}{\text{Original Design Discharge}} \times 100$$

$$\text{Percentage Difference} = \frac{1.447\times10^{-6}\ \text{m}^3/\text{sec}/\text{m}^2}{1.815\times10^{-6}\ \text{m}^3/\text{sec}/\text{m}^2} \times 100$$

The 10^{-6} terms cancel out:

$$\text{Percentage Difference} = \frac{1.447}{1.815} \times 100$$

$$\text{Percentage Difference} \approx 0.7972 \times 100$$

$$\text{Percentage Difference} \approx 79.72\%$$

Interpretation:

The discharge from the recommended modified foundation treatment (3.68×10−7 m3/sec/m2) is approximately 79.72% lower than the original design discharge (1.815×10−6 m3/sec/m2). This indicates a significant reduction in discharge based on the evaluation in the thesis and research, suggesting the modified treatment is effective in reducing flow.

(b) Comparing the Discharge of the Original and the Recommended Design at Chainage 0+802.7

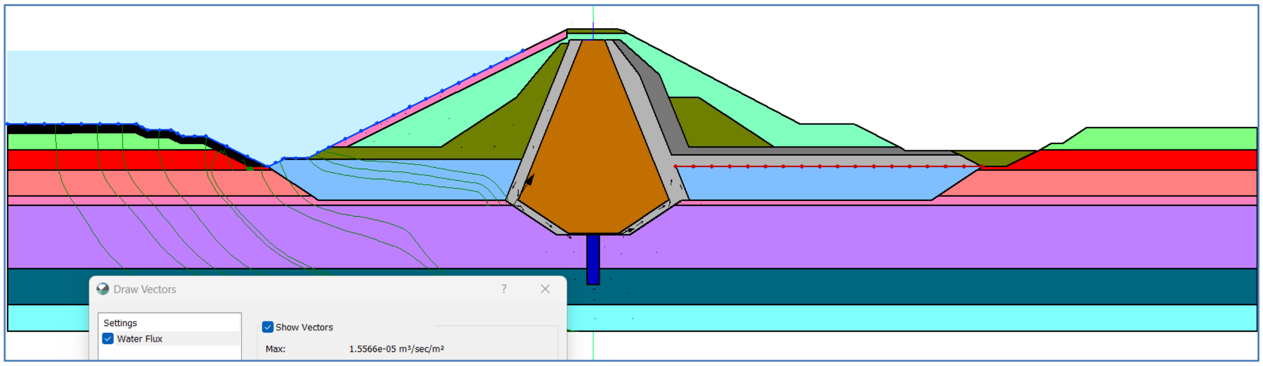

(a) The original design maximum discharge from the model is 1.5566e^{-05} m^3/sec/m^2

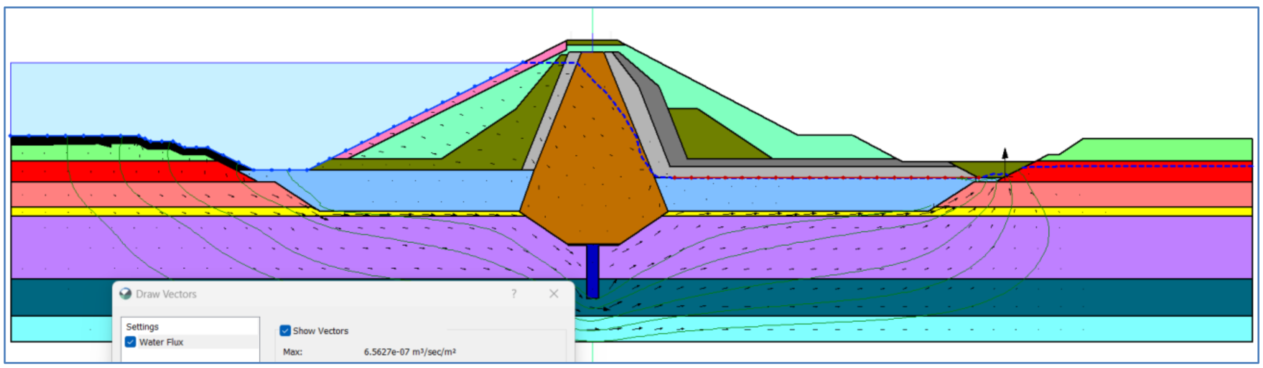

(b) Recommended foundation treatment's maximum discharge from the model is 6.5627e^{-07} m3/sec/m2

Figure 4. 38. Comparing the discharge of the original and recommended design at chainage 0+802.7

- Analyze the discharge values and calculate the percentage difference.

  Original design discharge: Original=1.5566×10−5 m3/sec/m2

  Modelled discharge: modelled=6.5627×10−7 m3/sec/m2

- With the following steps used at the chainage 0+640 above, the calculation has been done as follows;

The modeled discharge (6.5627e-07 m3/sec/m2) is significantly lower than the original design discharge (1.5566e-05 m3/sec/m2). The percentage difference calculation confirms this, showing a decrease of approximately 95.78% from the original design value.

(c) Comparing the Discharge of the Original and Recommended Design at Chainage 1+123

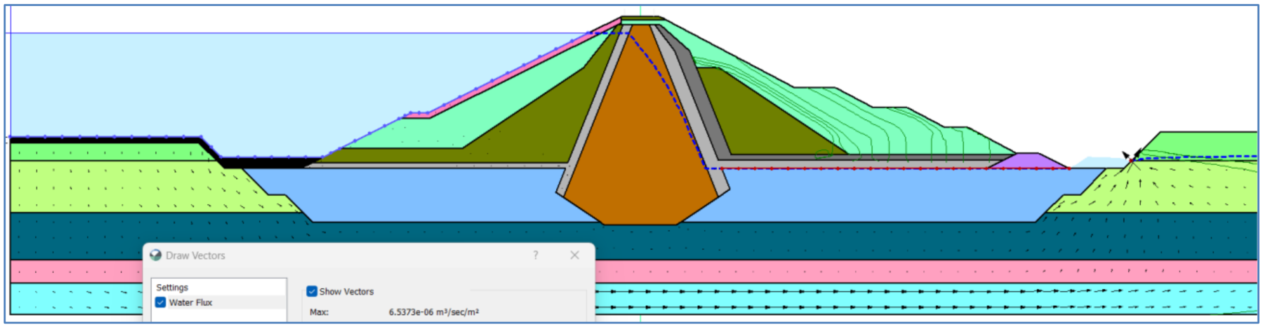

(a) The original design maximum discharge from the model is 6.5373e^{-06} m^3/sec/m^2

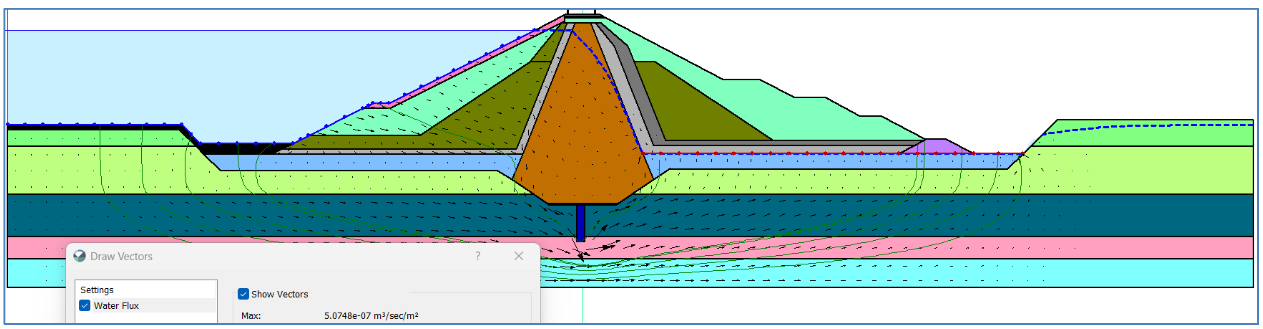

(b) Recommended foundation treatment's maximum discharge from the model is 5.0748e-07 m3/sec/m2

Figure 4. 39. Comparing the discharge of the original and recommended design at chainage 1+123

- **Analysis of the Discharges:**

According to the calculation, the modeled discharge (5.0748e-07 m3/sec/m2) is significantly lower than the original design discharge (6.5373e-06 m3/sec/m2). The percentage difference calculation confirms a decrease of approximately 92.24% from the original design value.

This still represents a large discrepancy. Potential reasons for this significant difference include: Differences in material properties, different boundary conditions, geometry or mesh differences, model simplifications, and errors in input data.

(d) Comparing the Discharge of the Original and Recommended Design at Chainage 1+228

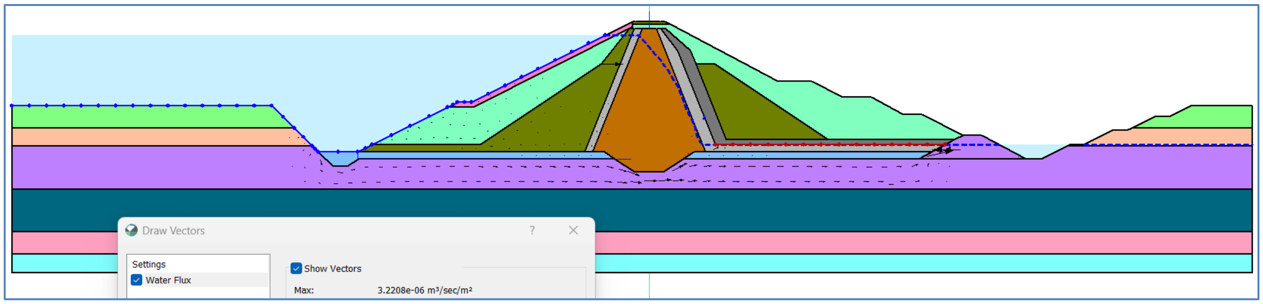

(a) Original design maximum discharge from the model is 3.2208e^{-06} m^3/sec/m^2

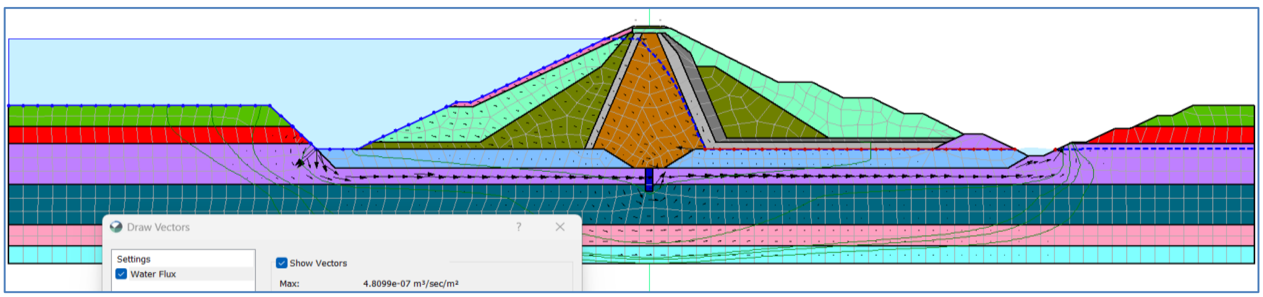

(b) Recommended foundation treatment's maximum discharge from the model is 4.8099e-07 m3/sec/m2

Figure 4. 40. Comparing the discharge of the original and recommended design at chainage 1+228

- **Analysis of the Discharges:**

According to the calculation, the modeled discharge (4.8099e-07 m3/sec/m2) is significantly lower than the original design discharge (3.2208e-06 m3/sec/m2). The percentage difference calculation confirms a decrease of approximately 85.07% from the original design value.

This still represents a large discrepancy. Potential reasons for this significant difference include: Differences in material properties, different boundary conditions, geometry or mesh differences, model simplifications, and errors in input data.

(e) Comparing the Discharge of Original and Recommended Design at Chainage 1+430

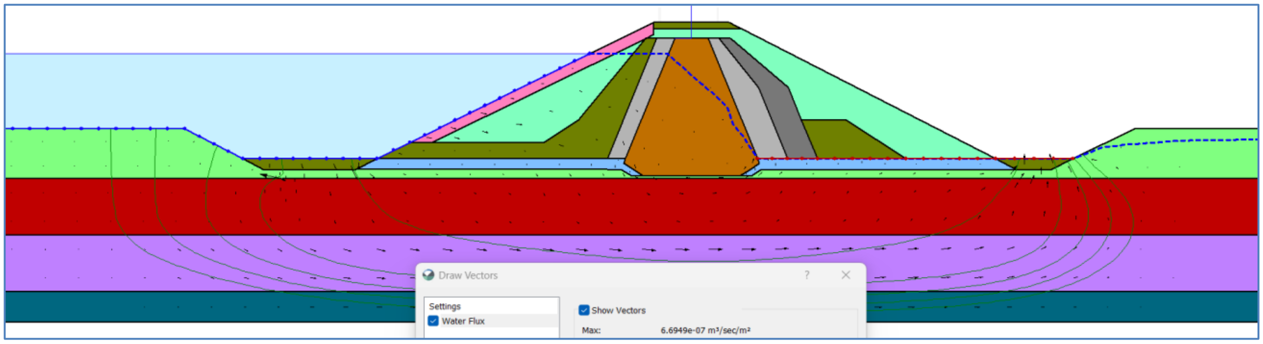

(a) The original design maximum discharge from the model is 6.6949e^{-07} m^{3}/sec/m^{2}

Figure 4. 41. Comparing the discharge of the original and recommended design at chainage 1+430

- **Analysis of the Discharges:**

  Analyzing the water flux along the cross-section at chainage 1+430, which is approximately located around borehole 6, reveals a value of 6.6949×10−7 m3/sec/m2

  When compared to the original design discharge values of the four sections mentioned previously, this water flux is relatively lower, suggesting potentially safer conditions in terms of seepage at this location. Furthermore, this calculated discharge value at chainage 1+430 is approaching the maximum water flux outputs observed in the modeled results for the other four sections, particularly after implementing the recommended foundation treatments based on a detailed evaluation of the original design.

- **Conclusion:**

  Considering the relatively low water flux at chainage 1+430 and its proximity to the acceptable range of modeled discharges achieved in other sections after treatment, it appears that this specific section may not require additional foundation treatment. The current seepage conditions at this location, as indicated by the calculated water flux, seem acceptable based on the analysis and comparisons made with the treated sections.

4.5 Cost Analysis and Evaluation

Following a comprehensive review and detailed modeling of the original drawings of the Kalid Dijo Dam, necessary modifications and foundation treatments have been identified and implemented across four specific sections: chainage 0+640, 0+802.5, 1+123, and 1+228. The cost implications of these modifications have been meticulously calculated, considering both additional and omitted construction components.

4.5.1 The process of measuring and pricing

4.5.1.1. Cost Analysis and Measurement Process

This study involves a systematic assessment of remedial measures implemented at critical locations along the dam, specifically at chainages BH 2, BH 7, BH 8, and BH 4. The process of evaluation and validation includes meticulous measurement of quantities from the final selected options outlined in the project drawings, followed by detailed cost estimation based on current unit rates.

4.5.1.2.Measurement Process

1st. Selection of Final Remedial Measures:

The remedial measures, including gravelly clay blankets, grouting, and drainage systems, were finalized based on detailed design evaluations. These are documented in the attached tables, which distinguish between measures adopted (additions) and those excluded (omissions).

2nd. Quantification from Drawings:

For each chainage, measurements were extracted directly from the final approved drawings. The quantities include:

- Volumes of materials (in cubic meters, m^3),
- Cross-sectional areas,
- Lengths of trenches or layers,
- Volumes of grouting and excavation.

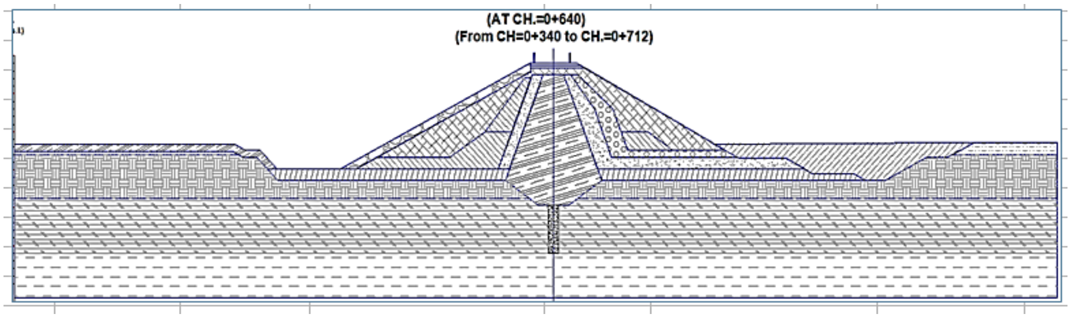

Figure 4. 42 Final Drawing for Measurement for pricing for BH-2

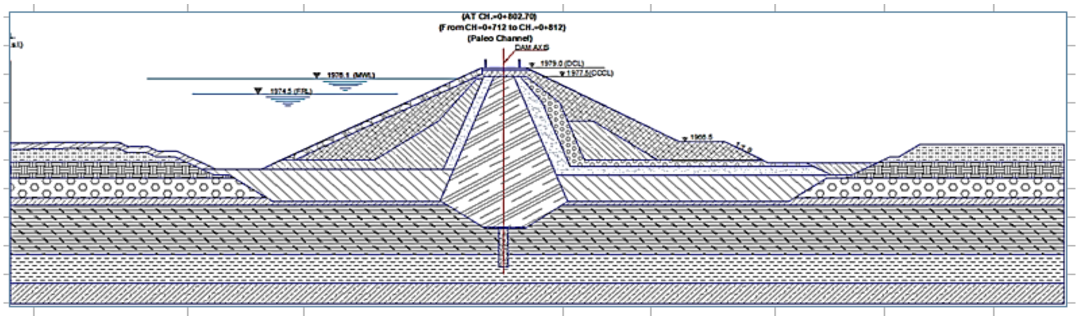

Figure 4. 43 Final Drawing for Measurement for pricing for BH-7

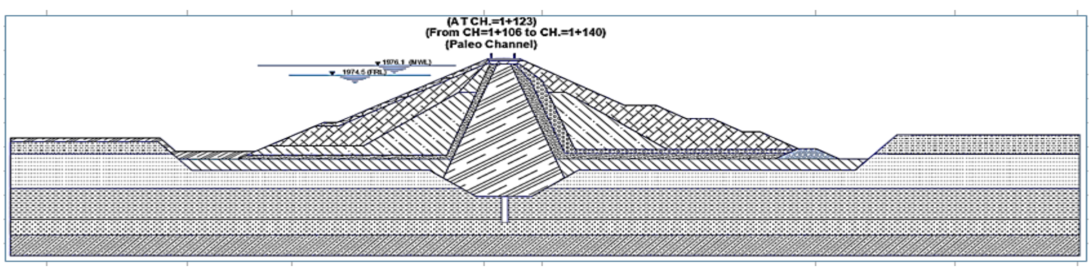

Figure 4. 44 Final Drawing for Measurement for pricing for BH-8

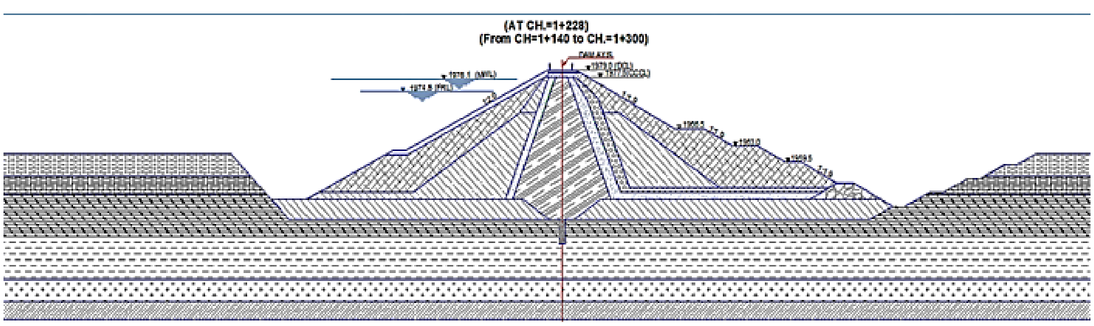

Figure 4. 45 Final Drawing for Measurement for pricing for BH-4

1st. Measurement of Additions and Omissions:

The tables specify the quantities for both additional measures incorporated into the final design and measures that were omitted. This helps in precise cost calculation and understanding the scope of remedial works.

4.5.1.3.Cost Analysis and Pricing

1st. Unit Rate Determination:

Cost per unit volume (m^3) was obtained based on current market rates, supplier quotations, and prevailing construction costs for materials such as gravelly clay, grout, and other construction materials.

2nd. Calculation of Material Costs:

For each remedial measure:

- The total volume of material was multiplied by the respective unit rate to determine the cost.
- For example, at BH 2, the volume of gravelly clay (11,492 m^3) was multiplied by the unit rate (978 per m^3) to get the total cost.

1st. Total Cost for Each Chainage:

The costs of individual measures, including additions and omitted materials, were summed to arrive at the total remedial cost at each chainage. The breakdown is as follows:

A. BH 2:

Table 4. 15. Measuring and Pricing for BH2 (chainage of 0+640)

BH 2			
ADDITIONAL MATERIAL			
Description	**Total Volume**	**Unit Rate**	**Amount**
	m^3	m^3	m^3
clay area	11,492	**978**	11,236,655.30
slurry x scrtion area FILL	3,435	**11557**	39,701,372.29
slurry x scrtion area EXC	3,435	**474**	1,627,546.67
	2,290.25	**11,557.61**	26,469,871.78
			52,565,574.25

BH 2			
OMMITED / DEDUCTED MATERAIL			
Description	**Total Volume**	**Unit Rate**	**Amount**
	m^3	m^3	m^3
U/S GC (0.5m) FILL	13,998.41	2317.02	32,434,584.53
U/S GC (0.5m) EXC	13,998.41	473.76	6,631,884.39
D/S GC (0.5) FILL	15,830.49	2317.02	36,679,562.79
D/S GC (0.5) EXC	15,830.49	473.76	7,499,853.12
U/S clay back FILL	14,088.74	977.82	13,776,250.57
U/S clay back EXC	14,088.74	473.76	6,674,680.89
			103,696,816.28

In summary,

- Additions: Gravelly clay blanket, slurry, and grout measures contributed to a total of approximately **52,565,574.25**.
- Omissions: Included measures like grout fill and excavation, totaling around **103,696,816.28**.

B. BH 7:

Table 4. 16. Measuring and Pricing for BH7 (chainage of 0+802.7)

BH 7			
OMMITED / DEDUCTED MATERAIL			
Description	**Total Volume**	**Unit Rate**	**Amount**
	m^3	m^3	m^3
U/S clay back FILL	24738.8988	**977.82**	24,190,190.02
Zone 2A-Filter Material (F1)	4769.3184	**2986.46**	14,243,378.63
			38,433,568.65

BH 7			
ADDITIONAL MATERIAL			
Description	**Total Volume**	**Unit Rate**	**Amount**
Unit	m^3	m^3	m^3
clay fill	5,513	**977.82**	**5,390,319.58**

In summary,

- Omissions measure approximately **38,433,568.65**.
- Additions are relatively minor, totaling **5,390,319.58**.

C. BH 8:

Table 4. 17. Measuring and Pricing for BH8 (chainage of 1+123)

BH 8			
OMMITED / DEDUCTED MATERAIL			
Description	**Total Volume**	**Unit Rate**	**Amount**
Unit	m^3	m^3	m^3
U/S GC fill	32,513.04	**2317.02**	75,333,359.03
D/S GC fill	35,266.34	**2317.02**	81,712,826.28
U/S GC excavation	22,346.55	**473.76**	10,586,902.90
D/S GC excavation	27,721.12	**473.76**	13,133,157.29
			180,766,245.49

BH 8			
ADDITIONAL MATERIAL			
Description	**Total Volume**	**Unit Rate**	**Amount**
Unit	m^3	m^3	m^3
slurry x scrtion area FILL	1,219.50	**11,558.61**	14,095,724.90
slurry x scrtion area EXC	1,219.50	**473.76**	577,750.32
			14,673,475.22

In summary,

- Omissions cost about **180,766,245.49**.
- Additions total approximately **14,673,475.22**.

D. BH 4:

Table 4. 18. Measuring and Pricing for BH4 (chainage of 1+228)

BH 4			
ADDITIONAL MATERIAL			
Description	**Total Volume**	**Unit Rate**	**Amount**
Unit	m^3	m^3	m^3
U/S GC FILL	40,796.79	2317.02	94,526,976.45
U/S GC EXC	40,796.79	473.76	19,327,886.84
U/S GC FILL	46,171.39	2317.02	106,980,022.69
U/S GC EXC	46,171.39	473.76	21,874,155.40
slurry x scrtion area FILL	1,440.00	11556.61	16,641,518.40
slurry x scrtion area EXC	1,440.00	473.76	682,214.40
	400.00	11,557.61	4,623,044.00
			260,032,774.18

In summary,

- Total measured cost for additions: **260,032,774.18**.

4.5.1.4.Summary of Cost Analysis:

The comprehensive cost across all chainages reflects the scope of remedial measures undertaken, considering both the implemented (additions) and excluded (omitted) measures. This detailed breakdown supports the validation of the selected remedial options and their associated costs. The measurement process involved the precise extraction of quantities directly from the final Options of selected drawings at specified chainages. These quantities were then multiplied by current unit rates to derive the cost estimates for each measure. The comparison of additions and omissions provided clarity on the scope of remedial works and their financial implications, forming a critical part of the overall project validation and economic evaluation.

This detailed cost analysis supports the thesis by demonstrating a transparent, data-driven approach to evaluating the effectiveness and economic feasibility of gravelly clay blankets and other remedial measures for piping control in the Kali Dijo Dam.

Table 4.19. Cost analysis of foundation treatment

Item No	Description	Unit	Added Quantity	Ommited Quantity	Unit Rate	Added Quantity	Ommited Amount	The Difference Amount
1	**BH= 2 @ Chainage 0+640**							
1.1	**Excavation of ordinary soil**	m^3	3,435.38	43,917.63	473.76	1,627,546.67	20,806,418.40	19,178,871.73
1.2	**Fill work**					-	-	-
1.2.1	Clay Material	m^3	11,491.54	14,088.74	977.82	11,236,655.30	13,776,250.57	2,539,595.27
1.2.2	GC Material	m^3	-	29,828.90	2,317.02	-	69,114,147.32	69,114,147.32
1.3	**Concrete Work**					-	-	-
1.3.1	Plastic Concrete	m^3	3,435.38	-	11,556.61	39,701,372.29	-	(39,701,372.29)
	Sub Total					**52,565,574.25**	**103,696,816.28**	**51,131,242.03**
2	**BH=7 @ Chainage 0+802.5**							
2.1	Fill work							
2.1.1	Clay Material	m^3	5,512.59	24,738.90	977.82	5,390,319.58	24,190,190.02	18,799,870.44
2.1.2	Zone 2A-Filter Material (F1)	m^3		4,769.32	2,986.46	-	14,243,378.63	14,243,378.63
	Sub Total					**5,390,319.58**	**38,433,568.65**	**33,043,249.07**
3	**BH=8 @ Chainage 1+123**							
3.1	**Excavation of ordinary soil**	m^3	1,219.50	50,067.67	473.76	577,750.32	23,720,060.19	23,142,309.87
3.2	**Fill work**					-	-	-
3.2.1	GC Material	m^3	-	67,779.38	2,317.02	-	157,046,185.30	157,046,185.30
3.3	**Concrete Work**					-	-	-
3.3.1	Plastic Concrete	m^3	1,219.50	-	11,556.61	14,093,285.90	-	(14,093,285.90)
	Sub Total					**14,671,036.22**	**180,766,245.49**	**166,095,209.28**
4	**BH=4 @ Chainage 1+228**							
4.1	**Excavation of ordinary soil**	m^3	88,408.17	-	473.76	41,884,256.64	-	(41,884,256.64)
4.2	**Fill work**					-	-	-
4.1.1	GC Material	m^3	86,968.17	-	2,317.02	201,506,999.14	-	(201,506,999.14)
4.3	**Concrete Work**					-	-	-
4.3.1	Plastic Concrete	m^3	1,440.00	-	11,556.61	16,641,518.40	-	(16,641,518.40)
	Sub Total					**260,032,774.18**	-	**(260,032,774.18)**
	Total Summary							**(9,763,073.80)**

The summarized cost analysis, as presented in the table above, indicates that the proposed remedial measures involve both additions and omissions in material and labor costs. Notably, the total cost resulting from additions exceeds that of omissions by approximately 9,763,073.80 Ethiopian Birr. Although the omission amount is lower than the cost of additional construction materials, the remedial measures have been implemented by adding necessary materials, which increased the overall contract amount by this figure.

Importantly, despite the higher total cost, the remedial measures have successfully enhanced the safety and stability of the dam. The steady-state slope analysis of the factors of safety shows that all safety factors are above the acceptable threshold of 1.5, indicating that the dam is now considered safe. This outcome demonstrates that the additional investments in materials and construction, though substantial, are justified by the improved safety performance.

From a financial perspective, while the total cost has increased, the primary goal of ensuring dam safety has been achieved. The higher expenditure reflects a strategic decision to prioritize safety and structural integrity, which is critical for the long-term sustainability of the project.

In conclusion, although the costs of additions are higher than the savings from omissions, the remedial measures have resulted in a safer, more reliable dam structure. The investment of approximately 9.76 million Birr is justified by the positive safety outcomes demonstrated through the slope stability analysis.

4.1.Evaluation and Calculation of the Discharge

Based on the evaluation conducted in this thesis/research and the output results obtained from GeoStudio modeling of both the original foundation design and the newly proposed foundation treatment for Kalid Dijo Dam, it is crucial to validate the effectiveness of the proposed remedial measures. After comprehensive analysis, calculating and assessing the discharge flow from upstream to downstream is an essential step to verify the accuracy and reliability of the modeling results. This process ensures that the modeled discharges accurately reflect the dam's behavior under both the original and modified foundation conditions. Validating these discharges is vital for confirming that the proposed foundation treatment effectively reduces seepage and flow, thereby enhancing dam stability and safety. Ultimately, this validation supports informed decision-making regarding the implementation of the remedial measures and contributes to the overall assessment of the dam's performance and safety in this study.

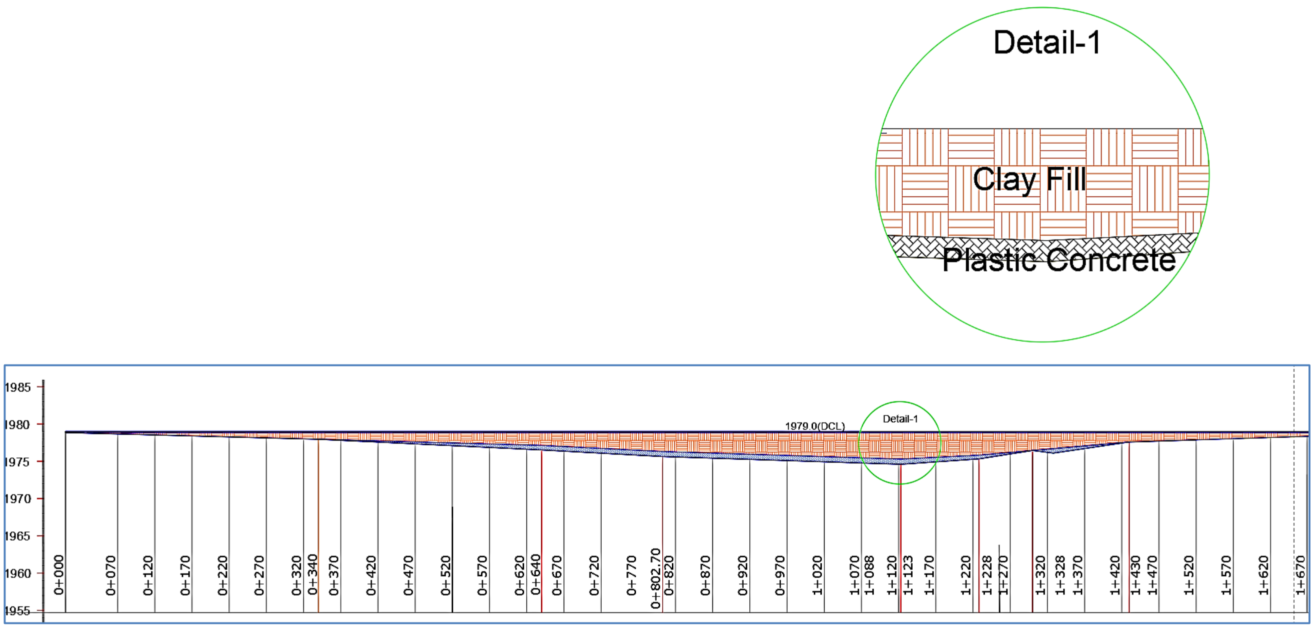

Figure 4.46. Longitudinal section of Kalid Dijo dam for discharge evaluation

Based on the above figure and the following summarized table, Discharge Comparison and Water Savings Analysis for Kalid Dijo Dam Foundation Treatment is going to be described as follows;

Table 4.20. Discharge calculation and analysis

Description	A	B	C	D	E	F	G	H
	Borehole	Max. Water Flux	Average Water Flux	Area of Gross Dam's Section Longitudinal	Area of Net Cross Section Longitudinal	Discharge	Sec/Year	Annual Discharge
		m3/Sec/m2	m3/Sec/m2	m2	New - Orginal	m3/Sec		m3/Year
						C*D		
Original	BH-2	1.82E-06	5.57E-06	28,928.03	5,377.50	0.030	31,536,000	**944,570.26**
	BH-7	1.56E-05						
	BH-8	6.54E-06						
	BH-4	3.22E-06						
	BH-6	6.69E-07						
New/ Proposed	BH-2	3.68E-07	5.36E-07	34,305.53		0.003	31,536,000	**90,964.97**
	BH-7	6.56E-07						
	BH-8	5.08E-07						
	BH-4	4.81E-07						
	BH-6	6.69E-07						

In conclusion to the above, the analysis of the tabulated data demonstrates a substantial reduction in water flux and annual discharge in the Kali Dijo Dam's foundation system after implementing proposed remedial measures. Specifically, the comparison between the original and new systems indicates that measures such as enhancing impermeable layers and installing cutoff structures are highly effective in controlling seepage and internal erosion risks.

The original system exhibited an annual discharge of approximately 944,570 m³, which posed a potential risk for internal erosion and piping. After applying the proposed foundation modifications, this discharge was reduced to roughly 91,000 m³ per year, representing a water saving of approximately 90.37%. This significant decrease underscores the effectiveness of the remedial measures in limiting seepage pathways, thereby enhancing the dam's stability and safety.

To calculate the percentage of water saving from the original to the proposed system, we compare the total annual discharge values:

- Original total annual discharge: 944,570.26 m^3/year
- Proposed total annual discharge: 90,964.97 m^3/year
- Water saving (volume):
  944,570.26 m^3/year – 90,964.97 m^3/year = 853,605.29 m^3/year

- Percentage of water saved:
  (Volume saved / Original volume) × 100 = (853,605.29 / 944,570.26) × 100 ≈ 90.37%

In Summary, the proposed measures reduce water flux significantly, resulting in approximately 90.37% water savings compared to the original system.

Purpose of this analysis in the research:

This data-driven evaluation confirms that targeted foundation improvements can drastically diminish water flux through the dam's foundation. The reduction in seepage not only decreases the risk of internal erosion but also contributes to the dam's long-term operational safety and sustainability. The findings support the conclusion that strategic foundation treatment is a vital component in dam safety management, especially in critical infrastructure like Kali Dijo Dam.

Output/result for the research:

The research concludes that implementing the proposed foundation modifications can achieve approximately a 90% reduction in seepage-related water flux. This substantial decrease enhances overall dam stability, reduces potential failure risks, and ensures safer downstream conditions. Such results validate the effectiveness of the recommended engineering interventions and provide a quantitative basis for their adoption in dam safety protocols and future infrastructure planning.

Analysis of Discharge Change Over Time

- **Before treatment (original design):** The dam discharges about 0.03 m^3/s, which results in significant seepage loss over time, potentially affecting dam stability and water resource management.
- **After treatment (proposed design):** The discharge is reduced to 0.003 m^3/s, significantly decreasing seepage and associated risks, while also conserving a substantial volume of water annually. This reduction not only enhances dam safety by minimizing seepage-induced instability but also supports water conservation efforts, especially in regions facing water scarcity.

4th. Discussion of Results

The approximately 90.37% reduction in discharge demonstrates the effectiveness of the proposed foundation treatment. The substantial annual water savings of about 853,605.29 cubic meters highlight the importance of implementing such remedial measures for both structural safety and resource conservation. The modeling results indicate that the foundation treatment successfully limits seepage, which is critical for maintaining dam integrity and prolonging its service life.

5th. Conclusion and Summary

In conclusion, the proposed foundation treatment for Kalid Dijo Dam effectively reduces seepage discharge from $0.03 m^3/s$ to $0.003 m^3/s$, achieving nearly 90.37% water conservation. This significant reduction translates to an annual savings of approximately 853,605.29 cubic meters of water, emphasizing the importance of such remedial measures. These findings validate the effectiveness of the new foundation design in improving dam safety and contributing to sustainable water resource management. Future recommendations include continued monitoring of seepage behavior and reassessment of discharge rates to ensure the long-term success of the remedial measures.

Economic and Water Conservation Analysis of Kali Dijo Dam

Table 4. 21. Economic and Water Conservation Analysis

No.	Descripition	m3	ha	Birr/ha/Month	Birr in a Year	Birr in 50Years
1	Volume Dam's Reservoir	**6,260,000**	1200	2869	41,313,600.00	2,065,680,000.00
2	Saved water due to New Foundation Treatment	**853,605**	163.6	2869	5,633,467.67	281,673,383.37
				Based on Ethiopia Sugar Corporation		

This table presents an analysis of water volume savings resulting from the implementation of new foundation treatment measures at Kali Dijo Dam. The data includes the total reservoir capacity, the amount of water saved, and the economic valuation based on resource data from Ethiopia Sugar Corporation for 2023.

Key points from the table:

1. **Reservoir Capacity:**

   The total volume of the dam's reservoir is 6,260,000 m³, covering an area of 1200 hectares.

2. **Water Saved Due to Foundation Treatment:**

   The measures have resulted in a water saving of approximately 853,605 m³. This corresponds to an area of 163.6 hectares.

3. **Economic Valuation Using Ethiopia Sugar Corporation Data:**

   - **Monthly revenue per hectare:** 2,869 Birr
   - **Annual revenue from saved water:** 5,633,467.67 Birr
   - **Revenue over 50 years:** 281,673,383.37 Birr

Conclusion:

This analysis, based on Ethiopia Sugar Corporation's resource valuation for 2023, quantifies the economic benefit of water savings achieved through foundation improvements. It highlights that leveraging water conservation not only enhances dam safety but also offers substantial economic returns over time.

Note:

This analysis is solely for research and thesis purposes related to the Kalid Dijo Dam. It uses resource data from Ethiopia Sugar Corporation in 2023 to illustrate potential economic benefits, emphasizing that the primary focus is academic research rather than direct financial assessment.

5. CONCLUSIONS AND RECOMMENDATIONS

5.1.Conclusions

The study systematically evaluates the potential risks associated with internal erosion and piping within the dam's foundation phenomena that, if unmitigated, could lead to catastrophic failure with devastating downstream consequences. This research carried out critical assessments of foundation treatment measures, notably the implementation of gravelly clay blankets and slurry cutoff walls, aimed at controlling seepage and preventing internal erosion. Through advanced geotechnical analysis utilizing GeoStudio 2022, the study demonstrates that strategically increasing the thickness of impermeable layers significantly reduces water flux and hydraulic gradients directly linked to piping risk. The comparison across multiple design options reveals that the optimized foundation treatment markedly lowers water flux, thereby substantially enhancing the dam's stability margins.

Furthermore, the detailed slope stability analyses have provided compelling evidence that the proposed remedial measures elevate the safety factors well above critical thresholds. The static analyses consistently show safety factors exceeding 1.6. These results affirm that the dam's structural components, when fortified with appropriate foundation treatments, can withstand steady-state conditions, safeguarding downstream communities and infrastructure.

The modeling and comparison of flow paths validate that the modified foundation treatments effectively reduce seepage by approximately 85–95%, contributing to enhanced dam safety and operational stability. This improvement aligns with sustainable water resource management objectives, especially in water-scarce regions.

Cost analysis further substantiates the economic viability of these remedial actions. The findings indicate that the additional expenditure incurred by implementing targeted foundation improvements is justified by the substantial safety benefits and long-term durability of the dam infrastructure. The overall investment ensures the dam's resilience against internal erosion risks, thereby protecting downstream populations and infrastructure.

In conclusion, this investigation affirms that well-designed foundation modifications such as increased impermeable layer thicknesses, effective cutoff walls, and strategic material placement are essential for mitigating internal erosion risks and ensuring the long-term stability of the Kalid Dijo Dam. The significant reduction in seepage and the enhancement of safety margins demonstrate that these measures effectively address the fundamental causes of piping, preventing potential dam failures. The comprehensive geotechnical evaluation, advanced modeling, and cost-effective strategies presented in this study contribute valuable insights to dam engineering. Ultimately, the implementation of these remedial measures will promote safer dam operation, protect downstream communities, conserve vital water resources, and extend the service life of this critical infrastructure, aligning engineering excellence with sustainable development goals.

5.2.Recommendations

Based on the comprehensive analysis and findings detailed in this thesis concerning the Kalid Dijo Dam project, it is evident that the implementation of targeted foundation treatments particularly the use of gravelly clay blankets and cut-off slurry walls are play a critical role after the construction of the Kalid Dijo Dam by enhancing the dam safety, reducing the internal erosion risks, and optimizing the water resource management. The following detailed recommendations are elaborated to guide future practices, improve current designs, and ensure long-term stability and sustainability of the dam:

5.2.1. Prioritize and Adopt Effective Foundation Treatments

(a) The study demonstrates that increasing the thickness of gravelly clay (GC) layers and implementing cut-off slurry walls significantly decreases seepage flow and the potential for piping failure.

(b) It is recommended that dam projects, especially those constructed on complex, ash-rich, or fractured foundation materials, incorporate these remedial measures during the design and construction phases.

(c) Specifically, foundation treatments such as a minimum of 3-meter GC layers combined with well-designed slurry cut-off walls should be adopted based on site-specific geotechnical and hydrological conditions. This approach effectively reduces water flux by over 85-90%, markedly improving structural integrity.

5.2.2. Optimize Cost-Effective Foundation Design:

(a) The cost analysis indicates that remedial foundation measures, though initially involving additional material and construction costs, are ultimately more economical than potential failure consequences.

(b) It is recommended that project budgets allocate sufficient resources for high-quality foundation treatments, considering long-term safety benefits and water savings.

(c) Regular review of material choices, construction techniques, and ongoing maintenance can ensure cost-effectiveness while maintaining safety standards.

5.2.3. Promote Water Conservation and Resource Management:

(a) The significant annual water savings achieved through improved foundation treatment underscore the importance of integrating seepage control with water resource planning.

(b) Dam operators should incorporate water savings calculations into operational protocols, adjusting reservoir management to maximize water conservation.

In conclusion, the evidence from this thesis underscores that proactive, site-specific foundation treatments such as increased GC layer thickness and effective slurry cut-offs are essential for minimizing seepage, preventing piping, and ensuring the long-term safety of the Kalid Dijo Dam. These recommendations advocate for integrating advanced modeling, continuous monitoring, cost-effective design, and robust emergency protocols to foster resilient dam infrastructure capable of supporting sustainable development and water resource management in Ethiopia and similar contexts.

6. REFERENCES

1. Ethiopian Construction Design and Supervision Works Corporation (ECDSWCo) (Insert Year). Study and Design of Kalid Dijo Dam and Irrigation Project
2. Ali Ghanbari and Sajjad Zaryabi 2. A simple method for calculating the seepage at the foundation of embankment dams with blanket and clay trench.
3. Hydraulics Branch, Research & Laboratory, Services Division, US Bureau of Reclamation, Hydraulics Program, Department of Civil Engineering, Colorado State University, Water Resource Section, HDR, Engineering, Incorporated. August 6, 1993. Dam Foundation Erosion Survey of Literature
4. Habtom Redda. Oct 2016. Evaluation Of Embankment Dam Failure And Remedial Measures (Case Study Of Gomit Dam In Amhara Region)
5. International Commission on Large Dams (ICOLD). (2019). Internal Erosion of Dams and Their Foundations. Bulletin 161. Paris: ICOLD. Available at: https://www.icold-cigb.org/
6. United States Society on Dams (USSD). (2018). Internal Erosion of Dams and Levees. Denver, CO: USSD. Available at: https://www.ussdams.org/
7. International Commission on Large Dams (ICOLD). (2019). Internal Erosion of Dams and Their Foundations. Bulletin 161. Paris: ICOLD. Available at: https://www.icold-cigb.org/
8. United States Society on Dams (USSD). (2018). Internal Erosion of Dams and Levees. Denver, CO: USSD. Available at: https://www.ussdams.org/
9. Federal Emergency Management Agency (FEMA). (2007). Risk Assessment for Dam Safety. FEMA P-1150. Washington, DC: FEMA. Available at: https://www.fema.gov
10. Terzaghi, K., & Peck, R. B. (1967). Soil Mechanics in Engineering Practice (2nd ed.). Wiley.
11. Lambe, T. W., & Whitman, R. V. (1969). Soil Mechanics. Wiley.
12. U.S. Army Corps of Engineers. (2003). Engineering and Design: Cut-off Walls for Dams. EM 1110-2-2300.
13. British Dam Society. (2017). Guidelines for the Design of Dam Improvements and Repairs
14. International Commission on Large Dams (ICOLD). (2019). Internal Erosion of Dams and

Their Foundations. Bulletin 161. Paris: ICOLD.

15. Federal Emergency Management Agency (FEMA). (2007). Risk Assessment for Dam Safety. FEMA P-1150.
16. International Commission on Large Dams (ICOLD). (2019). Internal Erosion of Dams and Their Foundations. Bulletin 161. Paris: ICOLD. Available at: ICOLD Publications
17. United States Society on Dams (USSD). (2018). Internal Erosion of Dams and Levees. Denver, CO: USSD. Available at: USSD Publications
18. Federal Emergency Management Agency (FEMA). (2007). Risk Assessment for Dam Safety. FEMA P-1150. Available at: FEMA Publications
19. Geo-Slope International Ltd. (2012). "GeoStudio 2012." Available at: https://www.geoslope.com/products/seep-w
20. Itasca Consulting Group, Inc. (2019). "FLAC - Fast Lagrangian Analysis of Continua." Available at: https://www.itascacg.com/software/flac
21. Bentley Systems, Inc. (2020). "PLAXIS 2D and 3D." Available at: https://www.bentley.com/en/products/brands/plaxis
22. Chowdhury, R., Sarker, A. (2014). "Seepage and Stability Analysis of Karnafuli Dam Using GeoStudio." Journal of Civil Engineering Research.
23. Itasca Consulting Group. (2007). "Numerical Analysis of Seepage and Piping at Wolf Creek Dam." Technical Report.
24. Chowdhury, R., & Sarker, A. (2014). "Seepage and Stability Analysis of Karnafuli Dam Using GeoStudio." Journal of Civil Engineering Research.
25. Geo-Slope International Ltd. (2012). "GeoStudio 2012." Available at: GeoStudio.